EXPERIMENTAL STUDY ON THE WAVE OVERTOPPING PERFORMANCE OF XBLOC+ ARMOUR UNIT

ALBA JIMÉNEZ MORENO

TUDelft Delft University of Technology   Delta Marine Consultants   CoMEM

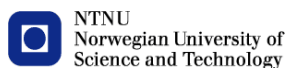ERASMUS +: ERASMUS MUNDUS MOBILITY PROGRAMME

Master of Science in

COASTAL AND MARINE ENGINEERING AND MANAGEMENT
CoMEM

Experimental study on the wave overtopping performance of Xbloc+ armour unit

Delft University of Technology
3th July 2017

Alba Jiménez Moreno

The Erasmus+: Erasmus Mundus MSc in Coastal and Marine Engineering and Management is an integrated programme including mobility organized by five European partner institutions, coordinated by Norwegian University of Science and Technology (NTNU).

The joint study programme of 120 ECTS credits (two years full-time) has been obtained at two or three of the five CoMEM partner institutions:

- Norges Teknisk- Naturvitenskapelige Universitet (NTNU) Trondheim, Norway
- Technische Universiteit (TU) Delft, The Netherlands
- Universitat Politècnica de Catalunya (UPC). BarcelonaTech. Barcelona, Spain
- University of Southampton, Southampton, Great Britain
- City, University London, London, Great Britain

During the first three semesters of the programme, students study at two or three different universities depending on their track of study. In the fourth and final semester an MSc project and thesis has to be completed. The two-year CoMEM programme leads to a multiple set of officially recognized MSc diploma certificates. These will be issued by the universities that have been attended by the student. The transcripts issued with the MSc Diploma Certificate of each university include grades/marks and credits for each subject.
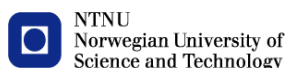
Information regarding the CoMEM programme can be obtained from the programme coordinator:

Øivind A. Arntsen, Dr.ing.
Associate professor in Marine Civil Engineering
Department of Civil and Transport Engineering
NTNU Norway

Telephone: +4773594625 Cell: +4792650455 Fax: + 4773597021

Email: oivind.arntsen@ntnu.no

CoMEM URL: https://www.ntnu.edu/studies/mscomem

CoMEM Master Thesis

This master thesis was completed by:

Alba Jiménez Moreno
Email: alba.jnez@hotmail.com

As a requirement to attend the degree of:

Erasmus+: Erasmus Mundus Master in Coastal and Marine Engineering and Management (CoMEM)

Under the supervision of:

Prof. dr.ir S.G.J Aarninkhof	*Hydraulic Engineering, TU Delft*
Ir. H.J. Verhagen	*Hydraulic Engineering, TU Delft*
Ing. C. Kuiper	*Hydraulic Engineering, TU Delft*
Dr.ir. B. Hofland	*Coastal Structures, TU Delft*
Ir. B. Reedijk	*Delta Marine Consultants*
Dipl.Ing. T. Eggeling	*Delta Marine Consultants*

In collaboration with:

Delft University of Technology
Faculty of Civil Engineering and Geosciences
Department of Hydraulic engineering

Delta Marine Consultants
BAM Infraconsult,
Coastal Engineering department

This master degree was taught at the following educational institutions:

- Norges Teknisk- Naturvitenskapelige Universitet (NTNU) – Trondheim, Norway
- Technische Universiteit (TU) Delft – Delft, The Netherlands
- University of Southampton - Southampton, Great Britain

At which the student has studied from August 2015 to June/July 2017.

Todo pasa y todo queda,
pero lo nuestro es pasar,
pasar haciendo caminos,
caminos sobre el mar.

- Antonio Machado

ACKNOWLEDGEMENTS

This thesis completes the MSc. in Coastal and Marine Engineering and Management (CoMEM) program carried out at three different universities: the Norwegian University of Science and Technology (NTNU), University of Southampton and Delft University of Technology. Research for this project was conducted in collaboration with Delta Marine Consultants.

Firstly, I would like to thank the CoMEM board for giving me the opportunity of pursuing this master degree. Studying this programme has become a challenging and enriching experience at all levels.

I would like to thank my committee for their support and contributions to this project. I would like to acknowledge Coen Kuiper and Henk Jan Verhagen for their guidance and advice. At Delta Marine I would like to say a special thanks to Tamara Eggeling. Thanks for all your time and patience throughout these past months and, especially, for sending support during the long days we spent in the lab.

To my fellow CoMEM classmates who make this whole experience unforgettable. Special thanks to my Pathé-mates, Xabi and Belén, for the movie sessions and long lunch breaks. I particularly want to thank Belén for her help and support during the ups and down I faced these last months; for working out with me at the lab and for being always willing for a NewYork NewYork pizza (or any other junk food we should not be eating). Moreover, I could not forget to mention my awesome Moholt's flatmate, Encarna. Although we took different paths after Norway, Lofoten hikings and our music sessions after library will be always stuck on me.

In addition, I would like to acknowledge Ana, who introduced me to the field of coastal engineering and motivated me to apply for this degree. Thanks for your constant support and valuable feedback.

Most of all, I would like to thank my family and especially my parents for their perpetual love, support and encouragement. Thanks for letting me experience this adventure. Going back home is always the best part of the journey.

Alba Jiménez Moreno
Delft, July 2016

SUMMARY

Nowadays, the use of concrete armour units on rubble mound breakwaters designs has become a common practice. Concrete armour units can be placed in a single layer system or in a double layer system and can its placement can be either random or uniform.

Recently, Delta Marine Consultants have designed a new armour unit called Xbloc+. This new block is applied as a one layer system and has a regular placement. As Xbloc+ is still under development, preliminary guidance on the performance of this new armour unit is required. This led this research to investigate how Xbloc+ behaves concerning wave overtopping.

To analyse wave overtopping, small scale tests were performed in a 2D wave flume. Wave overtopping was measured at a $3D_n$ distance from the seaward edge of the crest, which is made of rock. In front of the slope there is a flat transition of 0.3m followed by a sloping foreshore of 1/30. In total, 10 series of tests were conducted. In this research, three wave steepness (S_{op}) were tested (0.02, 0.04 and 0.06) to see the effect of wind waves and swell conditions on the armour layer and tests were performed in two different slope angles (1/2 and 3/4). Each series is formed by several sub tests conducted with increasing wave heights (and wave period in order to maintain a constant wave steepness). Tests were carried out until the failure of the armour slope was reached. Besides, a smooth slope was tested in a 1/2 slope angle to be able to compare smooth and rough results and determine the roughness coefficient of the armour unit more accurately.

The test results showed that wave overtopping rates increase exponentially with wave height (H_{m0}) and wave period ($T_{m-1,0}$). Moreover, waves with lower wave steepness (swell conditions) induce higher overtopping discharges as compared to larger wave steepness. Steeper slopes also lead to higher overtopping rates. Therefore, the larger the breaker parameter is, the larger the overtopping discharge results.

The influence of the armour roughness and armour permeability is also analysed and it is observed that swell conditions are less affected by these properties. This can be explained by means of the breaker type. Swell conditions are characterized by large surging waves. These waves have a thicker water tongue as compared with other type of breaking (e.g. spilling or plunging) and therefore, they tend to feel the top layer "smoother". This fact is supported by the analysis of the influence of the roughness coefficient since higher values are obtained for surging waves. in fact, the roughness coefficient ranges between 0.34 and 0.68 showing that, although empirical prediction consider this parameter as a constant, it is dependent on the wave conditions.

Concerning the comparison of dimensionless overtopping rate over Xbloc+ armour between test results and empirical prediction, it was found that the present formulae does not give a good estimation due its simplicity. In order to improve the representation of some parameters such as slope angle and wave steepness, correction factors are introduced in the empirical formulae leading to a better fit between prediction and measured data. Based on this modified empirical formula, roughness coefficients are calculated. A value of gf=0.55 is estimated for Xbloc+ unit.

LIST OF FIGURES

LIST OF TABLES

NOTATION

Symbol	Description	Units
Δ	Relative density	[-]
a	Empirical coefficient	[-]
A	Empirical coefficient	[-]
A_c	Armour crest freeboard of structure	m
b	Empirical coefficient	[-]
B	Empirical coefficient	[-]
C	Empirical coefficient	[-]
c	Empirical coefficient	[-]
D	Empirical coefficient	[-]
d	Water depth	m
D_n	Nominal diameter of concrete armour unit	m
D_{n50}	Nominal diameter of rock	m
D_{nx}	Diameter of stone that exceeds the x% value of the sieve curve	m
Fr	Froude number	[-]
g	Gravity (=9.81)	m/s^2
H	Wave height	m
$H_{1/3}$	Significant wave height defined as highest one-third of wave heights	m
$H_{2\%}$	2%-exceedance wave height	m
H_{m0}	Spectral significant wave height	m
$H_{m0,d}$	Design significant wave height	m
H_s	Significant wave height = $H_{1/3}$	m
K_d	Stability coefficient	[-]
K_r	Reflection coefficient	[-]
L_0	Deep water wave length based on $gT^2_{m-1,0}/2\pi$	m
L_p	Deep water wave length based on $gT^2_p/2\pi$	m
m_n	nth moment of the spectral density	m^2/s^n
N_{od}	Damage number	[-]
N_{ow}	Number of overtopping waves	[-]
N_w	Total number of incident waves	[-]
P_{ov}	Percentage of overtopping waves	[-]
q	Mean overtopping discharge	l/m/s
q*	Dimensionless overtopping discharge	[-]
R*	Dimensionless relative freeboard	[-]
R_c	Crest freeboard of the structure	m
Re	Reynolds number	[-]
S	Wave steepness	[-]
S_{0m}	Wave steepness with L_0 based on T_m	[-]
$S_{m-1,0}$	Wave steepness with L_0 based on $T_{m-1,0}$	[-]
S_{op}	Wave steepness with L_0 based on T_p	[-]
T	Wave period	s
$T_{1/3}$	Significant wave period	s

T_m	Mean wave period	s
$T_{m-1,0}$	Average spectral wave period defined by m_{-1}/m_0	s
T_p	Spectral peak wave period	s
V	Overtopping volume	l
W	Weight	kg
We	Weber number	[-]
X_{i-j}	Spacing between gauges	m
α	Angle between structure slope and horizontal	deg
γ	Peak-enhancement factor from JONSWAP-spectrum	[-]
γ*	Influence factor for a storm wall on slope or promenade	[-]
$γ_b$	Influence factor for a berm	[-]
$γ_f$	Roughness coefficient	[-]
$γ_v$	Influence factor for a vertical wall on the slope	[-]
$γ_β$	Influence factor for oblique wave attack	[-]
μ	Dynamic viscosity	kg/ms
v	Kinematic viscosity	m^2/s^n
$ξ_{m-1,0}$	Spectral breaker parameter based on $s_{m-1,0}$	[-]
$ρ_a$	Armour density	kg/m^3
$ρ_w$	Water density	kg/m^3
$σ_a$	Shape parameter from JONSWAP-spectrum	[-]
$σ_b$	Shape parameter from JONSWAP-spectrum	[-]

| TABLE OF CONTENTS

1 | INTRODUCTION

This chapter introduces the topic of this research. Firstly, a brief overview of breakwaters and existing single layer concrete armour unit is given in section 1.1. Secondly, the problem description is explained in section 1.2. The scope of this study is presented in section 1.3. Section 1.4 describes the general methodology followed in this study. Finally, section 1.5 outlines the structure of the report.

1.1 GENERAL OVERVIEW

1.1.1   COASTAL DEFENCE STRUCTURES

Historically, sloping dikes have been the most widely used option for sea defences along the coasts of the Netherlands, Denmark and many parts of the UK. However, coastal structures can also consist of a mound of layers of quarried rock fill, protected by rock or concrete armour units. This type of structures is known as rouble mound breakwater. The outer armour layer is designed to resist wave action without significant displacement of armour units. Underlayers of quarry or crushed rock support the armour and separate it from finer material in the embankment or mound. These porous and sloping layers dissipate a proportion of the incident wave energy in breaking and friction (EurOtop 2016).

Breakwaters can have many configurations. For this study, the effects of wave overtopping will be tested on a conventional rubble mound breakwater. Figure 1.1 gives an outline of the relevant parts of this type of breakwater.

Coastal defence structures are mainly protecting the inland against flooding. Therefore, wave overtopping is a principal concern and becomes a main parameter regarding the design of most coastal defence structures.
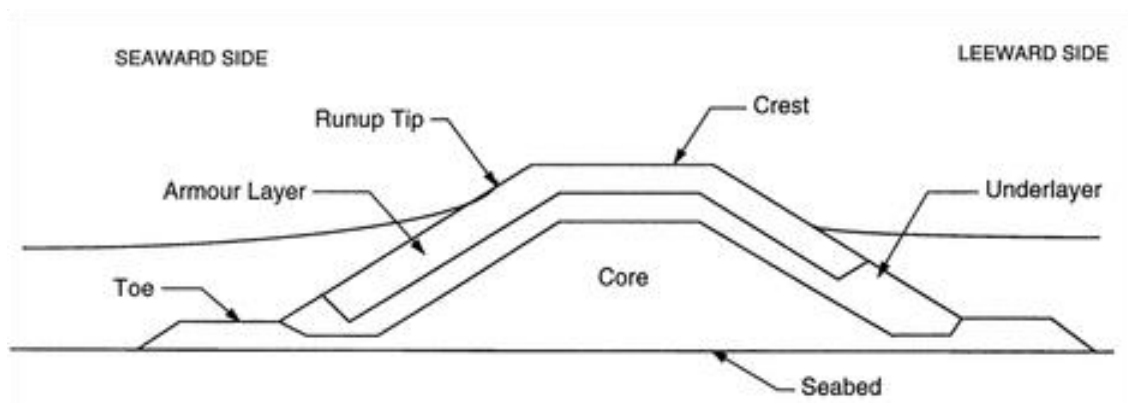
Figure 1.1 Cross section of a conventional rubble mound breakwater (Palmer & Christian 1998)
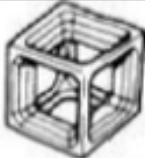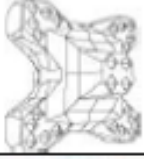
1.1.2   DEVELOPMENT OF THE DIFFERENT SINGLE LAYER CONCRETE ARMOUR UNITS

Concrete armour units become a more optimal alternative with respect to a rock protection when the armour rock size is economically too large in terms of production and transportation. The armour units can be placed in two layers or in a single layer. As stated by Muttray, M. and Reedijk, B. (2008), the first configuration covers the uncertainties regarding hydraulic stability and structural integrity of individual armour units. However, since 1980 higher safety margins have been achieved for armour units placed in a single layer with respect to the hydraulic design and the structural strength of individual units has been increased. Therefore in 1980, the Accropode, the first randomly placed single layer armour

unit, was presented. Core-loc and Xbloc were introduced some years later. The stability of the randomly placed armour units is governed by the interlocking force between the neighbouring units. Furthermore, armour units can also be placed in a uniformly distribution. In this case, friction is the governing factor that maintains the stability of the blocks. Seabee and Shed blocks are both examples of these type of blocks (Muttray & Reedijk 2008).

The most recent developments include the Cubipod (2005) and the Crablock (2007). The Cubipod was developed in order to improve the low hydraulic stability of Cubes (Vanhoutte 2008) and UAE created the Crablock to be applied in a damaged rubble mound breakwater (Saluddin, Md. 2015)

Table 1.1 summarizes the different single layer concrete armour units.

Randomly placed		Uniformly placed	
Interlocking		Friction	
Cube (Single layer)			
Accropode France, 1980		Cob UK, 1969	
Core-loc USA, 1996		Diahitis Ireland, 1998	
A-Jack USA, 1998		Seabee Australia, 1978	
Xbloc NL, 2003		Shed UK, 1982	
Accropode II France, 2004			
Cubipod Spain, 2005			

Table 1.1 Single layer concrete armour units

1.2 PROBLEM DESCRIPTION

Recently, Xbloc+ has been developed as a new single layer concrete armour unit by Delta Marine Consultants. This new development is introduced in order to allow for regular placement.

Xbloc is an armour unit that has high interlocking forces and resistance to wave impact as well as reduced wave overtopping. However, its characteristics rely on the random placement of the individual blocks. Some crane operators can have difficulties to place the units with a random orientation and the armour becomes more regularly placed than it is desirable. This results in a decrease of the interlocking force and thus, in a reduction of the hydraulic stability of the blocks. Besides, more concrete units might be used due to its more uniform placement.

The new armour unit Xbloc+ is presented as a single layer uniformly placed armour unit. The main distinct characteristic with the other armour units present in the world is that both interlocking force and friction are governing factors for its hydraulic stability. Furthermore, its uniform placement simplifies crane operations and gives higher aesthetic effects improving. In order to be used in future engineering projects, model tests must be done to ensure that the hydraulic stability of the new block is acceptable.

Figure 1.2 Regular placement of the Xbloc+

1.3 RESEARCH OBJECTIVES AND QUESTIONS

The main objective of this MSc research is to give an overview of the behaviour of the new Xbloc+ armour unit against wave overtopping. The following research objectives are aimed to be fulfilled:

- To investigate the wave overtopping over Xbloc+ armour layers
- To analyse the different parameters that might have an influence on wave overtopping
- To compare wave overtopping with empirical formulae
- To define the roughness coefficient for this new single layer armour unit

In order to give answer to these objectives, the following research questions are considered:

1. What is the wave overtopping discharge and percentage of overtopping waves over Xbloc+ armour layer?
2. What parameters have an influence on wave overtopping results?
3. Do the existing empirical formulae describe properly the wave overtopping?
4. How can the existing empirical prediction be improved in order to obtain more accurate estimations?
5. What value of roughness coefficient corresponds to this new armour unit?

1.4 RESEARCH METHODOLOGY

In order to fulfil the research objectives, the following methodology is adopted:

- First, a literature review is performed. This chapter includes a review of the previous researches on wave overtopping and the existing wave overtopping formulae. Scale and model effects resulting from physical modelling are also summarized.
- Secondly, the experimental set up is defined as well as the different hydraulic tests needed to be performed in a 2D wave flume. This laboratory plan contains a design for a suitable model for studying wave overtopping and considers the influence of relevant parameters such as slope and wave steepness.
- The following step includes the execution of the experimental tests. These tests are conducted for version 1 and 2 of Xbloc+ armour units.
- Next, the collection and processing of the necessary data is required in order to be able to determine the wave overtopping discharge and derive the roughness coefficient.
- After processing the data, the wave overtopping is analysed and the parameters that might influence the test results are discussed. A comparison of the results with existing formulae is also conducted along with the introduction of correctors factors to improve the overtopping prediction.
- Finally, conclusions are drawn and recommendations for further research are given.

This overview of the adopted methodology is presented in a flowchart in Figure 1.3.
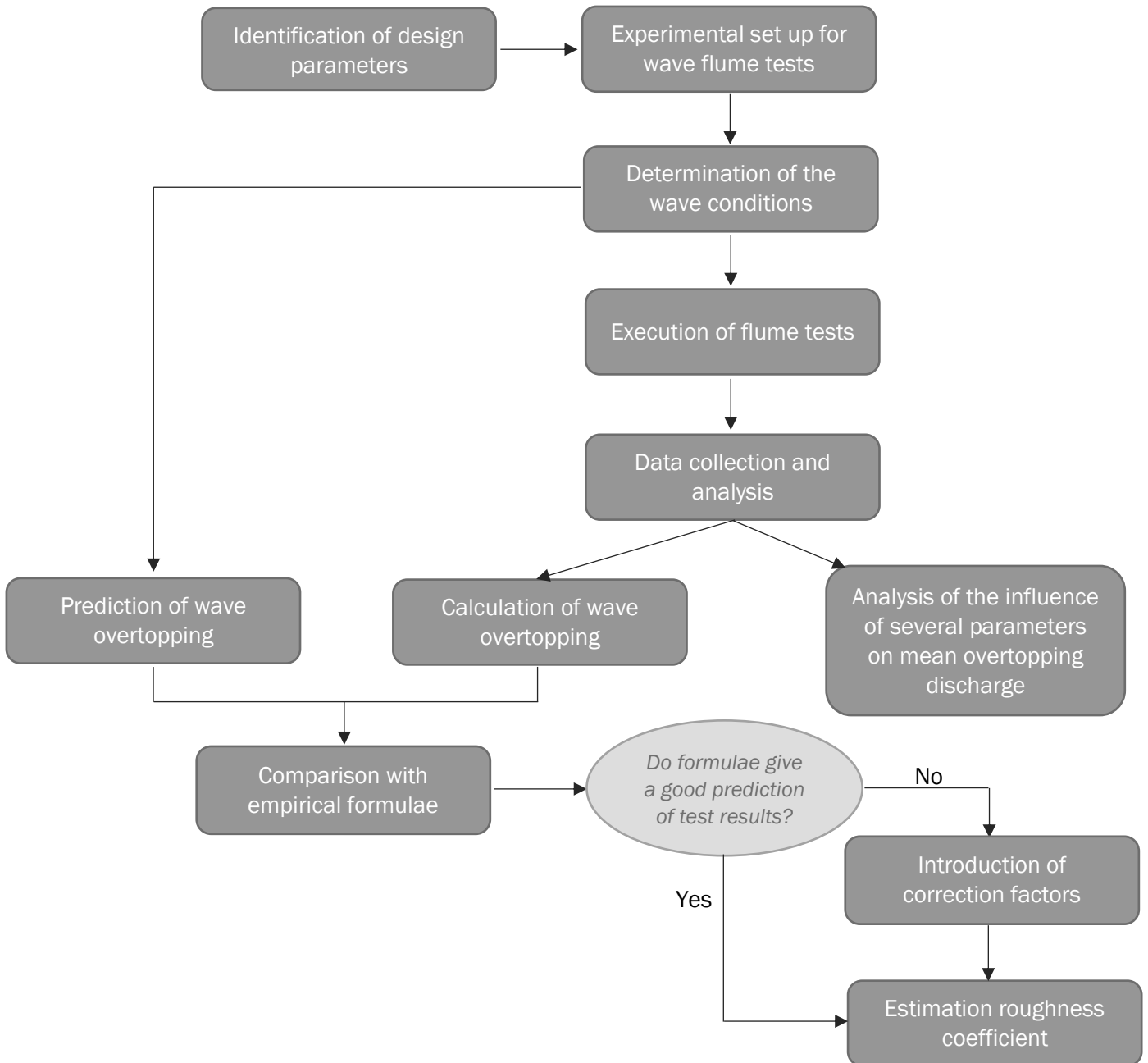
Figure 1.3 Research methodology

1.5 RESEARCH OUTLINE

The structure of this report contains the main steps considered in the research methodology. Chapter 1 gives an overview of the study and states the objectives and approach of the research. In chapter 2 the existing literature is discussed regarding wave overtopping phenomenon as well as some concerns about physical modelling such as scaling effects. The existing empirical formulae are also summarized. Chapter 3 describes the experimental set up designed for this study. The performance of the Xbloc+ unit on wave overtopping and the parameters that have an influence on it are analysed in Chapter 4. A comparison with empirical formulae is given in Chapter 5 as well as a modification of the actual formulae which provides a better prediction for the test results. Roughness coefficient is also defined at the end of that chapter. Finally, in Chapter 6, conclusions and recommendations for further research are stated.

2 | LITERATURE REVIEW

This chapter gives the state of art regarding wave overtopping on rouble mound breakwaters. The most relevant literature related to this phenomenon is reported. Finally, physical modelling is briefly explained as well as scale and model effects.

2.1 WAVE OVERTOPPING ON RUBBLE MOUND BREAKWATERS

Wave overtopping is defined as the quantity of water passing over the crest of a structure per unit of time (D'Angremond et al. 2008). The process of wave overtopping is very random in time, space and volume. While the highest waves can push large volumes of water over the crest in a short period of time (less than a wave period), lower waves may not generate any overtopping.

This process can be characterised by the wave overtopping discharge and the wave overtopping volume. Wave overtopping discharge, q, is the average discharge per linear meter of width and has units of m³/s per m or l/s per m. The reason for using mean overtopping discharges is that this parameter can be considered stable over about 1000 waves (Verhaeghe et al. 2008). In contrast, the wave overtopping volume can be calculated for given wave conditions and mean discharge q. It is expressed in m³ per wave per meter width.

Wave overtopping is often referred to as "green water" when full bodies of water overtop the structure. A second form of overtopping, termed "white water" or spray overtopping, occurs when waves break on the seaward face of the structure, generating non-continuous overtopping or large volumes of spray that can be transported along large distances by wind.

2.1.1 HAZARDS DUE TO WAVE OVERTOPPING

Wave overtopping can be damaging to other constructions, but also for the population. Indeed, as stated by Allsop (2003) at least 12 people have been killed in the UK by wave overtopping or related processes during 1999-2002 and approximately 60 were killed in Italy over last 20 years. EurOtop (2016) lists four general categories that should be analysed when assessing overtopping effects and their consequences:

- Damage to defence structure(s): either short-term or longer-term, with the possibility of breaching and flooding.
- Direct hazard of injury or death to people immediately behind the defence, whether they are pedestrians, cyclists or travelling in a vehicle;
- Damage to property, operation and/or infrastructure in the area defended, including loss of economic, environmental or other resource, or disruption to an economic activity or process;
- Low depth flooding (inconvenient but not dangerous)

The hazards caused by wave overtopping also depends on the geometry of the structure, the nature of the inland behind the structure, and the form and trajectory of overtopping.

2.1.2 TOLERABLE OVERTOPPING DISCHARGES

In order to prevent damages, maximum values of mean discharge overtopping have been determined. Guidance on overtopping discharges that can cause damage is described in the overtopping manual EurOtop. Furthermore, this manual gives maximum mean discharge

values for structural design of breakwaters since wave overtopping on rubble mound breakwater can lead to global failure of the structure. Table 2.1 summarizes the different limits that have been developed.

LIMITS FOR OVERTOPPING FOR STRUCTURAL DESIGN OF BREAKWATERS		
Hazard type and reason	Maximum mean discharge q (l/s per m)	Maximum volume Vmax (l per m)
Rubble mound breakwaters; $H_{m0} > 5m$; no damage	1	2.000 – 3.000
Rubble mound breakwaters; $H_{m0} > 5m$; rear side designed for wave overtopping	5 - 10	10.000 – 20.000
Grass covered crest and landward slope; maintained and closed grass cover; $H_{m0} = 1 – 3$ m	5	2.000 – 3.000
Grass covered crest and landward slope; not maintained grass cover, open spots, moss, bare patches; $H_{m0} = 0.5 – 3$ m	0.1	500
Grass covered crest and landward slope; $H_{m0} < 1m$	5 - 10	500
Grass covered crest and landward slope; $H_{m0} < 0.3m$	No limit	No limit
LIMITS FOR OVERTOPPING FOR PROPERTY BEHIND THE DEFENCE		
Hazard type and reason	Maximum mean discharge q (l/s per m)	Maximum volume Vmax (l per m)
Significant damage or sinking of larger yachts; $H_{m0} > 5m$	>10	>5.000 – 30.000
Significant damage or sinking of larger yachts; $H_{m0} = 3 - 5m$	>20	>5.000 – 30.000
Sinking small boats set 5 – 10 m from wall; $H_{m0} = 3 – 5m$. Damage to larger yachts	>5	>3.000 – 5.000
Safe for larger yachts; $H_{m0} > 5m$	<5	<5.000
Safe for smaller boas set 5 – 10 m from wall; $H_{m0} = 3 -5m$	<1	<2.000
Building structure elements; $H_{m0} = 1-3m$	≤1	<1.000
Damage to equipment set back 5 – 10 m	≤1	<1.000
LIMITS FOR OVERTOPPING FOR PEOPLE AND VEHICLES		
Hazard type and reason	Maximum mean discharge q (l/s per m)	Maximum volume Vmax (l per m)
People at structures with possible violent overtopping, mostly vertical structures	No access for any predicted overtopping	No access for any predicted overtopping
People at seawall / dike crest. Clear view of the sea $H_{m0} = 3m$ $H_{m0} = 2m$ $H_{m0} = 1m$ $H_{m0} < 0.5m$	 0.3 1 10 - 20 No limit	 600 600 600 No limit
Cars on seawall / dike crest, or railway close behind crest $H_{m0} = 3m$ $H_{m0} = 2m$ $H_{m0} = 1m$	 <5 10 - 20 <75	 2.000 2.000 2.000
Highways and roads, fast traffic	Close before debris in spray becomes dangerous	Close before debris in spray becomes dangerous

Table 2.1 Tolerable overtopping (EurOtop 2016)

2.1.3   PREVIOUS STUDIES

The wave overtopping phenomenon started to be investigated in the 1950's. Savile (1955) was one of the first researchers to conduct overtopping tests with regular waves. As different structures have been created, the interest in wave overtopping has increased and several models to predict wave overtopping have been developed through the years.

Initially, overtopping was simulated by physical model experiments and only regular waves were considered. Later, irregular waves started to be modelled, which resemble more to the natural waves found on the field. This made possible to gain accuracy in developing prediction methods. Owen (1980) developed the first overtopping formula based on irregular wave experiments. Owen's formula has become the base of empirical formulae, and even now, it is used for the design of sloping structure types (Verhaeghe et al. 2008). In 1995, Van der Meer and Janssen introduced a new approach by distinguishing breaking and non-breaking waves. This method is widely used in the determination of wave overtopping. In 2014 new physical insights and design formulae was introduced by Van der Meer and Bruce. These new formulae are presented in an updated version of the EurOtop manual released in 2016. Further details of wave overtopping formulae are given in section 2.1.5.

2.1.4   CLASH DATABASE

An extensive database on wave overtopping has been created within the CLASH project. This CLASH project (Crest Level Assessment of Coastal Structures by Full Scale Monitoring, Neutral Network Prediction and Hazard Analysis on Permissible Wave Overtopping), funded by European Union, investigated wave overtopping for different structures in prototype and in laboratory. This database covers over 10.000 tests performed around the world which is formatted in an Excel spreadsheet. There, small scale tests from 2D and 3D models and field data can be found. Besides, it includes all kind of coastal structures, from simple geometries to more complex situations. Some confidential tests also contribute to the database (Steendam 2004).

The reasons for the creation of this database are:

- The CLASH database is an inventory of data that can be used to analyse specific structure types. Data can be extracted to compare with similar structures or analyse further specific types of structures.
- The CLASH database was used to develop a neutral network prediction method for mean overtopping discharges on coastal structures.

In order to describe each overtopping test, 31 parameters are included in the spreadsheet, making it easy for users to conduct their analysis.

As the CLASH EU-Project was developed, different white spots were detected leading to additional tests. The CLASH committee considered the following points as the most important issues to investigate further:

- The influence of surface roughness/permeability
- The effect of obliqueness, short-crested waves and directional spreading

2.1.5   PREDICTION OF WAVE OVERTOPPING

Currently, a number of different methods exist to predict overtopping under given wave conditions and water levels. EurOtop (2016) gives a detailed description of the following different methods: analytical method, empirical methods, PC-Overtopping and Neural network tools from CLASH database, numerical methods and physical modelling.

In this research, physical modelling in a 2D flume is used to estimate wave overtopping and results are compared to empirical formulae proposed by EurOtop (2016).

2.1.5.1 Empirical methods

Empirical methods are regression models that are based on available overtopping data obtained from physical model experiments. Generally, these methods establish an exponential relationship between the mean discharge and the crest freeboard or its dimensionless forms.

In this section, the most relevant formulae found in literature is described.

2.1.5.1.1 *Owen's formula, 1980*

Owen's method calculates the overtopping discharge for smooth impermeable sloping structures. Equation [2.1] gives the relation between the dimensionless discharge (Q*) and freeboard (R*). These parameters are defined in equations [2.2] and [2.3] and they use the mean wave period and the significant wave height at the toe of the structure.

$$Q^* = a \cdot exp\left(\frac{-b \cdot R^*}{\gamma_f}\right)$$

[2.1]

$$R^* = \frac{R_c}{T_m\sqrt{gH_s}} = \frac{R_c}{H_s\sqrt{s_{0m}/2\pi}}$$

[2.2]

$$Q^* = \frac{Q}{T_m g H_s}$$

[2.3]

where 'a' and 'b' are empirical coefficients that depend on the cross-section and γ_f is the correction factor that accounts for the roughness of the slope. Owen (1980) considered this coefficient as the ratio between the run-up of a given wave on a rough slope and the run-up of the same wave on a smooth slope. He recommended γ_f= 0.5-0.6 for rock slopes and γ_f=1.00 for smooth slopes.

2.1.5.1.2 *EurOtop Manual, 2007*

Van der Meer and Janssen (1995) makes a clear distinction between breaking and non-breaking conditions. Therefore, two different formulae for mean wave overtopping discharge have been defined for irregular waves and slopping structures.

Equation [2.4] represents the basic overtopping expression in its dimensionless form.

$$\frac{q}{\sqrt{gH_{m0}^3}} = a \cdot \exp\left(-b\frac{R_c}{H_{m0}}\right)$$

[2.4]

where empirical coefficients 'a' and 'b' depends on the concerned method and accounts for the wave conditions, the reduction factors and the structure dimensions.

For breaking waves the wave overtopping formula can be described by using equations [2.5] and [2.6].

$$\frac{q}{\sqrt{gH_{m0}^3}} = \frac{A}{\sqrt{tan\alpha}}\gamma_b\xi_{m-1,0} \cdot \exp\left(-B\frac{R_c}{H_{m0}}\frac{1}{\xi_{m-1,0} \cdot \gamma_b \cdot \gamma_f \cdot \gamma_\beta \cdot \gamma_v}\right)$$

[2.5]

With a maximum of

$$\frac{q}{\sqrt{gH_{m0}^3}} = C \cdot \exp\left(-D\frac{R_c}{H_{m0}}\frac{1}{\gamma_f \cdot \gamma_\beta}\right)$$

[2.6]

This maximum represents the wave overtopping for non-breaking waves.

Note that the coefficients γ_b , γ_f , γ_β and γ_v accounts for the influence of a berm, roughness of the slope, oblique wave attack and or a wall at the end of the slope, respectively.

The presented formulae are valid for breaker parameters $\xi_{m-1,0}$<5. Formulae for breaker parameters $\xi_{m-1,0}$> 7 can be found in EurOtop Manual (2007).

- **Empirical coefficients**

The value of the empirical coefficients A, B, C and D vary depending on the undertaken approach (deterministic or probabilistic design). EurOtop (2007) proposed a more conservative approach for the deterministic design and one standard deviation has been recommended to be added to the mean overtopping discharge.

Table 2.2 summarizes the possible values they can take.

	Deterministic design	Probabilistic design
A	0.067	0.067
B	4.30	4.75
C	0.20	0.20
D	2.30	2.60

Table 2.2 Values for the different empirical coefficients in equations [2.5] and [2.6]

2.1.5.1.3   *New empirical formulae (EurOtop, 2016)*

Van der Meer and Bruce (2014) reviewed the empirical formulae provided by EurOtop (2007) and concluded that equations [2.5] and [2.6] overestimate wave overtopping discharge for slopping structures with very low or zero crest height. Therefore, new formulae have been developed to predict wave overtopping for slopping structures with zero and positive crest height more accurately. These new formulae are presented in the last version of the EurOtop manual.

The main difference is the addition of a third empirical coefficient, c, on the principal overtopping formula which makes the equation valid for the full range of $R_c \geq 0$. The general formula, which is applicable to dikes and embankments, is described in equation [2.7].

$$\frac{q}{\sqrt{gH_{m0}^3}} = a \cdot \exp\left(-\left(b\frac{R_c}{H_{m0}}\right)^c\right)$$

<div align="right">[2.7]</div>

This extra component modifies the general wave overtopping formulae as follows:

$$\frac{q}{\sqrt{gH_{m0}^3}} = \frac{A}{\sqrt{tan\alpha}}\gamma_b\xi_{m-1,0} \cdot \exp\left(-\left(B\frac{R_c}{H_{m0}}\frac{1}{\xi_{m-1,0} \cdot \gamma_b \cdot \gamma_f \cdot \gamma_\beta \cdot \gamma_v}\right)^{1.3}\right)$$

<div align="right">[2.8]</div>

With a maximum of

$$\frac{q}{\sqrt{gH_{m0}^3}} = C \cdot \exp\left(-\left(D\frac{R_c}{H_{m0}}\frac{1}{\gamma_f \cdot \gamma_\beta \cdot \gamma^*}\right)^{1.3}\right)$$

<div align="right">[2.9]</div>

Note that an influence factor γ^* has been added for non-breaking waves (relatively steep slopes) for a storm wall on a slope or promenade.

EurOtop (2016) suggests using equation [2.9] for rubble mound structures.

- ▪ **Empirical coefficients**

As mentioned for EurOtop (2007) the value of the empirical coefficients A, B, C and D vary depending on the taken approach (deterministic or probabilistic design). Table 2.3 summarizes the possible values they can take for the new formulae.

	Deterministic design	Probabilistic design
A	0.026	0.023
B	2.5	2.7
C	0.1035	0.09
D	1.35	1.5

Table 2.3 Values for the different empirical coefficients in equations [2.8] *and* [2.9]

Van der Meer and Bruce (2014) highlight that these new formulae give almost the same wave overtopping as the original formulae, equations [2.5] and [2.6], but represent nature better for R_c/H_{m0} < 0.5-1.0. As stated in EurOtop (2016), for breaking waves the new formulae may give up to 4% more overtopping discharge and up to 30% less than the old formulae. For non-breaking waves, it was up to 27% more and also about 30% less for the new formulae. Compared to the reliability of wave overtopping discharge prediction, which is estimated for a confidence band of 90% between a factor 2.5 and up to 20 or more (for very small overtopping) a deviation of up to 30% is small and insignificant. Therefore, the latest update of the overtopping prediction will be applied in this research.

2.1.5.1.4 *Percentage of overtopping waves*

The percentage of overtopping waves can also be estimated as described in EurOtop (2016). The empirical equation is a function of the armour freeboard, A_c, (instead of the crest freeboard, R_c), the nominal diameter, D_n, and the significant wave height, H_{m0}.

$$P_{ov} = \frac{N_{ow}}{N_w} = \exp\left(-\left(\frac{A_c \cdot D_n}{0.19 \cdot H_{m0}^2}\right)^{1.4}\right)$$

In which N_{ow} is the number of overtopping waves and N_w represents the total number of incident waves. This equation is based on the work of De Jong (1996) and various CLASH-test, see Figure 2.1.
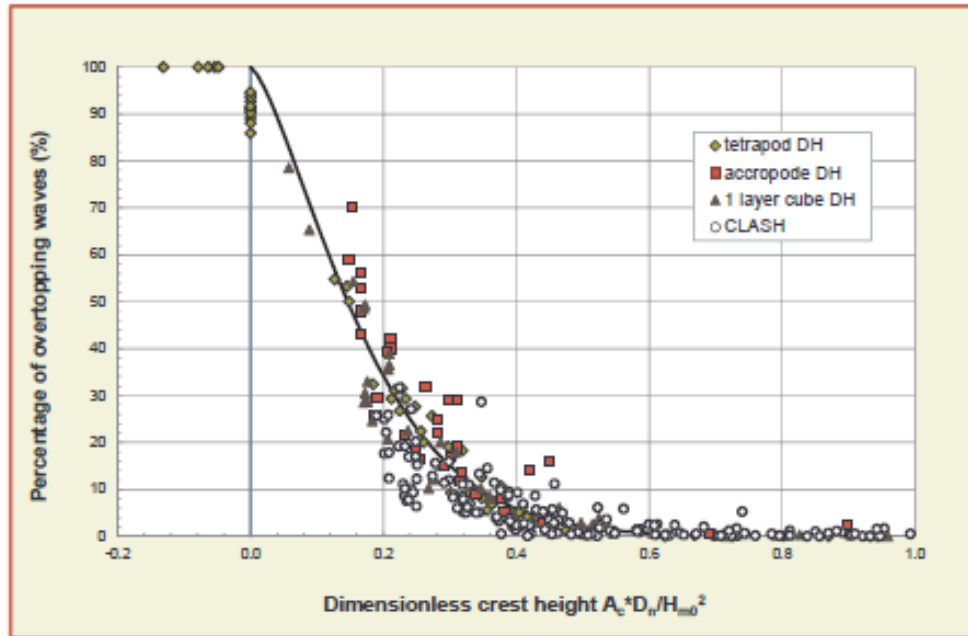
Figure 2.1 Percentage of overtopping waves for rubble mound breakwater as a function of relative armour crest height and armour size (Rc<Ac). (EurOtop 2016)

2.1.5.2 Estimation of the roughness coefficient

The roughness coefficient is one of the most important structural characteristics regarding the prediction of overtopping rates. Roughness is created by the irregular placement of the blocks or rocks forming the armour layer (more irregularities lead to higher roughness). However, the roughness factor, γ_f, not only takes into account how overtopping is influenced by the amour unit, but also the number of layers, the packing density and the permeability of armour layer (Molines and Medina 2015).

Roughness and permeability affect wave overtopping by decreasing the wave run-up as these induce wave dissipation. Therefore, the higher the roughness and permeability of the armour (the lower the roughness coefficient), the lower the overtopping discharge. A smooth slope has a roughness coefficient of 1.0.

The reduction factor, γ_f, is an empirical parameter that is generally estimated from the mean overtopping discharge, and hence, depends on the chosen wave overtopping predictor. Therefore, as the knowledge of the wave overtopping process increases and the formulae is modified, the roughness coefficient varies as well.

According to Molines and Medina (2015), the first roughness factors based on regular waves and run-up observations were published in Russian manuals. As mentioned in section 2.1.5.1, Owen (1980) considered the roughness factor as the ratio between the run-up of a given wave on a rough slope and the run-up of the same wave on a smooth slope. Later, Van

der Meer and Janssen (1995) proposed calculating the γ_f for dikes and rock slopes by comparing the run-up of a rough slope with that of a smooth one.

Within the CLASH EU-Project, Pearson et al. (2004) provided a set of roughness factors based on overtopping measurements for different armour units. Those roughness factors were calibrated considering the formula given by Van der Meer and Janssen (1995) and a 5% reduction was imposed on all values.

Furthermore, Bruce et al. (2006) analysed the results from Pearson et al. (2004) and listed γ_f for different armor units. These values were used in the formulas given by EurOtop (2007). Bruce et al. (2009) revised the tests reported by Bruce et al. (2006), suggesting changes in the γ_f and calculating the confidence intervals for each γ_f by analysing variance. This latest study also showed a dependency of the roughness coefficient with slope angle for rock (permeable core). The roughness factor decreases for smaller slope angles. EurOtop (2016) recommends using the revised values calculated by Bruce et al. (2009).

Table 2.4 summarizes the different coefficients found on literature.

Type of armor 2L=double-layer 1L=single-layer	Packing density (φ)	Owen (1980)	Hebsgaard et al. (1998)	Coeveld et al. (2005) CLASH NN	Pearson et al. (2004) Bruce et al. (2006) EurOtop (2007)	Smolka et al. (2009)	Bruce et al. (2009)	Kortenhaus et al. (2014)	CLASH NN Manual
Smooth	-	1.00	-	1.00	1.00	-	1.00	-	1.00
Rock (2L)	1.38	0.50-0.60	0.55	0.50	0.40	-	0.40	-	0.55
Cube(2L, random)	1.17	-	-	0.50	0.47	0.50	0.47	-	0.40
Cube (2L, flat)	1.17	-	-	-	0.47	-	0.47	-	-
Cube (1L, flat)	0.70	-	-	-	0.50	-	0.49	-	-
Antifer (2L)	1.17	-	0.65	0.50	0.47	-	0.50	-	-
Haro (2L)	-	-	-	0.47	0.47	-	0.47	0.57/0.63	-
Haro (1L)	-	-	-	-	-	-	-	0.57/0.63	-
Tetrapod (2L)	1.04	-	-	0.40	0.38	-	0.38	-	0.40
Accropode (1L)	0.62	-	0.55	0.49	0.46	-	0.46	-	0.40
Core-Loc (1L)	0.56	-	-	0.47	0.44	-	0.44	-	0.40
Xbloc (1L)	0.58	-	-	0.49	0.45	-	0.44	-	-
Dolos (2L)	-	-	0.45	0.43	_0.43_	-	_0.43_	-	0.40
Cubipod (2L)	1.18	-	-	-	-	0.44	-	-	-
Cubipod (1L)	0.61	-	-	-	-	0.46	-	-	-

Table 2.4 Different of roughness coefficient given in literature (Molines 2016)

Therefore, it becomes clear that the roughness factor is dependent on the specific overtopping formulae selected by the corresponding author and the dataset used. In this research, the coefficients recommended in the EurOtop manual (2016) are taken as reference since those are used in CLASH database to identify the armour type.

2.2 PHYSICAL MODELLING

Physical modelling is commonly used to assess wave overtopping and develop empirical formulae for predicting it. The large number of relevant parameters influencing this phenomenon makes it hard to develop theoretical or numerical approaches that represent the nature of overtopping well. In contrast, experimental tests are an established and reliable method for determining mean wave overtopping discharges for arbitrary coastal structures (EurOtop 2016).

However, the actual empirical formulae do not predict wave overtopping discharges and individual volumes very accurately due to scale and model effects present always at some degree in the physical model.

2.2.1 SCALE EFFECTS

Scale effects are the result of the incorrect reproduction of a prototype water-structure interaction in the scale model. Scaled models can only replicate reality by fulfilling Froude's and Reynolds' law simultaneously. However, this is not possible to achieve and therefore, scale effects always become an issue to consider when performing scaled model tests.

Most models are scaled according to Froude's law since gravity, pressure and inertial forces are the main relevant forces in terms of wave motion. However, viscosity forces are governed by Reynolds' law, elasticity by Cauchy's law and surface tension forces by Weber's law. These forces are neglected in most models leading to errors called scale effects.

EurOtop (2016) lists some generic rules that should be observed for physical model studies:

- Water depths in the model should be much larger than d = 2 cm
- Wave periods larger than T = 0.35 s and wave heights larger than Hs = 5 cm to avoid the effects of surface tension.
- For rubble mound breakwaters, the Reynolds number for the stability of the armour layers should exceed $Re = 3x10^4$
- For overtopping of coastal dikes $Re > 1x10^3$
- Stone size of the core of rubble mound breakwaters has to be scaled according to the velocities in the core rather than stone dimensions, especially for small models. This approach is detailed in Burcharth et al. (1999)

Moreover, Schüttrumpf and Oumeraci (2005) give some critical limits for the influence of viscosity and surface tension; see Table 2.5.

Process	Relevant forces	Similitude law	Critical limits
Wave propagation	Gravity force Friction forces Surface tension	Fr_w Re_w We	$Re_w > Re_{w,crit} = 1 \times 10^4$ $T > 0.35s; d > 2cm$
Wave breaking	Gravity force Friction forces Surface tension	Fr_w Re_w We	$Re_w > Re_{w,crit} = 1 \times 10^4$ $T > 0.35s; d > 2cm$
Wave run-up	Gravity force Friction forces Surface tension	Fr_q Re_q We	$Re_q > Re_{q,crit} = 1 \times 10^3$ $We > We_{crit} = 10$
Wave overtopping	Gravity force Friction forces Surface tension	Fr_q Re_q We	$Re_q > Re_{q,crit} = 1 \times 10^3$ $We > We_{crit} = 10$

Table 2.5 Critical limits for viscosity and surface tensions depending on wave processes

2.2.2   MODEL AND MEASURMENT EFFECTS

Besides scale effects, model and measurement effects may also disturb the model tests results. Model effects can be caused by the boundary conditions of a wave flume (such as side walls and wave paddle). On the other hand, measurement effects result from the different required equipment that it is installed in the wave flume.

These effects can lead to a high degree of discrepancy between prototype and model. Therefore, quantifying the model effects and the uncertainty related to the selected techniques is essential. However, since the main difference between model and prototype results will be induced by model effects, it is impossible to quantify these effects by comparing scaled and prototype models. Investigations performed by Kortenhaus et al. (2005), recommends quantifying the differences resulting from model effects by analysing the following effects in two flumes:

-   Effect of side walls: use flumes or wave basin with different widths so that the influence of the side walls plays a different role and see whether there is any difference in the results.
-   Effect of wave generator: different wave generators in identical flumes are needed to quantify any differences in the results.
-   Effect of wind: only possible if one of the flumes does have possibilities to study wind effects.
-   Effect of wave set-up: comparison of 2D wave flume and 3D basin (perpendicular wave attack) is needed to quantify this effect.
-   Generation of higher and lower harmonics: different wave generation software should be used in one flume so that a comparison of the generated wave spectra may give the magnitude of resulting differences.

The results of the mentioned research showed a large dependency on the magnitude of the overtopping rate itself. Differences of a factor of about 5.0 for large overtopping rates and a factor of about 40.0 for low rates were observed.

3 | EXPERIMENTAL SET-UP

This chapter contains the laboratory set up and the testing procedure. The objective of the physical tests is to obtain accurate measurements which intend to give answers to the scope of the study.

3.1 ENVIRONMENTAL PARAMETERS

3.1.1 WAVE HEIGHT AND WAVE PERIOD

Wave overtopping formulae is usually based on the spectral wave height, H_{m0} which is expressed as $H_{m0} = 4(m_0)^{1/2}$. This wave height is the incident significant wave height at the toe of the structure.

In terms of wave period, different definitions can also be used for a wave spectrum such as the peak period, T_p, the average period, T_m, or the significant period $T_{1/3}$. However, wave overtopping formulae usually use the spectral period $T_{m-1,0}$, defined as $T_{m-1,0} = m_{-1}/m_0$.

In case of a uniform (single peaked) spectrum, EurOtop (2016) establishes a fixed relationship between the spectral average period and the spectral peak period. The conversion factor is $T_p=1.1T_{m-1,0}$.

Considering the aforementioned, results are based on spectral wave height and period.

3.1.2 WAVE STEEPNESS

Wave steepness gives information about the wave's history and characteristics. It is defined as the ratio of wave height to wavelength: $s_0 = H_{m0}/L_0$ (EurOtop 2016).

In this research, and based on CLASH and DMC (2003) experiments, the nominal wave steepness based on the spectral peak period is derived (see expression [3.1]).

$$s_{op} = \frac{2\pi H_{m0}}{gT_p^2}$$

[3.1]

A steepness of $s_{0p}=0.01$ usually indicates a typical swell sea and values of steepness of $s_{0p}=0.04$ to 0.06 are representative of typical wind sea (EurOtop 2016).

As discussed in section 3.1.1 , the spectral peak period, T_p, is 1.1 times the average spectral period, $T_{m-1,0}$. This implies that the wave steepness based on $T_{m-1,0}$ is 1.21 times larger than the nominal wave steepness, s_{op}.

3.1.3 BREAKER PARAMETER

The breaker parameter, also known as Iribarren number, is defined as:

$$\xi_{m-1,0} = \frac{tan\alpha}{\sqrt{s_{m-1,0}}}$$

[3.2]

where α is the slope of the structure and $s_{m-1,0}$ is the wave spectral steepness derived from the $T_{m-1,0}$. Wave conditions are measured near the structure.

From the breaker parameter, the different types of wave breaking can be derived. For $\xi_{m-1,0}$ > 2 non-breaking conditions are considered, although there may be some breaking.

3.1.4   WAVE SPECTRUM

To represent reality irregular waves are tested. Irregular waves are best described by using a variance density spectrum which provides a statistical description of the fluctuations of the wave height. Therefore, in this research irregular waves are generated according to JONSWAP-spectrum.

JONSWAP-spectrum is based on Pierson-Moskowitz spectrum and it is characterized by three shape parameters: γ , σ_a and σ_b. For a standard JONSWAP-spectrum, the mean values of these shape parameters are γ = 3.3, σ_a = 0.07 and σ_b = 0.09.

3.1.5   DURATION TEST/NUMBER OF WAVES

JONSWAP-spectrum can be considered fully developed after 1000 waves (Victor et al. 2012). Therefore, in order to have the complete range of wave conditions, every test is run the corresponding duration depending its wave conditions to ensure that it contains at least 1000 waves.

3.2 SCALING PROCESS

Scale modelling must guarantee similarity in behaviour between the prototype and the model. Three types of similarity can be achieved: geometric similarity, kinematical similarity and dynamic similarity. To fulfil dynamic similarity, scaling needs to follow three laws based on Froude number, Reynolds number and Weber number. However, the fulfilment of these three criteria is not possible to achieve for a same model and therefore, scale effects occur.

Further description regarding these similitude requirements and scaling laws can be found in Appendix A.

3.2.1   BEST SUITABLE SCALING LAW

Geometric scaling between prototype and model is fulfilled by applying a certain scaling factor to the structural dimensions. However, scaling all the processes that occur in a breakwater is not possible since intrinsic properties of the fluid such as viscosity, surface tension and air content cannot be scaled for the same model.

Since overtopping phenomenon can be mainly considered as free surface flow and to reproduce waves correctly, Froude scaling is applied. Thus, gravity is assumed dominant over viscosity.

3.2.2   SCALE EFFECTS

As a consequence of scaling based on Froude criterion, a disproportion of viscosity and surface tension occurs. This leads to the introduction of scale effects in the model. From the observation of physical model studies some generic rules has been derived in order to avoid scale effects (EurOtop 2016).

The effects of surface tension can be avoided by defining wave periods larger than T=0.35s and wave heights larger than Hs=5 cm. Besides, water depths in the model should be larger

than d=2cm. Otherwise, dampening of the waves might occur. In this research, these requirements are fulfilled avoiding scale effects due to surface tension.

Besides, the permeability of the core influences the armour layer stability. In case flow velocities and rock grading are small, viscous forces may be greater in the model resulting in scale effects. In order to avoid them, stone size of the core of the structure has to be scaled according to the velocities in the core rather than stone dimensions. Therefore, the core is not scaled geometrically. Instead, the approach proposed by Burcharth et al. (1999) is used. This method results in a diameter for the core material that ensures that Froude scaling law holds for a characteristic pore velocity. The pore velocity is defined as the average velocity of a most critical area in the core with respect to the pore velocity.

According to Wolters et al. (2014) for core material with a D_{n50} > 7mm and Re > 300, viscous scale effects can be neglected. In this research, this last requirement is not met since Re = 67 based on an average pore porosity of $8 \cdot 10^{-3}$ m/s obtained from Burcharth's method. This means that in the core, the flow is more laminar than in the prototype core since in reality the flow would be turbulent at least in a considerable part of the core and, thus, scale effects due to viscosity might be present. However, these scale effects present in the core have no influence on the measured overtopping since this process is governed mainly by the armour layer and its permeability rather than the permeability of the core. Therefore, the viscous forces associated with the armour layer are important to investigate. Usually, the armour layer is large enough to ensure fully turbulent flow since the characteristic dimension of the armour unit is sufficiently large. As described in Appendix B the Reynold number in this research is greater than 10^3 and therefore, viscous effects can be neglected.

3.3 MODEL'S CONFIGURATION

Due to the fact that this research is part of the preliminary study of the behaviour of a new armour unit, the hydraulic tests were not based in any prototype model that needs to be tested. Although the parameters used in the experiments were not scaled from a prototype present in reality, a scale of 1/50 is considered in order to be able to generalize the results to a real situation.

3.3.1   SET-UP AND DIMENSIONS

The set-up of the tested cross-section has been designed by considering the set-up of CLASH by Pearson et al. (2004) and the set-up of the first experiments done by DMC (2003) when studying standard Xbloc units.

3.3.1.1 Xbloc+ units

The small scale tests were performed using available Xbloc+ units (version 1) provided by Delta Marine Consultants. The model units were made also in a scale of 1:50 representing 7.2 ton of prototype units. They are made of plastic, in order to properly scale the roughness, with a mass density of 2.28 g/cm³ and a mass of 58.6 gr.

After the performance of the first series of tests, the shape of the armour units was modified by the introduction of an 8 mm hole in the centre of the unit. This modification is meant to release uplift pressures and make the armour units more stable. The modified block has a mass of 55.95 gr and corresponds to version 2 of the block.

The nominal diameter of the unit is calculated based on its design armour size as defined in equation [3.3]:

$$D_n = \left(\frac{W}{\rho_a}\right)^{1/3}$$

Therefore, the nominal diameter is 2.95 cm for the unit used initially (version 1) and 2.91 cm for the modified unit (version 2).
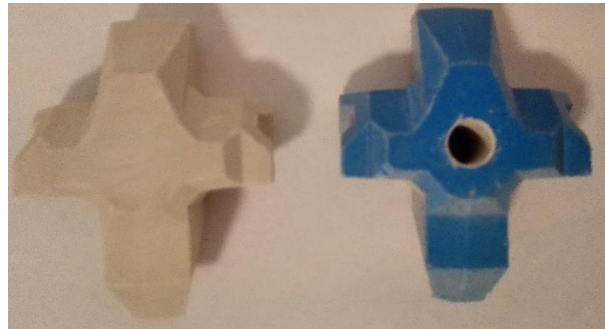
Figure 3.1 Version 1 (left) and version 2 (right) Xbloc+ armour unit

3.3.1.2 Breakwater cross-section and slope

The design cross-section consists of:

- Single layer Xbloc+ armour
- Under layer
- Core
- Stone protection at the toe
- Stone protection at the crest in order to make it stable. It has the same thickness as the armour layer.
- Glued rock protection at the rear slope of 5 cm width
- Block row enable stable position of the chute: three 20 m long blocks were available at the lab (W=4.8 cm; H=6.8 cm)

The thickness of the armour layer is assumed as 3.6 cm based on studies performed by Rada Mora (2017). The under layer has a thickness of 2.6 cm representing $2D_{n50}$ (see section 3.3.2 for more details).

Most of the studies of single layer concrete armour are performed with a slope of 1 in 1.5. However, in this research a slope of 1 in 4/3 is used since the previous tests done by DMC for Xbloc where set up with that slope. Besides, a 1 in 2 slope is also tested to analyse the influence of the slope angle on the overtopping. Test with a wooden plate are also performed in a 1:2 slope. Those tests also maintained the rock crest berm.

The rear slope is fixed as 1 in 4/3 and in order to ensure its stability it is protected with a layer of glued rock.

3.3.1.3 Crest freeboard

The crest freeboard of the design cross-section is chosen based on other small scale tests performed on single layer units. Within the CLASH project, a freeboard of 1.3 and 0.8 times the significant wave height were selected for the conducted tests in order to analyse small overtopping and higher overtopping rates. Hydraulic tests on Xbloc armour (DCM, 2003) were performed with a variable freeboard between 1.1 and 1.9 times the significant wave height.

Besides, Van der Meer (1987) stated that by using a freeboard of 1.33 times the significant wave height the wave overtopping is restricted to only 5 to 10%.

Based on all these experiments, the relative freeboard is fixed as 1.3 allowing some waves overtopping. In this research, tests are planned to be running until the failure of the armour layer which means higher wave heights than the design significant wave height are programmed. Therefore, large overtopping for these higher wave heights is expected.

3.3.1.4 Crest width

In order to design the width of the crest, the distance from where the overtopping is measure needs to be fixed. Based on previous experiments such as CLASH and the 2D hydraulic tests on Xbloc armour (DMC, 2003), and to enable further comparisons with those tests, the overtopping needs to be measured at a distance of 3Dn (or 8.9 cm) from the seaward edge of the structure. In order to place the chute in a stable position, a block of 5 cm width is placed leading to a wider crest of 13.9 cm.

3.3.1.5 Foreshore

A sloping foreshore of a uniform slope of 1:30 is placed. Besides practical reasons, this 1:30 slope is selected based on previous experiments performed on Xbloc armour by DMC (2003).

The sloping foreshore has a length of 8.7m starting from the bottom of the flume up to depth 0.29 m above the bottom.

Due to positioning of connection points for the foreshore in the flume the structure had to be shifted 0.3m backwards to facilitate observations of the slope from the side window. Therefore, there is a flat transition of 0.3 m from the foreshore to the structure. This horizontal section in front of the structure might have some little impact on the wave conditions at the toe of the structure.

3.3.1.6 Design significant wave height

The Hudson formula can be used to derived the design significant wave height:

$$H_s = \Delta \cdot \left(\frac{W}{\rho_a} \cdot K_d \cdot cot\alpha \right)^{1/3}$$

[3.4]

Where $\Delta = \frac{\rho_a}{\rho_w} - 1 = 1.28$ assuming an armour density of 2281 kg/m³. Previous studies done by Vos (2017) showed that the stability coefficient K_d should be lower than $K_d = 16$ (as fixed for Xbloc units). Therefore, for this research, K_d is fixed as 12.

Based on the aforementioned data, the design significant wave height is calculated for the two slopes planned to be tested. Table 3.1 summarize the results based on the tested unit.

	Xbloc+ v1	Xbloc+ v2
W (gr)	58.6	55.95
$H_{m0,d}$ (cm) – slope 3:4	9.52	9.32
$H_{m0,d}$ (cm) – slope 1:2	10.9	10.74

Table 3.1 Design significant wave height for a slope 3:4 and 1:2

3.3.1.7 Water depth

DMC (2003) designed their experimental tests on Xbloc armour using a water depth of 0.35m and 0.40m at the structure. Tests performed within CLASH framework considered a water depth at the structure of 2.5 and 3 times of the design wave height, although these tests were conducted without a foreshore.

Based on discussed researches and the limiting capacities of the wave flume, the water depth was fixed as 21 cm at the toe of the structure that means 2.2 times the design significant wave height. At the paddle, the water depth is 50 cm.

This water depth implies that the structure is placed in intermediate waters. Therefore, the bottom configuration will have some effect on the wave propagation. Shoaling is expected.

3.3.1.8 Dimension of the overtopping box

In order to design the overtopping box a preliminary prediction of the expected overtopping volume needs to be done. The overtopping rates can be estimated from the empirical formulae described in EurOtop. Therefore, equation [2.9] is used to estimate the overtopping discharge.

Since these experiments correspond to the first insight on the behaviour of the Xbloc+ concerning wave overtopping, there is no information about the roughness coefficient, γ_f. In order to be able to make a first estimation, a roughness coefficient of 0.45 is considered, therefore, assuming slightly higher overtopping rates as compared to the standard Xbloc units (γ_f=0.44).

The mean overtopping discharge is calculated for the design wave conditions. A chute width of 25 cm (only chute width available at the laboratory) and a test duration of 30 minutes is assumed in order to estimate the expected volume of overtopping water. Table 3.2 presents a summary of this calculation.

	Slope 3:4							
%Hm0,d	60%	80%	100%	110%	120%	130%	140%	150%
Hm0,toe (cm)	5.71	7.62	9.52	10.48	11.43	12.38	13.33	14.29
Rc (cm)	12.4	12.4	12.4	12.4	12.4	12.4	12.4	12.4
Rc/Hm0	2.2	1.6	1.3	1.2	1.1	1.0	0.9	0.9
g_f	0.45	0.45	0.45	0.45	0.45	0.45	0.45	0.45
q* (-)	1.85E-07	1.10E-05	1.06E-04	2.33E-04	4.41E-04	7.46E-04	1.16E-03	1.68E-03
q(l/m/s)	7.92E-06	7.25E-04	9.79E-03	2.48E-02	5.34E-02	1.02E-01	1.77E-01	2.85E-01
V(l) - chute 25 cm; duration = 30 min	0.004	0.33	4.41	11.15	24.03	45.83	79.53	128.13
	Slope 1:2							
%Hm0,d	60%	80%	100%	110%	120%	130%	140%	150%
Hm0,toe (cm)	6.44	8.59	10.74	11.81	12.88	13.96	15.03	16.10
Rc (cm)	14.00	14.00	14.00	14.00	14.00	14.00	14.00	14.00
Rc/Hm0	2.17	1.63	1.30	1.19	1.09	1.00	0.93	0.87
g_f	0.45	0.45	0.45	0.45	0.45	0.45	0.45	0.45
q* (-)	1.80E-07	1.08E-05	1.05E-04	2.30E-04	4.36E-04	7.39E-04	1.15E-03	1.67E-03
q(l/m/s)	9.22E-06	8.51E-04	1.16E-02	2.93E-02	6.32E-02	1.21E-01	2.10E-01	3.38E-01
V(l) - chute 25 cm; duration = 30 min	0.00	0.38	5.20	13.18	28.43	54.29	94.31	152.05

Table 3.2 Estimation mean overtopping discharge and overtopping volume

The previous estimations show a large variability of volume. In order to be able to measure also the large overtopping expected for the highest waves an overtopping box of a capacity of 8 litres is selected together with a submerged pump that pumps water from the little overtopping box to a set of larger boxes placed outside the flume.

The overtopping box is placed inside an outer box to protect it from the water running over the rear slope and ensure its stability.

More details of the overtopping measuring equipment can be found in section 3.4.5.

3.3.1.9 Toe protection

Standard toes have a height of 2-3Dn and a width of 3-5Dn (D'Angremond et al. 2008). Therefore, a height of 2Dn (5.9 cm) and a width of 3Dn (8.9cm), as it is selected in the experiments conducted within CLASH project, is chosen.

3.3.1.10   Sketch of the cross-section

Figure 3.2 and Figure 3.3 indicates some important dimensions of the cross-section design for a 3:4 and 1:2 angle slope configuration.
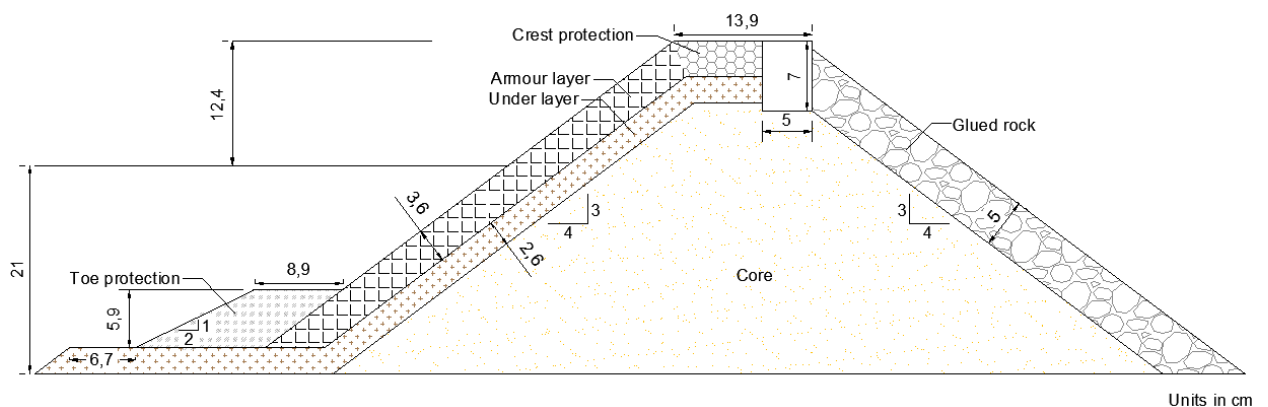
Figure 3.2 Cross-section design for structure with a 3:4 slope
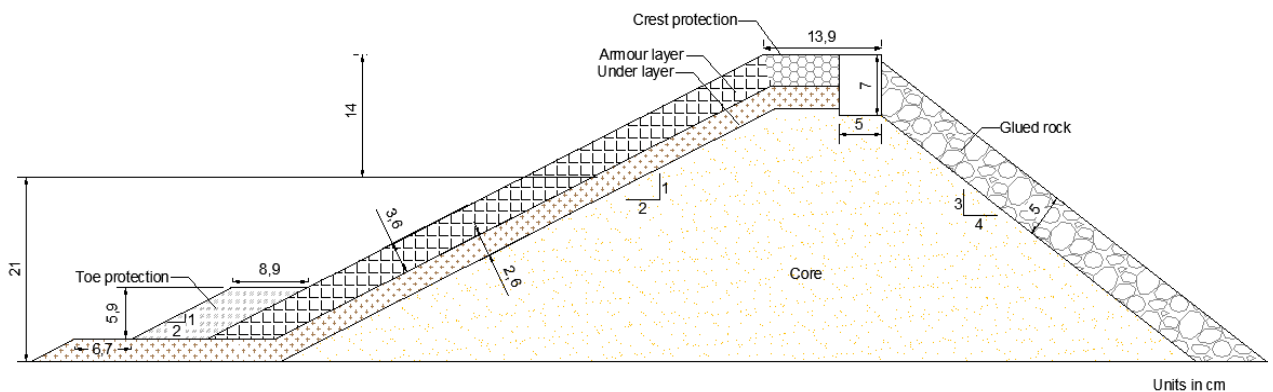
Figure 3.3 Cross-section design for structure with 1:2 slope

To perform the tests with the smooth 1:2 slope, the concrete units are replaced by a wooden plate of 60 x 73 x 1.8 cm. The underalyer is increased 1.8 cm so the wooden sheet rests on the slope. The crest and toe protection remain unchanged.

3.3.2 MATERIAL

3.3.2.1 Armour layer

The armour layer consists of Xbloc+ units placed as one layer system. The units were placed with a spacing of 1.1 times the width of the unit in order to provide the maximum interlocking to each row and be realistic regarding crane operations.

	Xbloc+ v1	Xbloc+ v2
W (gr)	58.6	55.95
D_n (cm)	2.95	2.91

Table 3.3 Characteristic values of the different Xbloc+ units tested

In general, for single armour layers, the thickness of the armour layer is equal to the D_n of the unit. However, due to the asymmetric shape of this unit, the layer thickness is greater than the Dn. Based on investigations performed by Rada Mora (2017) the layer thickness is 0.76 times the characteristic length of the unit which, for the unit used in this research, this results in a layer thickness of 3.6 cm.

3.3.2.2 Under layer

The underlayer material has a rock density of 2.65 g/cm^3. It has been constructed out of the available standard grading of 11.2 -16 mm. The grading is based on a D_{n50} 13 mm assuming one tenth of the armour layer design weight.

Filter stability is checked based on Terzaghi's theory. More details are provided in Appendix B.

3.3.2.3 Core material

As discussed in section 3.2.2, the core material is scaled according to Burcharth's approach which results in a required D_{n50} of 9.6 mm. Standard available grading of 8 – 11.2 mm has been selected for the core material.

3.3.2.4 Toe protection

The material of the toe has a rock density of 2.65 g/cm^3. The grading has been composed out of available standard grading of 16 – 22.4 mm based on toe stability. Stones are handpicked and weighed.

More information regarding the toe stability can be found in Appendix B.

3.3.2.5 Crest protection

The material of the crest has a rock density of 2.65 g/cm^3. The grading has been composed out of available standard grading of 16 – 22.4 mm. Stones are handpicked and weighed.

3.4 LABORATORY EQUIPMENT

3.4.1 WAVE FLUME

The experimental tests have been performed at the DMC 2D wave flume located in Utrecht. The flume has a length of 25m, a width of 0.6m and a height of side walls of 1.0m. The effective length of the flume is approximately 20m.

It allows water depths of between 40 and 75cm and it can be filled and emptied with pump valves which are placed on both sides of the flume.

Figure 3.4 Wave flume
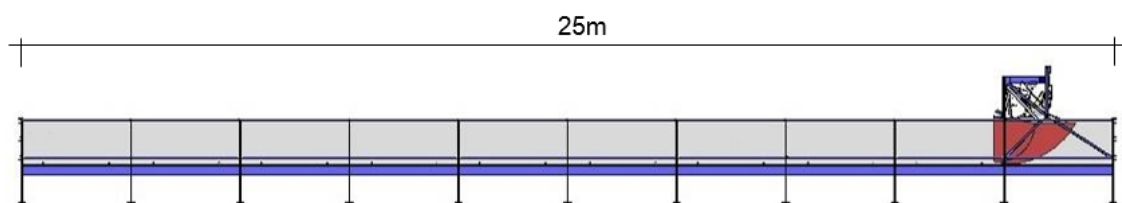
Figure 3.5 Longitudinal section of the wave flume

3.4.2 WAVE GENERATOR

The wave generation is induced by a fully absorbing piston type spectral wave maker provided by Edinburg Designs. The wave maker is able to measure the reflected wave and correct the paddle motion to absorb it.

The incoming and reflected wave fields are measured by resistance wave gauges. The reflection analysis is based on the method of Mansard and Funke (1980) for which the WaveLab3 software, created by Aalborg University, has been applied.

The wave generation of the piston is based on a steering file which contains all the wave information such as the significant wave height and peak period, the type of the spectrum, its characteristics and the duration. Time series of water level elevations have been recorded at a frequency of 32Hz.

The maximum wave height which can be generated is a significant wave height of $H_{m0}=20cm$.
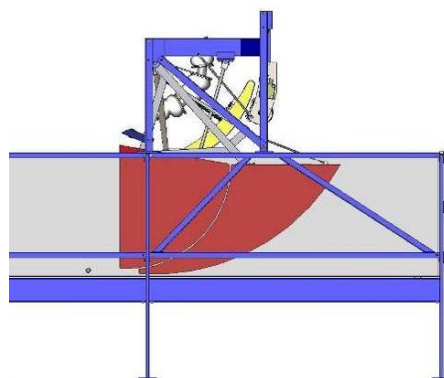
Figure 3.6 Piston type wave maker

3.4.3 WAVE GAUGES

Two sets of three wave gauges are placed in the flume; one at deep water and the other one near the structure. The array at deep water is located at 8m from the wave generator just before the foreshore structure. The position of the other array is based on a compromise: it needs to be placed as close as possible to the structure (as it is the place of interest) but a sufficient distance from the structure (as this will improve the quality of reflection analysis). Water depth should be constant for all 3 wave gauges. Thus, positioning them on the breakwater slope or on the toe is not an option. Besides, dissipation of wave energy by breaking while passing the gauge array will reduce the accuracy of the reflection analysis.

Based on these considerations, the gauge array near the structure is placed at 1m from the toe.

The spacing between the gauges is set based on the following conditions given by Mansard & Funke (1980):

$$X_{1-2} = \frac{L_p}{10}$$

$$\frac{L_p}{6} < X_{1-3} < \frac{L_p}{3} \ and \ X_{1-3} \neq \frac{L_p}{5} \ and \ X_{1-3} \neq \frac{3L_p}{10}$$

[3.5]

According to these recommendations, a distance of 0.3m between the first and second gauge and 0.7m between the first and third gauge is selected.

3.4.4 BALANCE AND PUMP

The overtopping water is collected behind the structure and pumped into larger buckets when needed. The volume of water is weighed using an electronic balance. The water is pumped using a submergible pump.

3.4.5 OVERTOPPING TANK AND CHUTE

The dimensions of the chute and overtopping tank are 25x66 cm and 60x50 cm respectively.

Due to limitation of time, the equipment available in the laboratory is used, although the capacity is lower than needed. Therefore, water is collected inside the overtopping tank in a bucket with a capacity of 8L and pumped it outside the flume into larger buckets when higher wave heights are tested.

Figure 3.7 Top and profile view of the overtopping box and chute

3.4.6 VIDEO CAMERAS

In order to record video footages and images of all the executed tests, two video cameras are installed. One is placed on the top of the flume focusing on the armour slope and another in a lateral of the flume recording the cross-section. Pictures of the slope are taken before and after each test.

3.5 MEASUREMING SYSTEM

3.5.1 FINAL MEASUREMENT SET-UP

The final measurement set-up used for the performed tests on a 3:4 slope structure is detailed in Figure 3.8 and Figure 3.9. The same measuring set-up is used for series performed in a 1:2 slope.
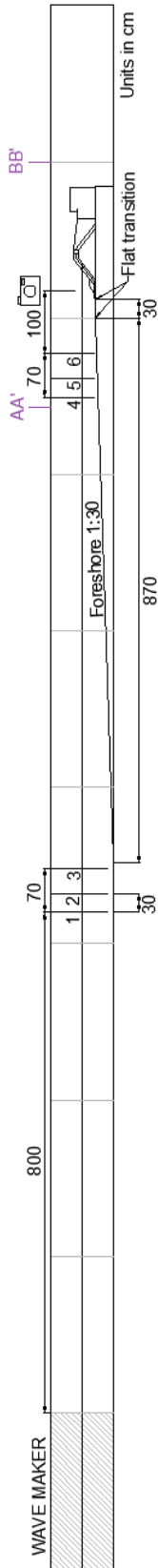
Figure 3.8 Final measuring set-up used for the performed tests
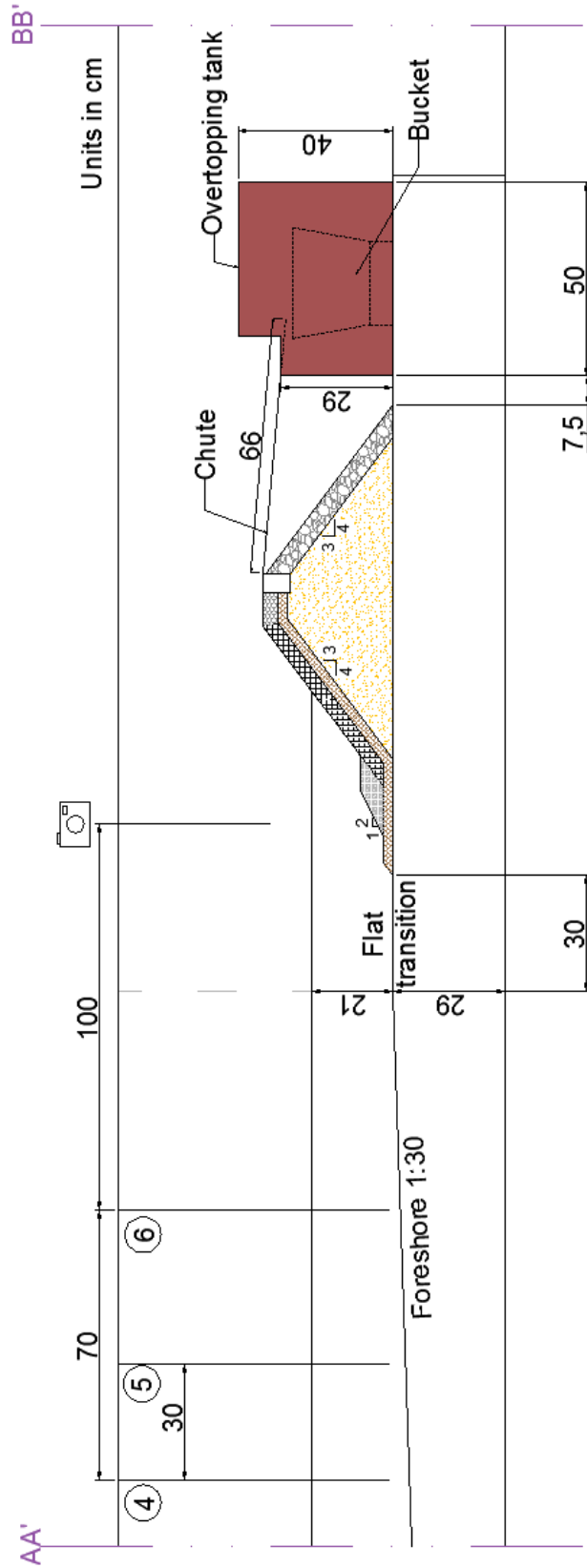
Figure 3.9 Close-up of the final measuring set-up (slope 3:4)

3.5.2   TEST PROCEDURE

The performance of a test requires three main phases: a preparation phase before the generation of waves, the actual performance of the test where waves are generated and data is collected and the final phase after the test where data is analysed.

- ▪ **Before the test**

Before starting testing, laboratory equipment need to be calibrated and checked. The input files with the corresponding wave characteristics are created and the overtopping buckets are weighted empty. The initial water level is also checked. Moreover, the pump is introduced in the overtopping box in case its use is required.

- ▪ **Wave generation**

During the performance of the test wave data is recorded by the wave gauges. The number of overtopping waves is counted manually and the water is pumped outside the flume (when needed).

In case of initiation of armour failure, the test is stopped before the filter layer is damaged.

- ▪ **After the test**

After the wave generation is completed (after 1000 waves), the wave generator is switched off. The recorded wave data is analysed and checked in order to confirm the reliability of the test. Finally, the overtopping water is weighted and the final water depth is measured. The overtopping water is returned to the flume in order to keep a constant water depth.

Pictures of the armour slope are taken before and after each test.

3.6 TEST PROGRAM

3.6.1   RANGE OF VARYING PARAMETERS

The main varying parameters are three: the wave height, the wave steepness and the slope angle. The ranges of these parameters are specified in next subsections.

3.6.1.1 Wave height

Wave height is increased in order to test until armour failure. Therefore, the following wave heights percentages are chosen:

- ▪ 60%$H_{m0,d}$
- ▪ 80%$H_{m0,d}$
- ▪ 100%$H_{m0,d}$
- ▪ 110%$H_{m0,d}$
- ▪ Increments of 10% until failure or flume limitations

The first two tests are needed to allow for compaction and initial settlements of the armour slope.

$H_{m0,d}$ corresponds to the design significant wave height described in Table 3.1.

3.6.1.2 Wave steepness

Based on the test program designed by DMC for the study of the Xbloc armour in 2003, the tested wave steepness groups are:

- $S_{op,1}$= 0.02
- $S_{op,2}$= 0.04
- $S_{op,3}$= 0.06

The first steepness is representative of swell waves.

3.6.1.3 Slope angle

In order to investigate the influence of the slope, two different slope angles are tested:

- $\tan\alpha_1 = 3:4$
- $\tan\alpha_2 = 1:2$

3.6.2 TEST PROGRAM

Based on the varying range presented above, the set of performed experiments for each slope is:

Series	Test	Type of unit	Slope	% H_{m0}, design	H_{m0}, design [m]	T_p [s]	S_{op}	R_c [m]	R_c/H_{m0}
1	a	v1	3/4	60%	0.0571	0.960	0.04	0.124	2.17
	b	v1	3/4	80%	0.0761	1.100	0.04	0.124	1.63
	c	v1	3/4	100%	0.0952	1.240	0.04	0.124	1.30
2	a	v2	3/4	60%	0.0563	1.343	0.02	0.124	2.20
	b	v2	3/4	80%	0.0750	1.551	0.02	0.124	1.65
	c	v2	3/4	100%	0.0938	1.734	0.02	0.124	1.32
	d	v2	3/4	110%	0.1032	1.818	0.02	0.124	1.20
	e	v2	3/4	120%	0.1125	1.899	0.02	0.124	1.10
	f	v2	3/4	130%	0.1219	1.977	0.02	0.124	1.02
	g	v2	3/4	140%	0.1313	2.051	0.02	0.124	0.94
3	a	v2	3/4	60%	0.0563	0.950	0.04	0.124	2.20
	b	v2	3/4	80%	0.0750	1.097	0.04	0.124	1.65
	c	v2	3/4	100%	0.0938	1.226	0.04	0.124	1.32
	d	v2	3/4	110%	0.1032	1.286	0.04	0.124	1.20
	e	v2	3/4	120%	0.1125	1.343	0.04	0.124	1.10
	f	v2	3/4	130%	0.1219	1.398	0.04	0.124	1.02
	g	v2	3/4	140%	0.1313	1.451	0.04	0.124	0.94
	h	v2	3/4	150%	0.1408	1.502	0.04	0.124	0.88
4	a	v2	3/4	60%	0.0563	0.775	0.06	0.124	2.20
	b	v2	3/4	80%	0.0750	0.895	0.06	0.124	1.65
	c	v2	3/4	100%	0.0938	1.001	0.06	0.124	1.32
	d	v2	3/4	110%	0.1032	1.050	0.06	0.124	1.20
	e	v2	3/4	120%	0.1125	1.097	0.06	0.124	1.10
	f	v2	3/4	130%	0.1219	1.141	0.06	0.124	1.02
	g	v2	3/4	140%	0.1313	1.184	0.06	0.124	0.94

Series	Test	Type of unit	Slope	% H_{m0}, design	H_{m0}, design [m]	T_p [s]	S_{op}	R_c [m]	R_c/H_{m0}
5	a	v2	1/2	60%	0.064	1.44	0.02	0.14	2.17
	b	v2	1/2	80%	0.086	1.66	0.02	0.14	1.63
	c	v2	1/2	100%	0.107	1.86	0.02	0.14	1.30
6	a	v2	1/2	60%	0.064	1.02	0.04	0.14	2.17
	b	v2	1/2	80%	0.086	1.17	0.04	0.14	1.63
	c	v2	1/2	100%	0.107	1.31	0.04	0.14	1.30
	d	v2	1/2	110%	0.118	1.38	0.04	0.14	1.19
	e	v2	1/2	120%	0.129	1.44	0.04	0.14	1.09
7	a	v2	1/2	66%	0.078	0.91	0.06	0.14	1.79
	b	v2	1/2	80%	0.086	0.96	0.06	0.14	1.63
	c	v2	1/2	100%	0.107	1.07	0.06	0.14	1.30
	d	v2	1/2	110%	0.118	1.12	0.06	0.14	1.19
	e	v2	1/2	120%	0.129	1.17	0.06	0.14	1.09
8	a	Smooth	1/2	60%	0.064	1.44	0.02	0.14	2.17
	b	Smooth	1/2	80%	0.086	1.66	0.02	0.14	1.63
	c	Smooth	1/2	100%	0.107	1.86	0.02	0.14	1.30
9	a	Smooth	1/2	60%	0.064	1.02	0.04	0.14	2.17
	b	Smooth	1/2	80%	0.086	1.17	0.04	0.14	1.63
	c	Smooth	1/2	100%	0.107	1.31	0.04	0.14	1.30
	d	Smooth	1/2	110%	0.118	1.38	0.04	0.14	1.19
	e	Smooth	1/2	120%	0.129	1.44	0.04	0.14	1.09
10	a	Smooth	1/2	66%	0.078	0.91	0.06	0.14	1.79
	b	Smooth	1/2	80%	0.086	0.96	0.06	0.14	1.63
	c	Smooth	1/2	100%	0.107	1.07	0.06	0.14	1.30
	d	Smooth	1/2	110%	0.118	1.12	0.06	0.14	1.19
	e	Smooth	1/2	120%	0.129	1.17	0.06	0.14	1.09

Table 3.4 Test program

4 | ANALYSIS OF OVERTOPPING PERFORMANCE OF XBLOC+ UNIT

This chapter presents and discusses the results of the experimental tests performed in the 2D wave flume. Firstly, a description of the measuring accuracy is given. Secondly, an overview of the measured wave conditions is presented. The next section analyses the test results on wave overtopping. Finally, a discussion about the different parameters playing a role on wave overtopping is conducted.

Note that the analysis does not include the series performed with the version 1 of Xbloc+ unit (without hole) since this study is focused on the latest version (version 2) of the block.

4.1 MEASURING ACCURACY

The measuring error is mainly induced by the measuring system and the accuracy of the used instruments. In this research, 6 parameters where measured: the overtopping volume, the duration of the test, the wave height and period, the water depth (and freeboard) and the angle of the slope.

4.1.1 OVERTOPPING VOLUME

The overtopping is measured with an electronic balance; its accuracy is ±1gr.

During the tests, it was observed that for higher wave heights some waves overtopped the structure at high velocities exceeding the bucket used for water collection. The water that remained in the overtopping tank was pumped and weighted. This extra overtopping volume is also included in the calculations in order to improve the accuracy of the results.

Based on the relationship between measured overtopping inside and outside the bucket the accuracy is estimated. An average error of ±1.3kg is defined, which implies a 2.5% error.

Furthermore, the lower overtopping discharges might be more affected by the crest as compared to higher overtopping rates. During the execution of the tests, it was observed that large surging waves (which generated high overtopping rates) were so energetic that passed over the structure with little interaction with the crest and therefore, less water might become infiltrated. Besides, the volume infiltrated through the crest has a greater impact in lower overtopping discharges since it corresponds to a higher percentage of the total overtopping volume.

4.1.2 DURATION OF THE TEST

The duration of the test is measured by the wave data recorder. The initiation and conclusion of the recording is done manually. However, in a wave record the time limits are easily noticeable and hence, the accuracy of this measurement is not compromised.

4.1.3 WATER DEPTH AND FREEBOARD

Wave overtopping is extremely sensitive to variations of the relative freeboard (Molines & Medina 2015b). The fact that the crest is protected by rocks might lead to some variations on the design freeboard since rocks are not uniform and can slightly move or settle. Besides, due to water depth fluctuations derived from overtopped water, the crest freeboard might vary.

In order to analyse the variations in the crest freeboard, the water depth was measured before and after each test. Table 4.1 shows the measured differences in water depth for the performed tests. In most of the tests there is no or little reduction of the water depth. The maximum decrease in water depth is observed under smooth conditions for the test performed with a 100% of the design wave height where a difference of 2.2 cm was measured between the beginning and the end of the test.

The reduction of the water depth during the performance of some tests implies an increase in the crest freeboard. To account for this effect, the crest freeboard R_c is corrected based on the measured difference in water depth as defined in equation [4.1]. The modified values of the crest freeboard are given in Table 4.1.

$$R_c^* = R_c + \frac{|d_{final} - d_{initial}|}{2}$$

[4.1]

By introducing this correction, the accuracy of the largest overtopping discharges is improved, reducing the scatter of the results.

	Series	Test	Δdepth [m]	Rc* [m]		Series	Test	Δdepth [m]	Rc* [m]
Slope 3:4	2	a	0	0.124	Slope 1:2	6	a	0	0.140
		b	0	0.124			b	0	0.140
		c	-0.002	0.125			c	0	0.140
		d	-0.006	0.127			d	0	0.140
		e	-0.009	0.129			e	0	0.140
		f	-0.012	0.13		7	a	0	0.140
		g	-0.02	0.134			b	0	0.140
	3	a	0	0.124			c	0	0.140
		b	0	0.124			d	0	0.140
		c	0	0.124			e	0	0.140
		d	0	0.124	Slope 1:2 smooth	8	a	-0.001	0.141
		e	0	0.124			b	-0.01	0.145
		f	-0.002	0.125			c	-0.022	0.151
		g	-0.005	0.127		9	a	0	0.140
		h	-0.007	0.128			b	-0.001	0.141
	4	a	0	0.124			c	-0.006	0.143
		b	0	0.124			d	-0.009	0.145
		c	0	0.124			e	-0.012	0.146
		d	0	0.124		10	a	0	0.140
		e	0	0.124			b	0	0.140
		f	0	0.124			c	-0.003	0.142
		g	0	0.124			d	-0.006	0.143
Slope 1:2	5	a	0	0.140			e	-0.007	0.144
		b	0	0.140					
		c	-0.002	0.141					

Table 4.1 Measured decrease in water depth and corrected crest freeboard

4.1.4 PARAMETERS DERIVED FROM REFLECTION ANALYSIS

The reflection analysis is done by WaveLab3 based on Mansard and Funke's method (1983). This method requires a simultaneous measurement of the waves at three positions in the flume. Parameters such as wave heights and wave periods are obtained from this reflection analysis based on the wave data recorded by the wave gauges. The accuracy of the wave gauges is around 0.01 – 0.1 mm.

By comparing signals from the wave gauges placed near the structure, a signal deviation of 0.3% is found. Therefore, the accuracy of the parameters derived from the spectral analysis such as wave height and period are assumed to be equal to the signal deviation.

4.1.1 SLOPE

The slope is built manually based on a drawing placed at the glass wall. The slope angle is measured after the structure is built resulting in a slope angle of 36° and 27° for a design slope of 3:4 and 1:2, respectively. The measured slope angle is used for the analysis and therefore, no error is considered for this parameter.

4.1.2 DIMENSIONLESS WAVE OVERTOPPING DISCHARGE

The measured dimensionless wave overtopping is the key parameter in this research. Its accuracy can be derived from the individual parameters described above.

The dimensionless wave overtopping discharge is calculated from the measured overtopping volume, the duration of the test and the width of the chute. In order to make the parameter dimensionless, it is divided by $\sqrt{gH_{m0}^3}$. The inaccuracy in the determination of these parameters induce errors in the measured dimensionless wave overtopping.

Based on the errors defined above, the overall error of the measured dimensionless wave overtopping is calculated as 1.5%. This error is insignificant compared to errors induced by model effects (see section 2.2.2), especially when small quantities of water are measured.

4.2 MEASURED WAVE CONDITIONS

Prior to the analysis of the results, an analysis of the measured wave conditions is performed. Due to shoaling and wave breaking caused by depth limited conditions, the wave height near the structure differs from the wave height at deep water. Moreover, the wave is partly reflected when reaching the structure, thus influencing the measured incident wave. In order to optimize the desired wave conditions, a previous calibration without the structure is performed.

Appendix D presents the measured wave conditions at deep waters and near the structure for each individual test series.

4.2.1 VARIATION IN WAVE STEEPNESSES

Wave steepness is maintained constant throughout the duration of each test series. The measured nominal wave steepness near the structure is presented in Figure 4.1, Figure 4.2 and Figure 4.3, plotted against the nominal wave steepness introduced in the wave maker.
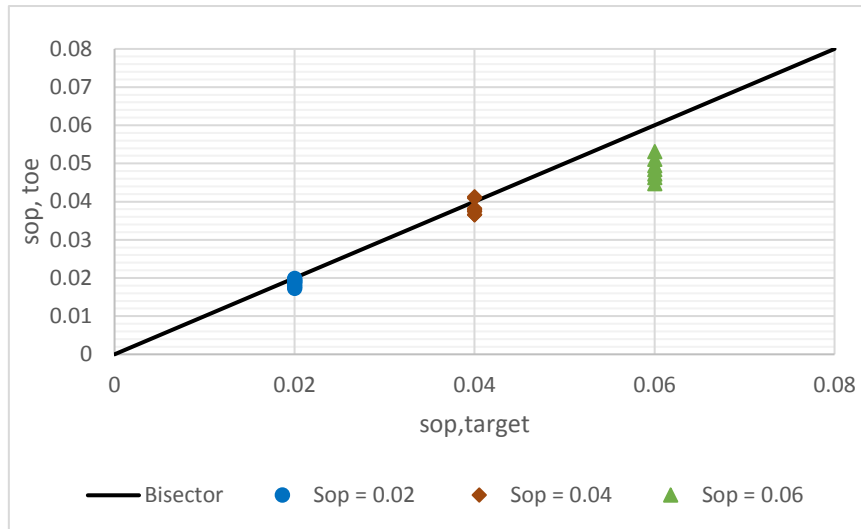
Figure 4.1 Measured wave steepness for tests performed on a 3:4 slope
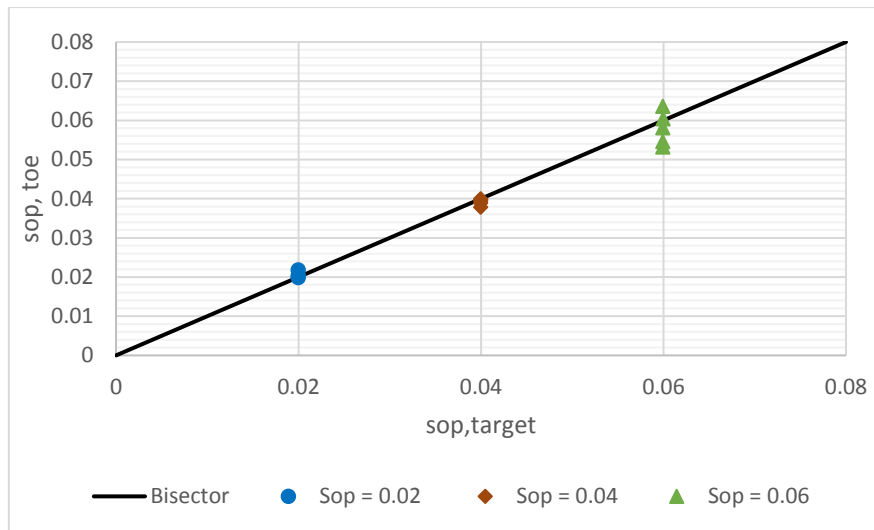
Figure 4.2 Measured wave steepness for tests performed on a 1:2 slope
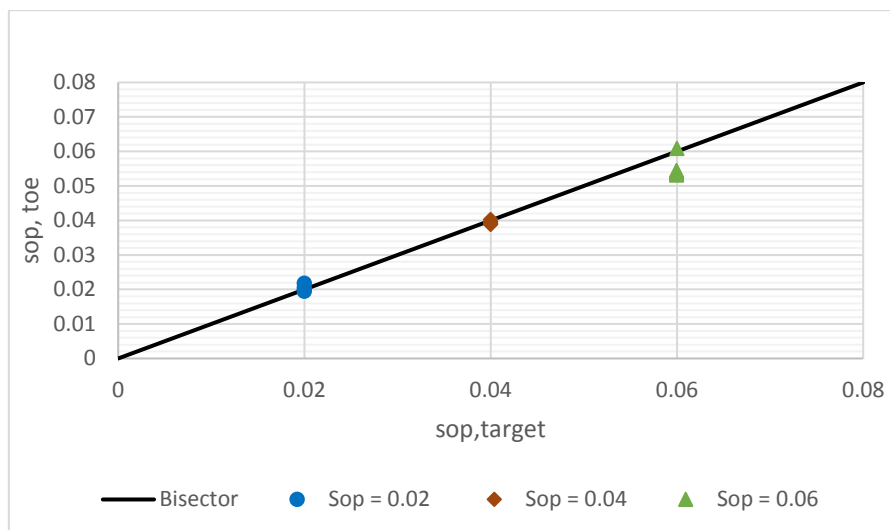
Figure 4.3 Measured wave steepness for tests performed on a smooth 1:2 slope

It can be observed that the target wave steepness near the structure is achieved fairly well in most of the tests. However, the difference between measured and target wave steepness is more noticeable for the higher wave steepness. This is due to the loss of energy occurring when waves break. The larger the wave height and smaller the period, the larger the energy dissipation due to breaking and hence, the larger the difference between target and measured conditions. It is also important to bear in mind that, near the structure, uncertainties of the reflection analysis for breaking wave conditions (non-linear waves) might also be affecting the calculation of the real incident wave heights.

Besides, the 6% wave steepness in the smooth 1:2 slope presents slightly lower wave steepness with respect to the same tests performed in 1:2 armoured slope, although the same steering file, calibrated without the structure, is used. In Figure 4.4 the measured reflection coefficients for the three tests series are shown in relation to the Iribarren number. It can be seen that the impermeable wooden plate leads to higher reflection coefficients than the armoured slopes. This might cause the differences in the measured wave steepness. Moreover, limitations on the absorption control might also have an influence.
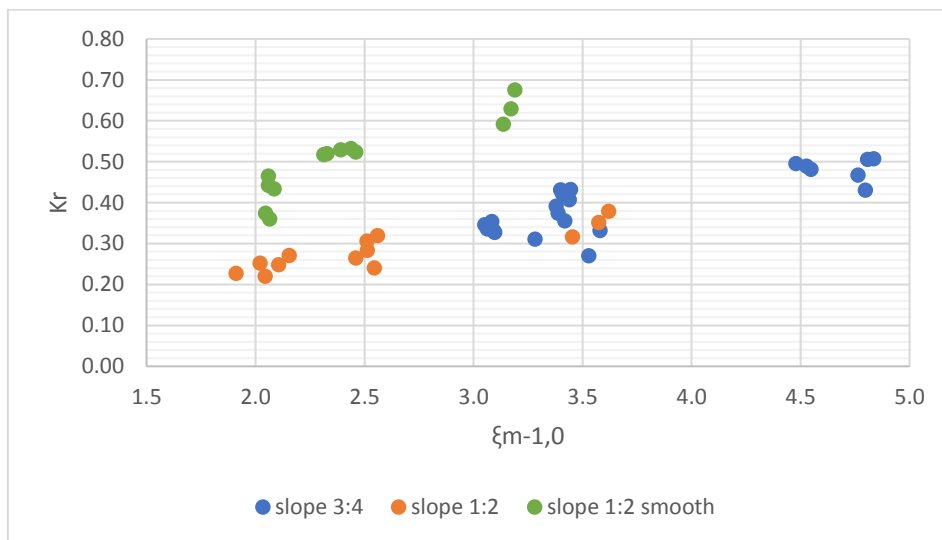
Figure 4.4 Measured reflected coefficient

The wave breaking can be noticed in the wave height exceedance curves. In Figure 4.5, the wave distribution of test 4f corresponding to a 6% wave steepness and a target wave height of 12.19 cm (130% of design Hm0) on 3:4 slope is shown. It can be seen that for greater wave heights the wave distribution is not following a Rayleigh distribution. This deviation of the wave distribution is caused by wave breaking. Besides, the wave spectrum, presented in Figure 4.6, shows larger differences between the measured and target spectrum for higher frequencies (smaller periods) as a result of energy losses.
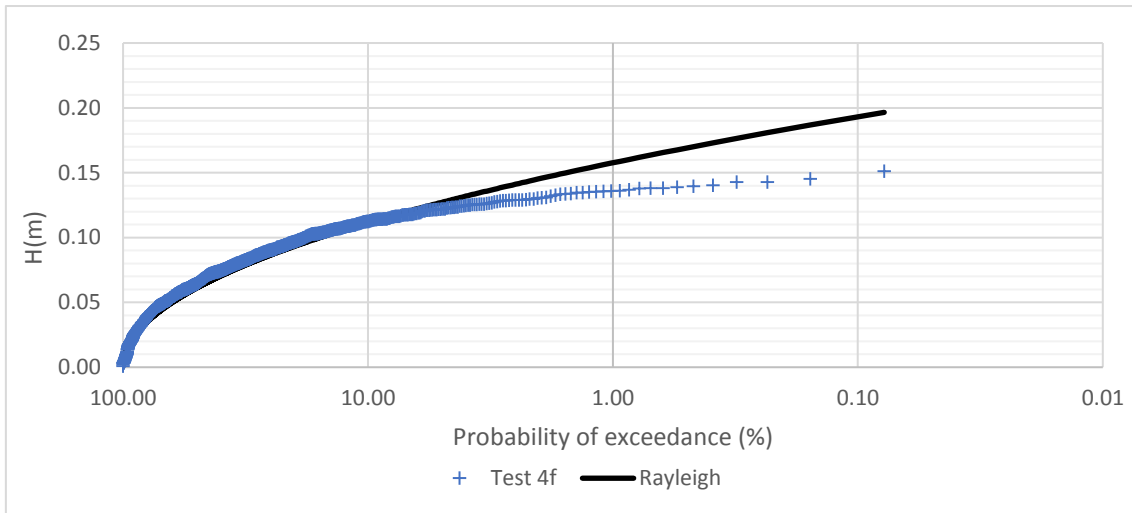
Figure 4.5 Wave distribution of Test 4f (130%Hm0, s=0.06, 3:4 slope)
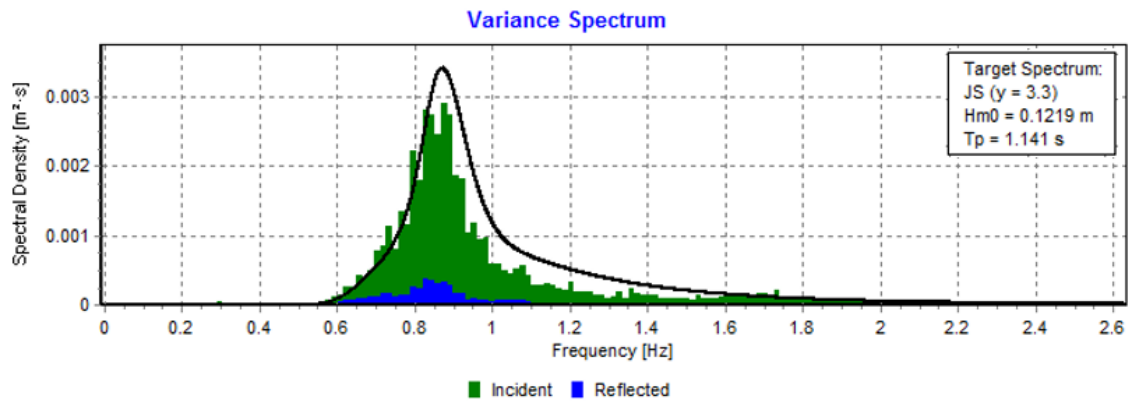
Figure 4.6 Wave spectrum of Test 4f (130%Hm0, s=0.06, 3:4 slope)

4.2.1 VARIATIONS IN WAVE HEIGHT

During the performance of the test, the wave height was measured at deep water and near the structure. Figure 4.7 presents the relationship between the spectral significant wave height, H_{m0}, at those two locations. Wave breaking caused by depth limited conditions makes the measured wave height decreases. This can be observed in Figure 4.7 where it is clearly noticed that wave height near the structure is lower than in deep water.
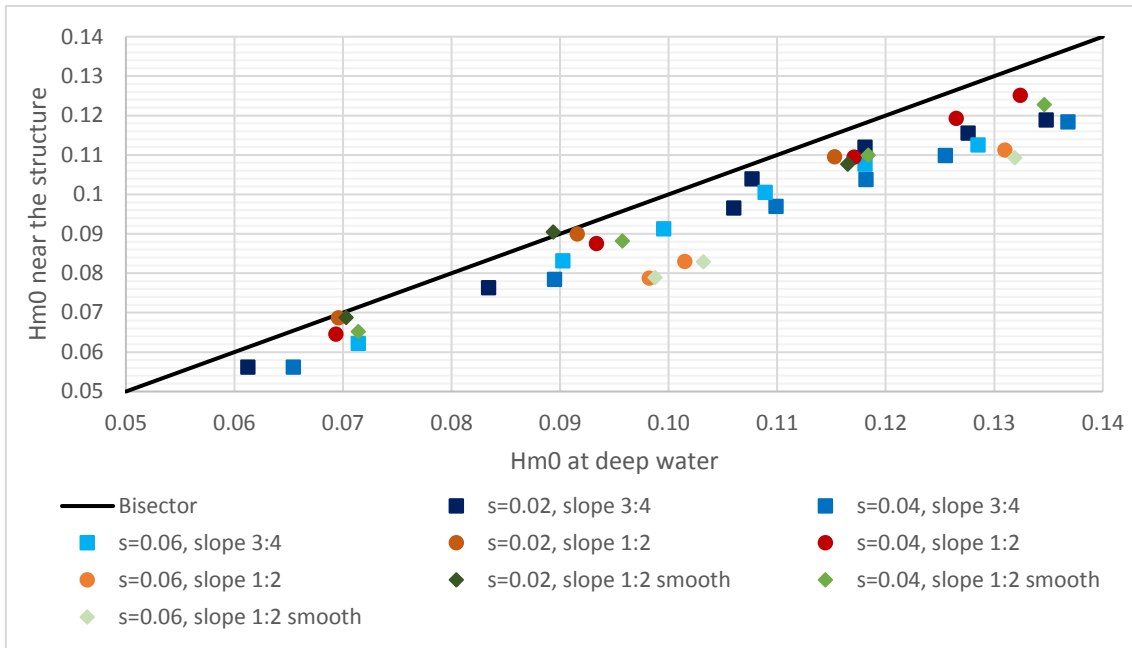
Figure 4.7 Relationship between measured Hm0 at deep water and near the structure

Due to wave breaking, the spectral significant wave height, H_{m0}, also varies from the statistical significant wave height $H_{1/3}$. Figure 4.8 describes the relationship between these two measured wave height near the structure. Slightly greater deviations are noticed for the highest measured wave heights as wave breaking process increases.
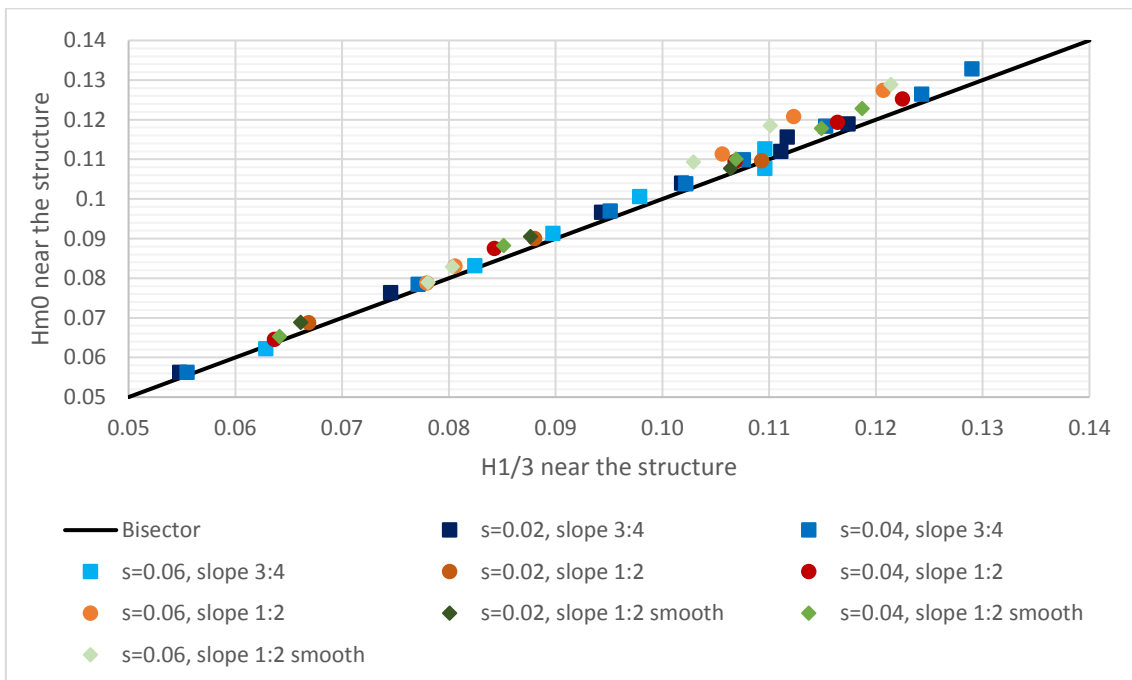
Figure 4.8 Relationship between measured Hm0 and H1/3 near the structure

4.2.2 VARIATIONS IN WAVE PERIOD

In this experimental research, the wave period is estimated from spectral analysis performed with WaveLab3. Figure 4.9 describes the relationship between wave periods measured at deep water (d=0.5m) and near the structure (d=0.21m) which represents intermediate waters. On one hand, it is observed that the peak wave period tends to be slightly higher near the structure in most of the series. On the other hand, less scatter is obtained for the average spectral wave period although deviations increase for swell conditions.
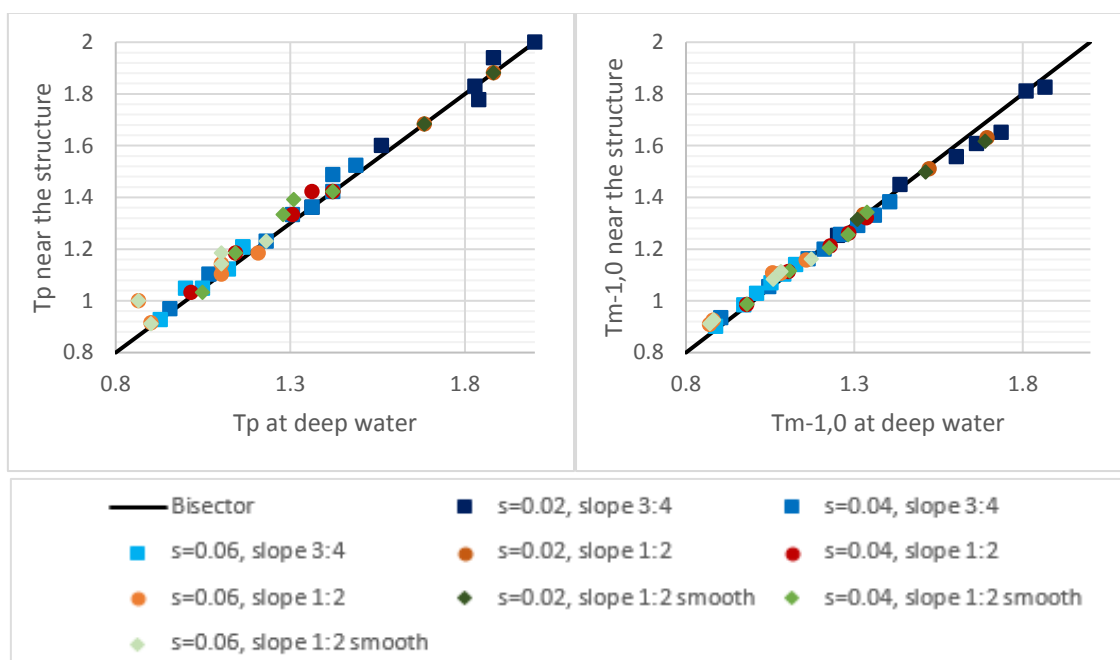
Figure 4.9 Relationship between wave periods at deep water and near the structure

EurOtop Manual (2016) describes a relationship between the spectral peak wave period (T_p) and the spectral average wave period ($T_{m-1,0}$) for a single peaked spectrum with Rayleigh distribution in deep water where T_p is assumed 1.1 times $T_{m-1,0}$. However, in shallow water this relationship is not always valid as the spectrum in shallow water deviates from the spectrum in deep water due to wave breaking (Verhagen et al. 2007). Figure 4.10 shows the relationship between these two spectral wave periods in deep waters and near the structure. Test results show that this relationship is mostly maintained in deep water. However, near the structure a slight deviation is found due to the fact that the structure is placed at intermediate waters and, thus, Rayleigh distribution is no longer followed (as Figure 4.5 shows) and wave breaking occurs.
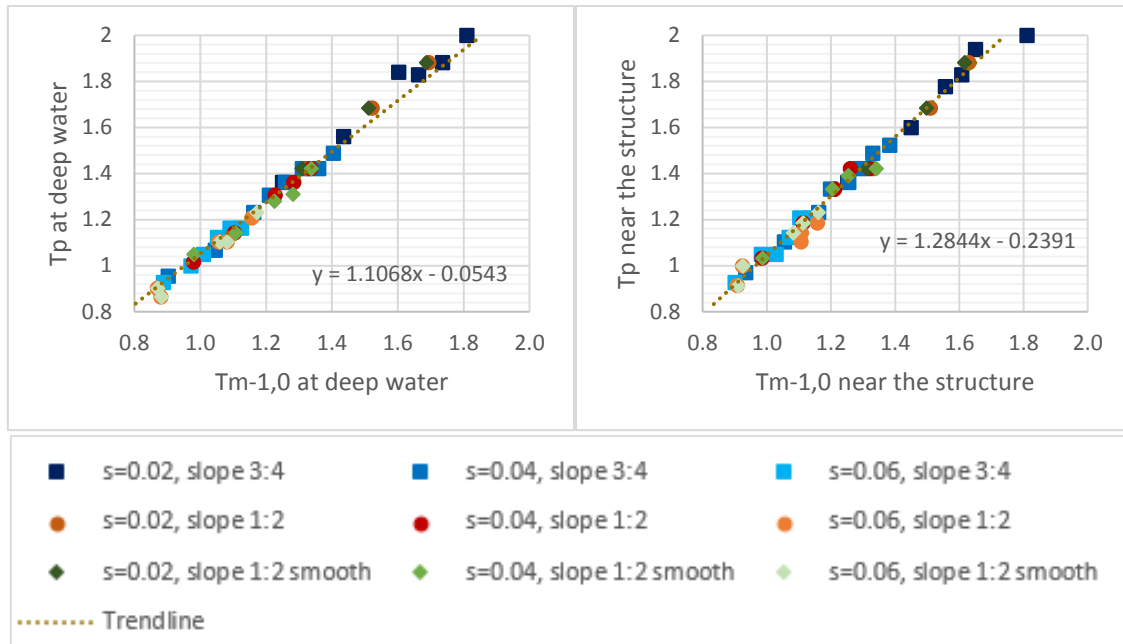
Figure 4.10 Relationship between Tp and Tm-1,0 both at deep water and near the structure

4.2.3 INFLUENCE OF THE FORESHORE ON WAVE BREAKING CONDITIONS

The wave breaking type, as defined by the average spectral breaking parameter $\xi_{m-1,0}$ (see equation [3.2]), depends on the combination of structure slope and wave steepness. EurOtop (2016) considers waves not to be breaking (surging waves) for $\xi_{m-1,0} > {\sim}2$. As it is shown in Figure 4.4, the breaker parameters derived from the measured conditions are higher than 2 which imply that tests are performed under non-breaking conditions. However, during the laboratory tests, collapsing and plunging waves were observed in the laboratory.

The foreshore used in the model induces wave shoaling and thus, an increase in height. As the wave advances, breaking occurs either due to the structure or depth limitations. Severe breaking is not observed since the foreshore is placed at intermediate water and hence, the target wave steepness can be obtained in most of the tests.

Miche breaking limit (1944) indicates that wave breaking occurs when H_s is greater than 0.4-0.5 times the water depth. This limit is exceeded in most of the series after the 100% design wave height is tested. Furthermore, during tests of 6% wave steepness some whitecappping is observed due to wave steepness limitation.

4.2.4 RANGE OF MEASURED WAVE CONDITIONS

A summary of the wave conditions measured near the structure during the performance of the test (with the structure) is presented in Table 4.2.

	Test series	Tp (s)	Hm0 (cm)	Sop	ξm-1,0
3:4 slope	2	1.36 – 2.07	5.62 – 11.89	0.018 – 0.020	4.86 – 5.01
	3	0.97 – 1.52	5.62 – 13.28	0.037 – 0.046	3.52 – 3.63
	4	0.78 – 1.21	4.26 – 11.26	0.045 – 0.053	3.62 – 3.13
1:2 slope	5	1.42 – 1.88	6.88 – 10.96	0.025 – 0.026	3.22 – 3.26
	6	1.03 – 1.42	6.46 – 12.52	0.039 – 0.040	2.36 – 2.46
	7	0.91 – 1.19	7.88 – 12.74	0.053 – 0.063	1.97 – 2.02
Smooth 1:2 slope	8	1.42 – 1.88	6.88 – 10.77	0.019 – 0.022	3.18 – 3.28
	9	1.03 – 1.42	6.53 – 12.28	0.039 – 0.040	2.19 – 2.44
	10	0.91 – 1.23	7.89 – 12.89	0.053 – 0.061	1.95 – 1.97

Table 4.2 Summary of measured wave conditions near the structure

4.3 MEASURED WAVE OVERTOPPING

The overtopping volume and the number of overtopping waves are measured for each test series. The mean overtopping rate is then calculated based on the measured overtopping volume and the duration of the test. Appendix E presents all the details of the measured wave overtopping for each specific test.

4.3.1 DEFINITION OF MEASURED WAVE OVERTOPPING

Wave overtopping can take different definitions as it is shown in Figure 4.11. This research is based on the wave overtopping measured at 3Dn from the seaward edge of the crest. Therefore, the discharge is influenced by the crest berm. The crest berm is made by rock and thus, water infiltration occurs through the crest (Q3). Besides, water might also go through the armour layer (Q2) due to its permeability.
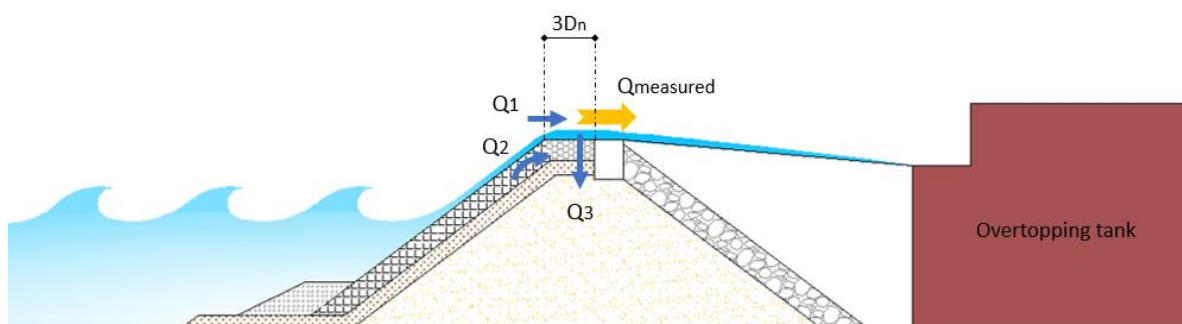
Figure 4.11 Definition of measured overtopping

4.3.2 DIMENSIONLESS WAVE OVERTOPPING

In general, mean overtopping discharge is displayed as dimensionless overtopping rate so a comparison of wave overtopping for different conditions can be made. In Figure 4.12, the experimental data is plotted based on an exponential distribution between the dimensionless overtopping discharge $[q/(gH_{m0}^3)^{0.5}]$ and the dimensionless freeboard (R_c*/H_{m0}). H_{m0} corresponds to the wave height measured near the structure.

No overtopping occurred during test 3a, 4a, 4b, 6a, 7a and 7b (see Table 3.4 for details of each run). Note that these runs are not included in the graphs.
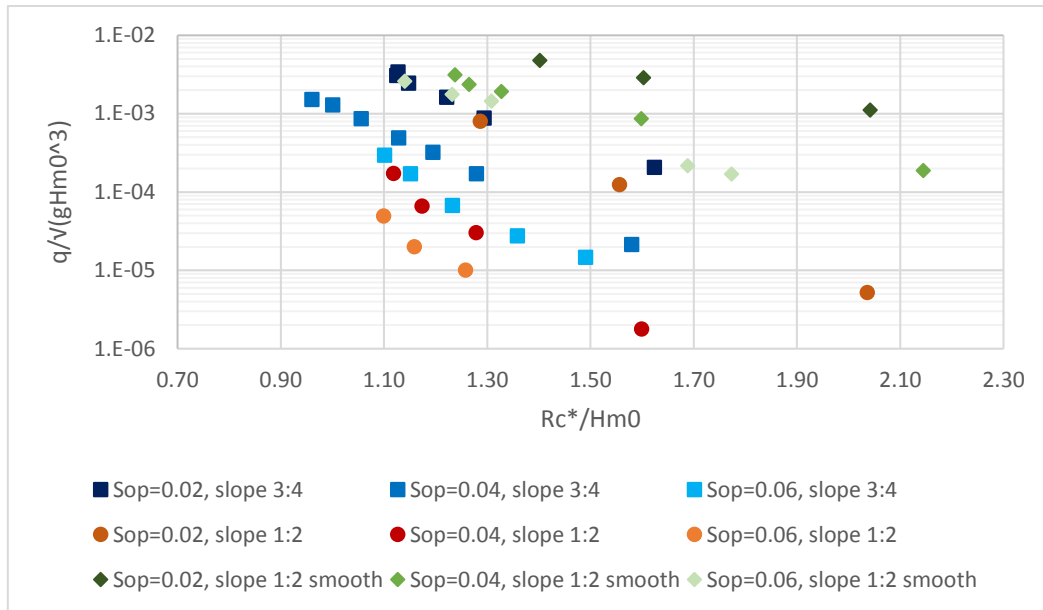
Figure 4.12 Measured dimensionless mean overtopping discharge

Figure 4.12 shows that all series follow the same trend: as wave height increases (relative freeboard decreases), dimensionless overtopping discharge increases as well. However, a high degree of scatter among the different tested conditions is noticed.

As expected, it is observed that smooth conditions give greater overtopping rates as compared with rough armoured slopes. Moreover, steeper slopes (3:4) induce higher overtopping rates when compared with gentler slopes such as 1:2. This is due to the fact that mild slopes are larger and therefore, there is more room for dissipation, which results in less wave overtopping.

Furthermore, it is observed that the wave steepness influences wave overtopping. For longer waves a higher amount of overtopping is obtained while a higher wave steepness (shorter waves) leads to reduced overtopping. For example, overtopping rates obtained in series 2 (swell conditions in 3:4 slope) are 20 times higher (in average) with respect to series 4 (6% wave steepness in 3:4 slope).

Further analyses of the different parameters influencing wave overtopping are provided in section 4.4.

4.3.3   PERCENTAGE OF OVERTOPPING WAVES

The number of overtopping waves (N_{ow}) is determined visually at the laboratory for each performed test. The total number of waves (N_w) is calculated from the time series analyses obtained from WaveLab3.

Figure 4.13 shows the measured percentage of overtopping waves with respect to the dimensionless freeboard and is expressed as $A_c D_n / H_{m0}^2$ and therefore, taking into account the nominal diameter, D_n. In this research, the armour freeboard (A_c) is equal to crest freeboard (R_c).
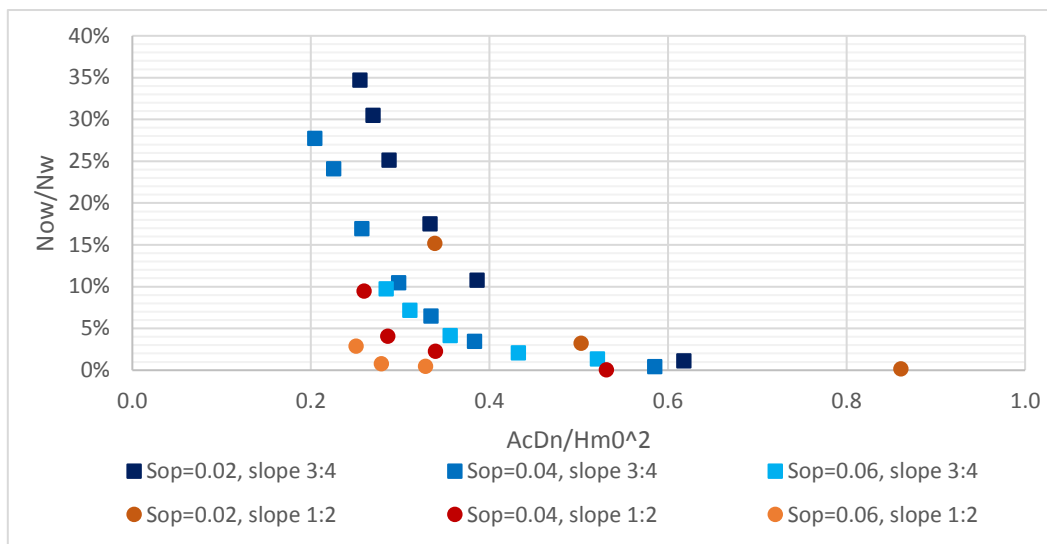
Figure 4.13 Percentage of overtopping as a function of dimensionless crest freeboard

From Figure 4.13 it becomes clear that the percentage of wave overtopping increases as wave height increases or, in other words, a reduction of the relative freeboard results in a higher percentage of overtopping waves. It is also noticed that, the longer the wave period, the higher the number of overtopping waves. This can be explained based on wave energy. The longer the wave period, more energetic the waves are and hence, they are able to produce more overtopping discharge.

Furthermore, the test results show that a 3:4 slope induces a higher number of overtopping waves as compared with a 1:2 slope. As mentioned before, this is due to the fact that the 1:2 slope is larger as compared with the 3:4 slope and thus, there is more space for dissipation and less waves are able to overtop the structure.

4.4 PARAMETERS INFLUENCING WAVE OVERTOPPING

Wave overtopping is a complex phenomenon that is sensitive to many different parameters related to breakwater geometry, construction materials and hydraulic data. To understand the performance of the Xbloc+ armour unit on wave overtopping, the influence of the main factors on overtopping rates is analysed. Some of these main parameters are listed below:

- Geometrical parameters: crest freeboard, crest berm width, *slope angle of the structure*.
- Construction material parameters: *porosity*, *roughness*, crest configuration, armour layer configuration.
- Hydraulic parameters: *wave height, wave period*, angle of wave attack, *wave steepness,* water level.

In this research, tests are performed under perpendicular wave attack, a rock crest width of 3Dn and a constant armour porosity and water level. Therefore, only the influence of some of the aforementioned parameters can be analysed (which are remarked in italics).

4.4.1   INFLUENCE OF WAVE HEIGHT

Wave overtopping is considered to increase almost exponentially with the wave height. This trend is confirmed by the present model tests as Figure 4.14 shows. Besides, similar trendlines are observed regardless of the wave steepness and slope angle.

It should be noted that within the same series the wave period changes due to the fixed wave steepness.
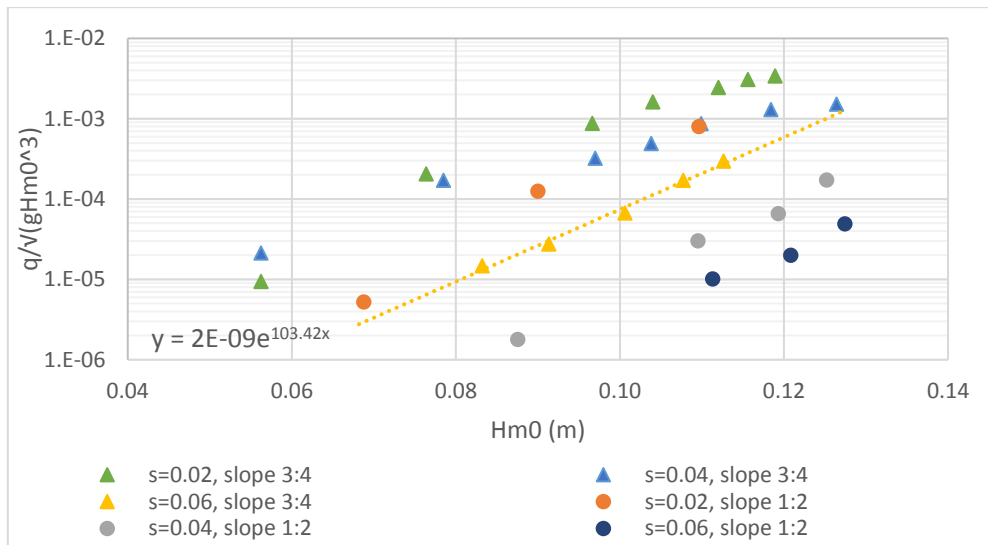
Figure 4.14 Influence of wave height on wave overtopping

For instance, in series 4 (Sop=0.06, slope 3:4) the wave overtopping discharge increases by e^{100Hm0} approximately.

4.4.2 INFLUENCE OF WAVE PERIOD

The wave period is not included directly in wave overtopping formulae defined for armoured structures. However, the tests results depicted in Figure 4.15 show that wave overtopping increases almost exponentially with wave period.

It should be noted that for the tests performed within the same series the wave heights vary in order to keep the wave steepness constant.
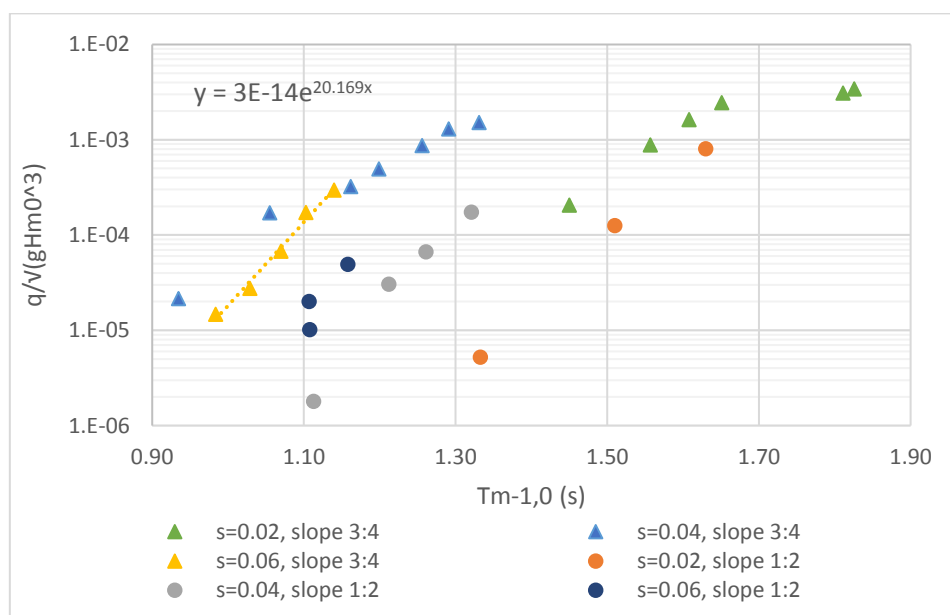
Figure 4.15 Influence of wave period on wave overtopping

For instance, in series 4 (S_{op}=0.06, slope 3:4) the wave overtopping discharge increases by $e^{20T_{m-1,0}}$ approximately. It becomes clear that, although the wave period has a lower influence on wave overtopping than the wave height, it has also an effect on wave overtopping. Consequently, empirical formulae for breakwaters might not consider properly the influence of the wave period in wave overtopping.

4.4.3 INFLUENCE OF WAVE STEEPNESS

The influence of the wave steepness is shown in Figure 4.16 and Figure 4.17 for a 3:4 slope and 1:2 slope respectively. Data from tests is depicted by dividing it based on the wave height measurements near the structure. Series are identified by the percentage of design wave height that corresponds to the measured wave heights near the structure. Bear in mind that due to the influence of the foreshore wave heights near the structure differ from the target value (as it is explained in section 4.2) and hence, the series are formed with data with slightly different wave height. Table 4.3 and Table 4.4 indicates the percentage of design wave height that each data point represents.
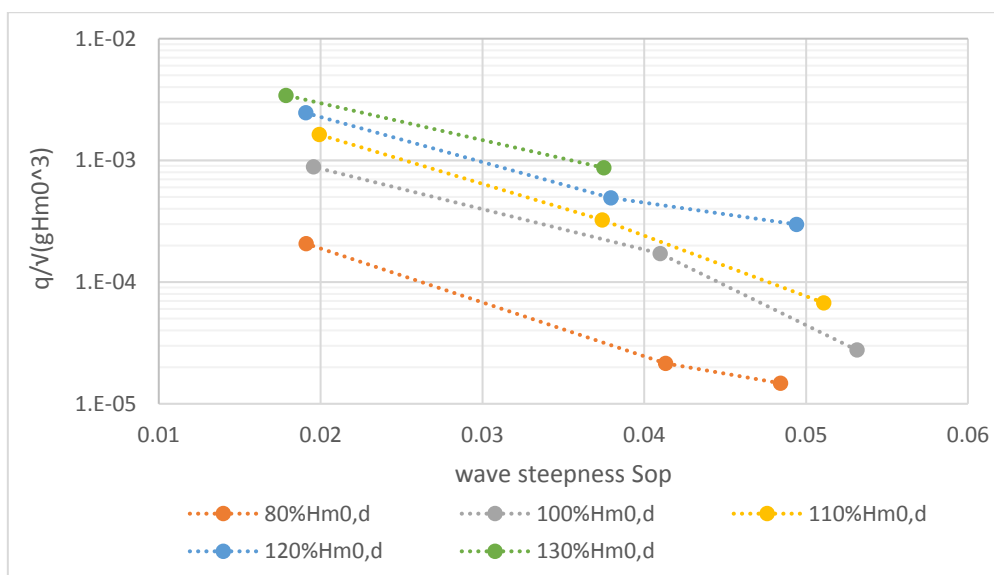
Figure 4.16 Influence of wave steepness on wave overtopping for a 3:4 slope

		Wave steepness S_{op}		
		0.02	*0.04*	*0.06*
Series	*80%Hm0,d*	81%	84%	89%
	100%Hm0,d	103%	103%	97%
	110%Hm0,d	111%	111%	107%
	120%Hm0,d	119%	117%	120%
	130%Hm0,d	127%	126%	-

Table 4.3 Percentage of design Hm0 that corresponds to each wave steepness for a slope 3:4.
Design Hm0 = 0.0938m
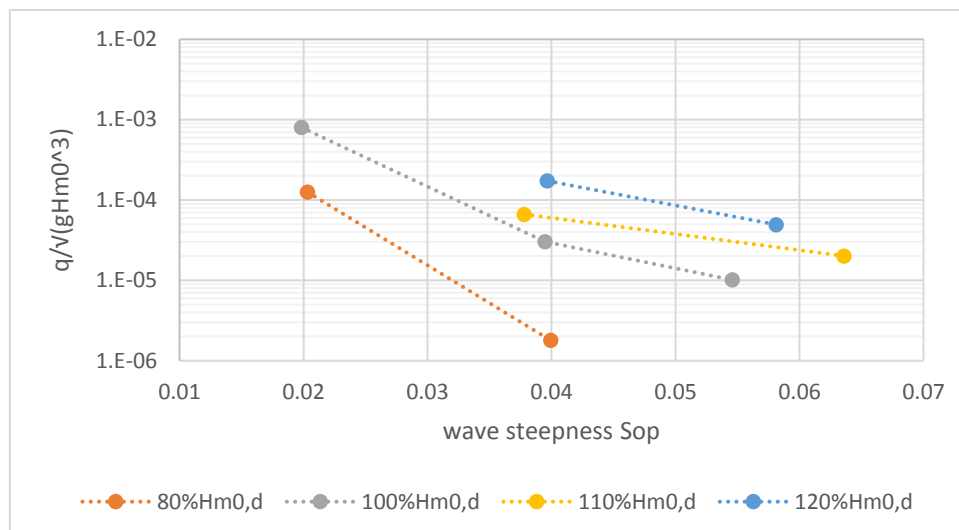
Figure 4.17 Influence of wave steepness on wave overtopping for a slope 1:2

		Wave steepness S_{op}		
		0.02	*0.04*	*0.06*
Series	*80%Hm0,d*	84%	82%	-
	100%Hm0,d	102%	102%	104%
	110%Hm0,d	-	111%	113%
	120%Hm0,d	-	117%	119%

Table 4.4 Percentage of design Hm0 that corresponds to each wave steepness for a slope 1:2.
Design Hm0 = 0.107m

Figure 4.16 and Figure 4.17 clearly show a tendency for increasing overtopping rates by a decrease in wave steepness. Note that the differences in the trendlines are induced by the differences in wave height. For instance, the series that describes the 100% of the design wave height is formed by data points that represent 101%, 102% and 96% of the design H_{m0} for a 0.02, 0.04 and 0.06 wave steepness respectively.

Moreover, as wave height exceeds the design wave height (which corresponds to $H_{m0,d}$=0.0938m and $H_{m0,d}$=0.107m for 3/4 slope and 1/2 slope, respectively) overtopping discharges increases with a lower rate compared to smaller wave heights. For instance, in a 3/4 slope and for a 2% wave steepness, the 101%$H_{m0,d}$ gives 4.3 times more overtopping discharge compared to the measured discharge for 81%$H_{m0,d}$ (H_{m0}=0.0764m) and the overtopping discharge for 119%$H_{m0,d}$ (H_{m0}=0.112m) is only 2.8 times higher than the discharge relative to the design wave height. This reduction in the increase of the overtopping rates might be a result of the decrease of the water level due to the overtopped water which leads to an increase of the crest freeboard.

4.4.4 INFLUENCE OF SLOPE ANGLE

Wave overtopping is also affected by the slope angle of the structure. The gentler the slope, the larger it needs to be in order to maintain the same crest height. This increase in length provides more space for wave dissipation. Waves can run up and down along a larger surface and therefore, more energy can be dissipated.

Test results, depicted in Figure 4.18, shows slightly higher overtopping rates for steeper slopes, confirming the previous statement. It is also noticed that in swell conditions the slope angle has almost no influence. As observed during the physical tests, wave steepness of 2%

is characterized by large surging waves. Those waves have a thick water layer running up and down the slope and therefore, the incoming waves did not feel the top layer with the same "intensity" as waves with a 4% and 6% wave steepness did.

In contrast, the increase in wave overtopping is significant in wind conditions. For example, for a 4% wave steepness, overtopping rates are 6 times higher in the steeper slope compared to the milder slope 1 in 2.

Note that the connection lines depicted in Figure 4.18 connects data points with almost the same relative crest freeboard but these points do not have the exact same R_c/H_{m0} due to differences in the measured wave height near the structure (that differs from the target wave height). For instance, the lowest discharges if the 4% wave steepness have a slightly different trendline compared with higher discharges. This effect is induced by a lager difference between the two relative crest freeboard R_c/H_{m0}.
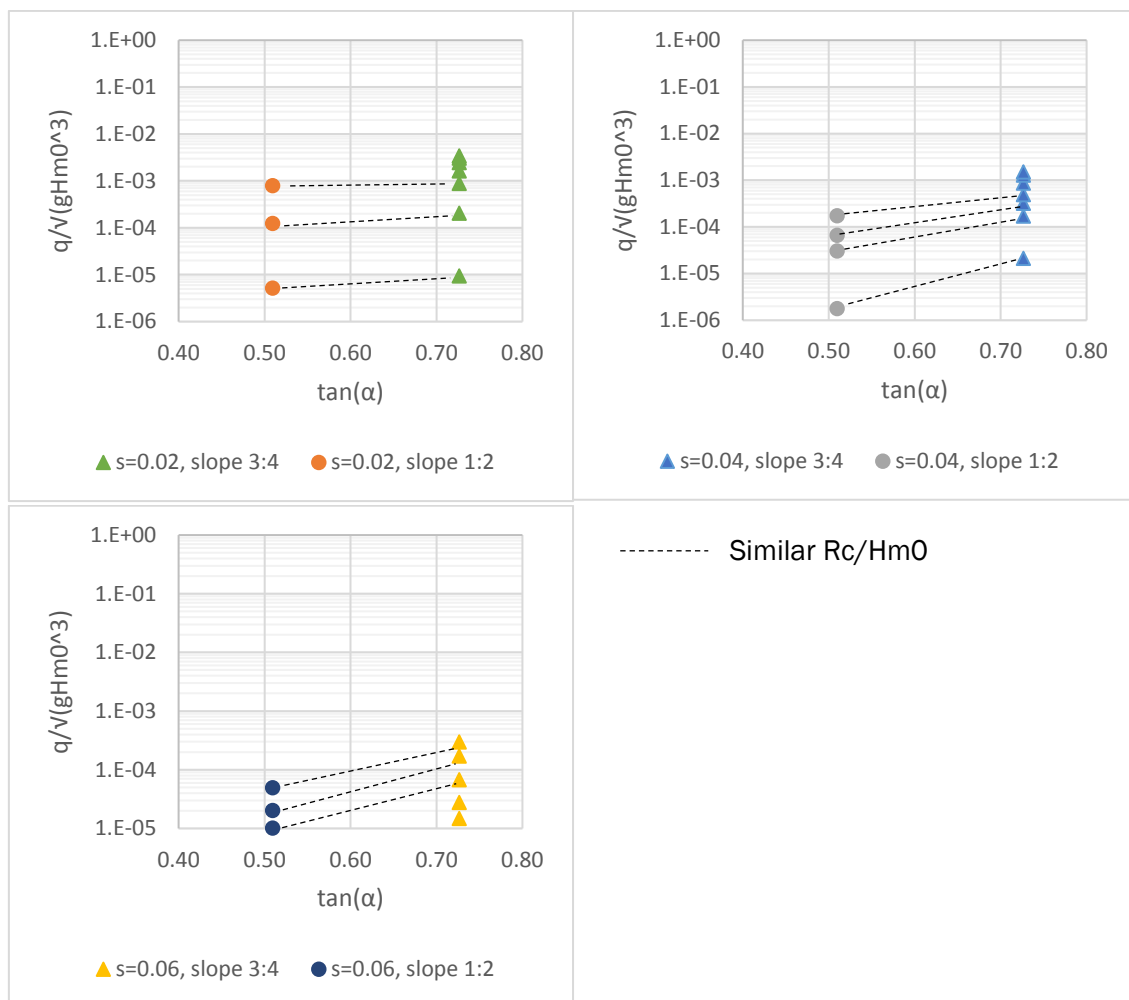
Figure 4.18 Influence of slope angle on wave overtopping

4.4.5   INFLUENCE OF BREAKER PARAMETER

As described in sections 4.4.3 and 4.4.4, the slope angle and wave steepness has an influence on wave overtopping. Therefore, the breaker parameter is also affecting overtopping rates. Figure 4.19 describes the breaker parameter based on the spectral average wave steepness, $S_{m-1,0}$.
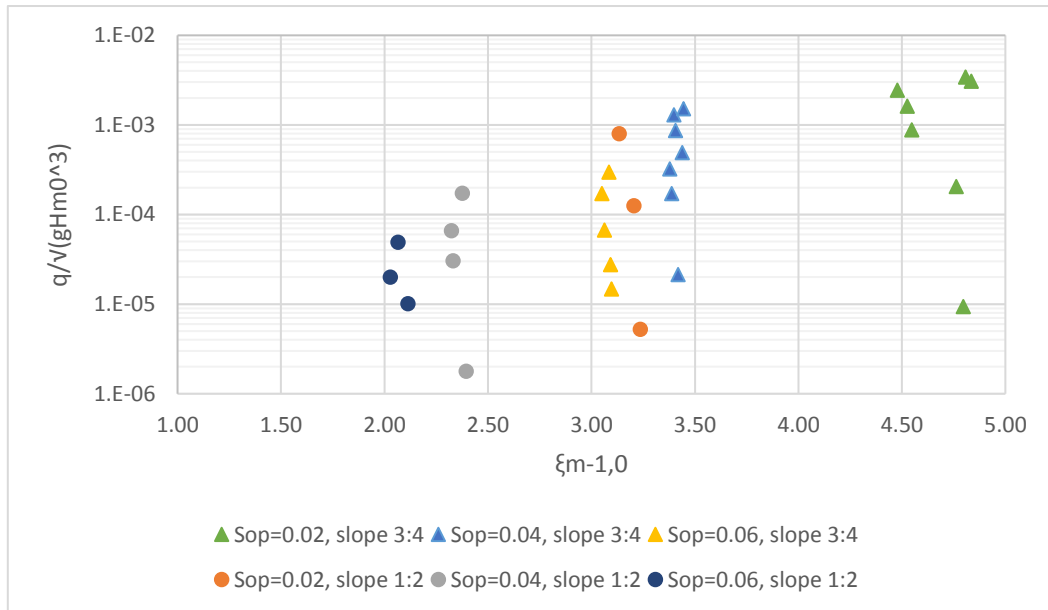
Figure 4.19 Influence of breaker parameter on wave overtopping

It is noticed that larger breaker parameters induce higher overtopping discharges. Furthermore, similar trendlines are observed for the different performed tests: as wave height (and wave period) increases within the same series, although the breaker parameter remains constant, the overtopping discharge increases due to a decrease in the relative crest freeboard.

Note that the series testing swell conditions in a slope 3:4 have three data points that deviates from the trend due to a higher $S_{m-1,0}$ (closer to 3% wave steepness) as compared to the other data from that series.

4.4.6 INFLUENCE OF THE ROUGHNESS COEFFICIENT

Roughness is somewhat included in the wave overtopping empirical formulae by a correction factor, γ_f. However, roughness is not properly represented by a constant value as it is confirmed by the test results depicted in Figure 4.20.

In order to investigate the influence of the roughness of the armour layer, the roughness coefficient is derived from the overtopping formula for armoured structures. Rewriting the overtopping equation leads to equation [4.2]. The roughness coefficient is, then, expressed as:

$$\gamma_f = -1.5 \frac{R_c}{H_{m0}} \cdot \left(\ln\left(\frac{q}{0.09\sqrt{gH_{m0}^3}} \right) \right)^{1/1.3}$$

[4.2]
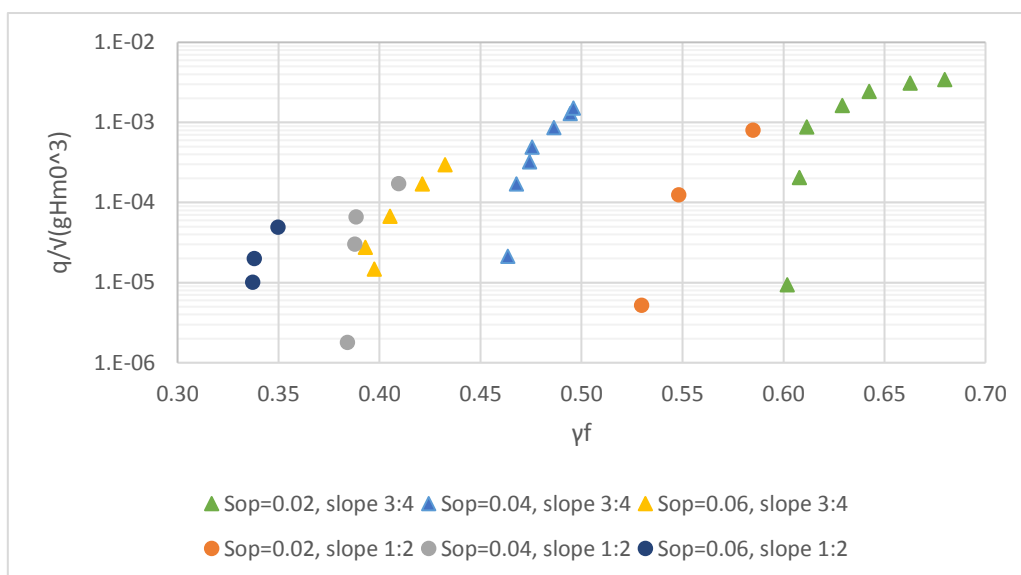
Figure 4.20 Influence of roughness coefficient in wave overtopping

Figure 4.20 shows that the roughness coefficient ranges between 0.34 and 0.68 with an average of 0.49. Within tests runs with the same wave steepness and slope angle, it is perceived that the increase in wave overtopping is correlated with an increase in the roughness coefficient. Therefore, it can be inferred that as the wave height increases, the thickness of the water layer covering the armoured slope increases as well, reducing the influence of roughness of the following incoming waves and the armour layer is identified as "smoother". This can also be related to the type of wave breaking as lower wave steepness presents large surging waves (i.e. large breaker parameters). Under surging waves, roughness becomes less important and thus, the armour layer is felt "smoother" by the incoming waves. Consequently, overtopping rates are higher for swell conditions as well as their corresponding roughness coefficients.

4.4.7 INFLUENCE OF THE PERMEABILITY, POROSITY AND ROUGHNESS

The roughness coefficient previously analysed does not only account for the roughness of the armour layer but also for the permeability and porosity of the structure. Actually, this factor absorbs information of any parameter not directly listed in the empirical formulae.

The influence of the permeability and roughness of the armour slope can also be observed based on the test results from the 1:2 armoured and smooth slope. By placing a wooden plate on the top layer, both the roughness and the permeability of the structure disappears. Therefore, the influence of the porosity and the roughness of the armour layer can be studied. However, these two factors cannot be investigated separately under the conditions tested in this research.

The armour porosity allows part of the wave to penetrate through the armour units and dissipate energy. Moreover, due to the permeability of the core and underlayer, water can infiltrate through the structure which decrease the run-up and the wave overtopping discharge.

Figure 4.21 shows the test results of the armoured slope and the smooth slope. Steeper trends are observed for the armoured slope test series regardless of the wave steepness. Therefore, as the relative freeboard crest decreases the differences between the discharge of the armoured slope and the smooth slope are reduced. In fact, a smaller R_c/H_{m0} has less

room for run-up and run-down and thus, the influence of the properties of the armour on the incoming waves become less significant, which leads to a lower reduction of the overtopping discharge.
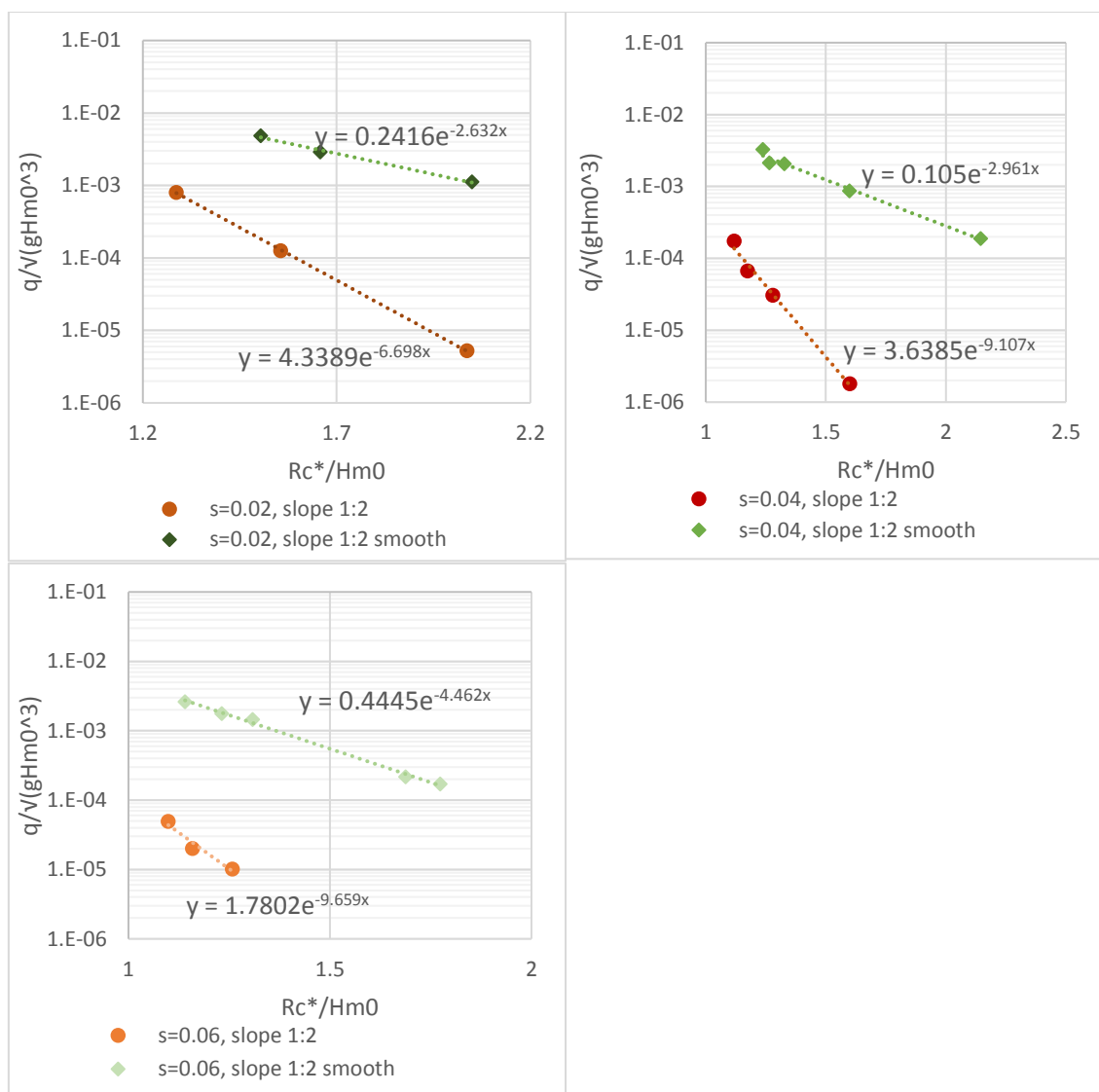
Figure 4.21 Measured dimensionless overtopping discharge for 1:2 armoured and smooth slope

Based on the trendlines depicted in Figure 4.21, the ratio of the dimensionless overtopping discharge of the armoured slope over the discharge of the smooth slope can be calculated for each wave steepness (i.e. $q*_{armoured}/q*_{smooth}$).

Figure 4.22 depicts the ratio $q*_{armoured}/q*_{smooth}$ (where $q*$ represents the dimensionless discharge) as a function of the relative crest freeboard, R_c*/H_{m0}. It is perceived that 2% wave steepness is less affected by the armour porosity/roughness as compared with wind conditions for a given relative crest freeboard. For instance, considering a $R_c*/H_{m0}=1.3$, the ratio $q*_{armoured}/q*_{smooth}$ is equal to 0.09, 0.012, 0.005 for the 2%, 4% and 6% wave steepness, respectively. Therefore, the reduction of overtopping discharge induced by the armour porosity/roughness is more effective for higher wave steepness.

As already mentioned in section 4.4.6 which analyses the influence of the roughness coefficient, surging waves are less affected by the armour layer as the water tongue is thicker for these types of breakers. Therefore, properties such as porosity and roughness are not

able to dissipate as much energy as compared to higher wave steepness. This leads to a lower decrease in wave overtopping rates.
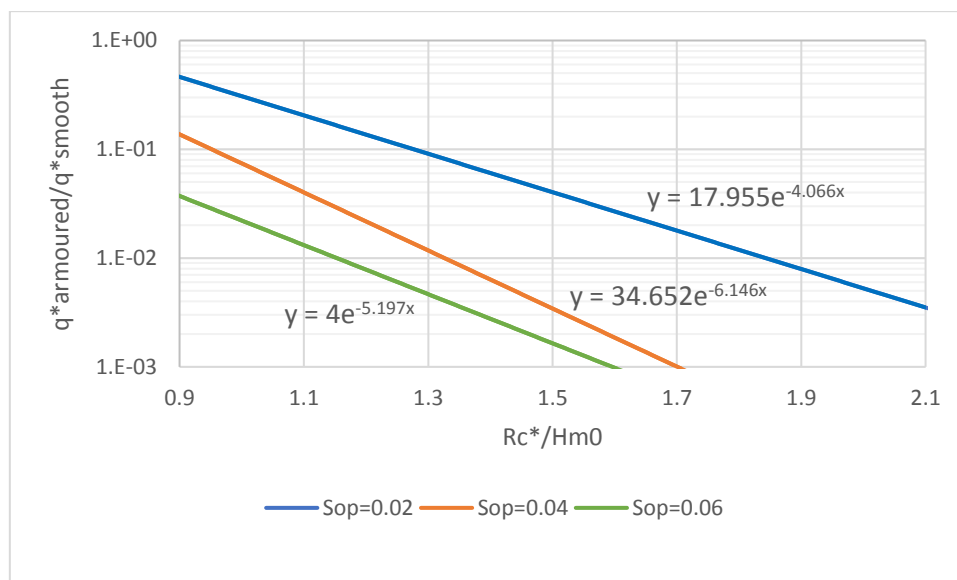
Figure 4.22 Ratio armoured and smooth dimensionless discharge as a function of the relative crest freeboard

4.4.8 INFLUENCE OF THE ROCK CREST BERM

During the performance of the tests of 2% wave steepness it was observed that most of the incoming waves had high velocities and they passed over the structure with little interaction with the crest. Therefore, swell conditions were less affected by the rock crest berm.

This fact is confirmed in Figure 4.23 where the dimensionless overtopping discharges measured in this research are compared to the CLASH tests performed under standard smooth conditions. The overtopping discharge in these tests is measured at the seaward edge of the structure and, thus, they are not affected by any crest berm.
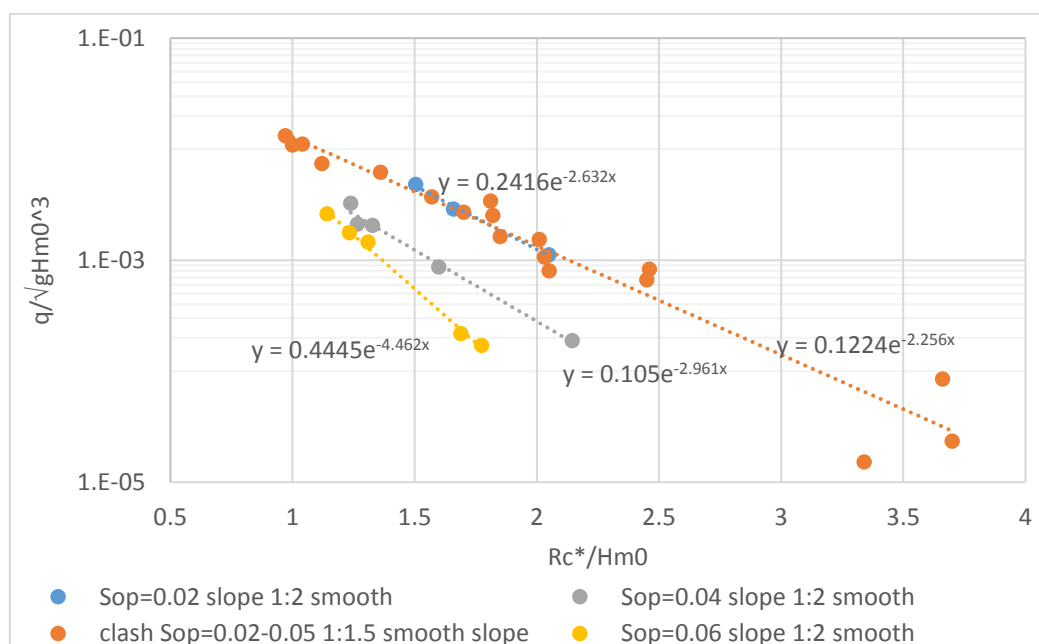
Figure 4.23 Influence of the rock crest berm

Note that although the model set-up is based on the model design defined for CLASH tests and they are both similar, there are still differences between both configurations that need to be considered. The main differences between the model set-up designed for this research and CLASH set-up are:

- The CLASH tests were performed with a 1:1.5 breakwater slope. The structure used in this study has a slope angle of 1:2 and 3:4. Hence, slightly higher overtopping rates are measured in CLASH programme.
- The CLASH tests were conducted with a horizontal bed. In contrast, tests in this research are performed with a sloping foreshore of 1:30. Therefore, wave shoaling occurs and wave height near the structure increases and waves can break due to the influence of the sloping foreshore.

5 | COMPARISON WITH EMPIRICAL FORMULAE

This chapter compares the measured wave overtopping discharge with the empirical formulae presented in the literature review of this research, included in Chapter 2. Moreover, a discussion of the deviations found between measurements and prediction is given. Finally, some correction factors are introduced in the empirical formulae in order to improve the overtopping prediction and reduce the scatter.

5.1 REGIONS OF VALIDITY FOR WAVE OVERTOPPIG FORMULAE

EurOtop manual (2016) specifies that the wave overtopping discharge can be described by two formulae for coastal dikes and embankments, one for breaking waves on the slope and, one for non-breaking (surging) waves. These two expressions correspond to equation [2.8] and [2.9] respectively and they are repeated here as equation [5.1] and [5.2].

$$\frac{q}{\sqrt{gH_{m0}^3}} = \frac{0.023}{\sqrt{tan\alpha}} \gamma_b \xi_{m-1,0} \cdot \exp\left(-\left(2.7 \frac{R_c}{H_{m0}} \frac{1}{\xi_{m-1,0} \cdot \gamma_b \cdot \gamma_f \cdot \gamma_\beta \cdot \gamma_v}\right)^{1.3}\right)$$

[5.1]

$$\frac{q}{\sqrt{gH_{m0}^3}} = 0.09 \cdot \exp\left(-\left(1.5 \frac{R_c}{H_{m0}} \frac{1}{\gamma_f \cdot \gamma_\beta \cdot \gamma^*}\right)^{1.3}\right)$$

[5.2]

In case of armoured slopes such as rubble mound structures, EurOtop (2016) indicates that mainly equation [5.2] has to be used since these types of structures often have steep slopes of about 1:1.5, leading to the overtopping equation that gives the maximum (Eq. [5.2]).

In order to determine which empirical formulae corresponds to the present research conditions, measured wave overtopping discharge is depicted as a function of the breaker parameter. Figure 5.1 shows that the test results are within the region where Eq. [5.2] is valid as predicted in EurOtop manual.

In this thesis H_{m0} is taken as the wave height in front of the structure and $\xi_{m-1,0}$ is calculated using wave period $T_{m-1,0}$ in front of the structure, the wave height in front of the structure and the slope angle of the breakwater.
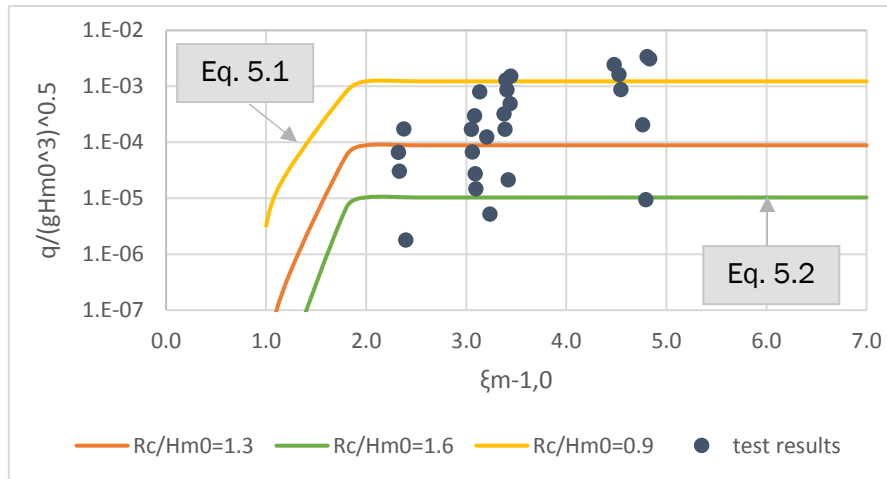
Figure 5.1 Wave overtopping discharge as a function of the breaker parameter ξm-1,0 and for three relative freeboards

Note that in further sections, Eq.5.1 is also named dike's formula and its maximum, Eq.5.2, is cited as breakwater's formula.

5.1.1 COMPARISON WITH EMPIRICAL FORMULAE FOR BREAKWATERS

Based on last section's conclusion, the test results are compared with the empirical prediction given by the breakwater's formula. Firstly, a comparison with the test results of a 1:2 smooth slope is performed. Figure 5.2 presents the measured overtopping results for this case. It clearly shows that the empirical prediction does not give a good fit. There is large scatter between different wave steepness. This scatter is emphasized in swell conditions.

Due to the presence of the rock crest, lower overtopping discharges are expected as compared with the empirical prediction for smooth slopes (γ_f=1.0). However, a roughness coefficient of 1.0 gives a good fit for swell conditions since, as discussed in section 4.4.8, swell conditions are not affected by the rock crest berm. Higher wave steepness present much lower overtopping rates, which results in a smaller roughness coefficient.
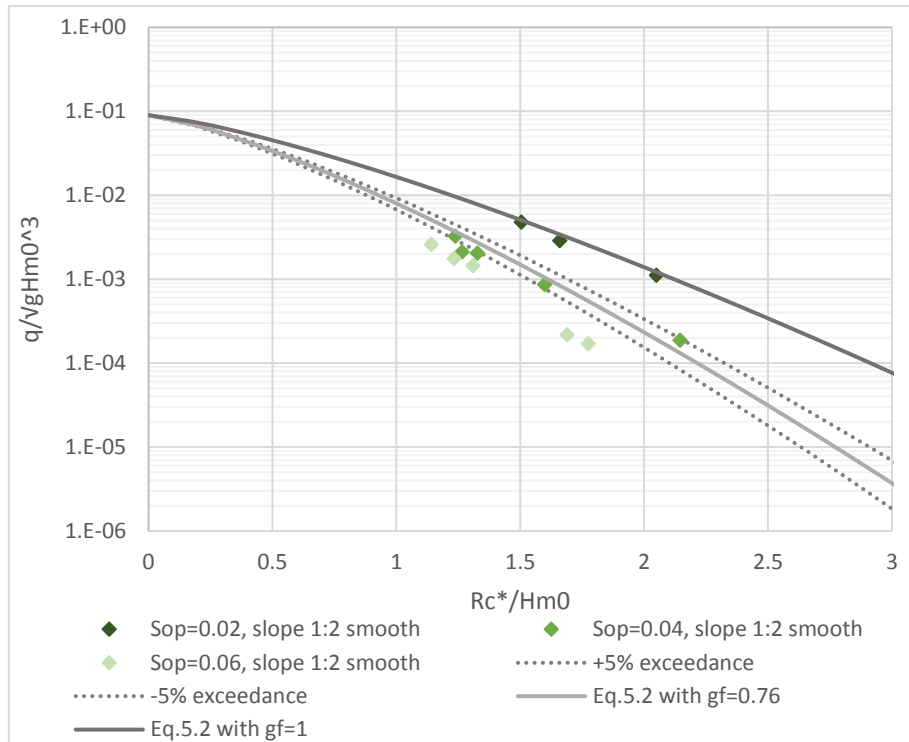
Figure 5.2 Dimensionless overtopping discharge of smooth slope compared to empirical prediction (Eq.5.2)

Measured overtopping discharges of 3:4 and 1:2 armoured slopes are presented in Figure 5.3 and Figure 5.4. Large scatter is also observed in both cases. As already seen in the results for the smooth slope, swell conditions have larger deviations as compared to the results of 4% and 6% wave steepness.
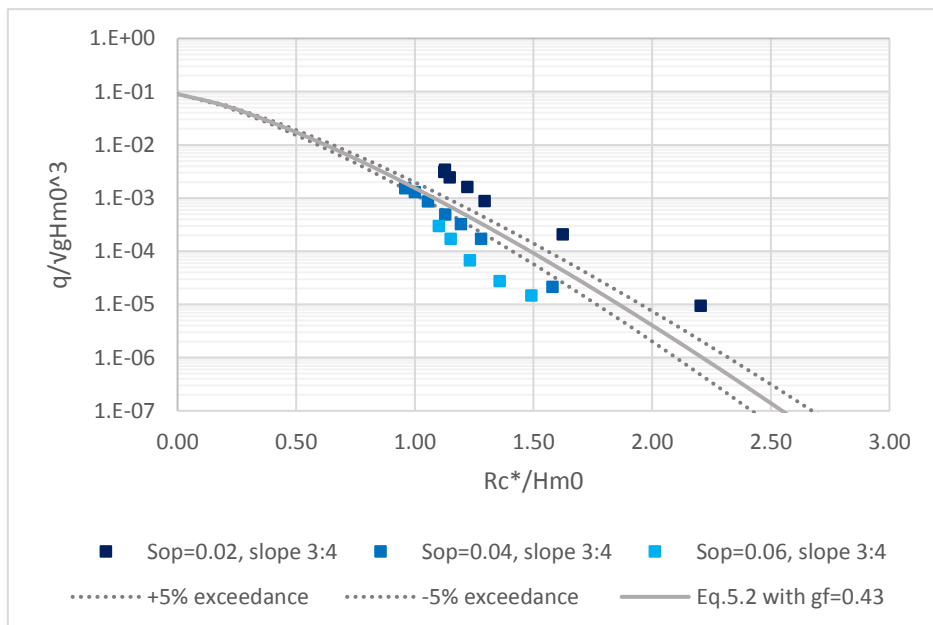
Figure 5.3 Dimensionless overtopping discharge of 3:4 slope compared to empirical prediction (Eq.5.2)
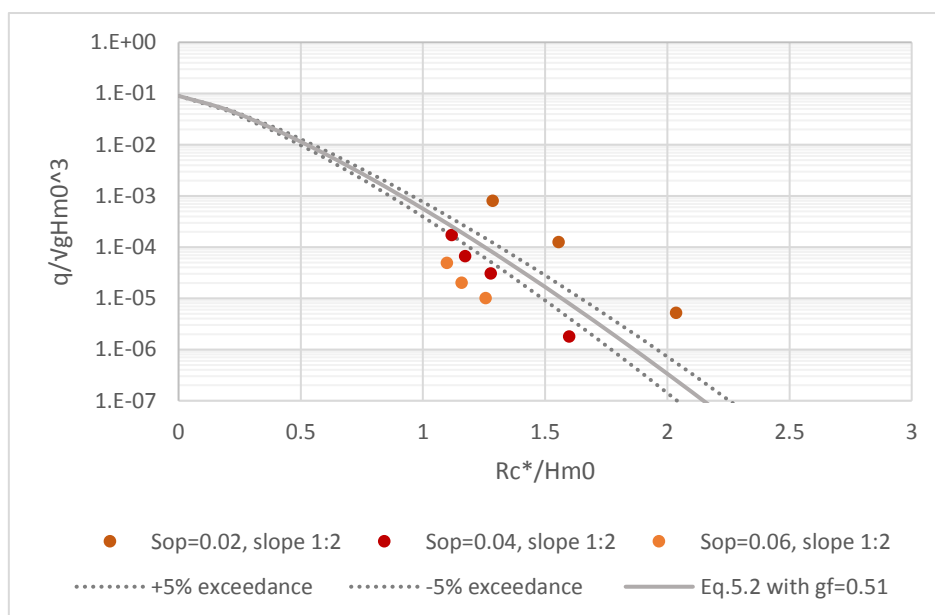
Figure 5.4 Dimensionless overtopping discharge of 1:2 slope compared to empirical prediction (Eq.5.2)

Note that for all graphs a prediction is given with a 90% confidence band. The roughness coefficient used for these predictions is derived by averaging the roughness values obtained from equation [4.2] and depicted in Figure 4.20. These values are presented in Table 5.1 along with its calibrated coefficient assuming γ_f=1.0 for the smooth slope. They should be taken as a first and rough estimation but they cannot be considered representative for the armour unit since the standard overtopping formula does not give a good fit due to the high scatter present in the results. Besides, roughness coefficients for the two tested slopes differs significantly. Although the 1:2 slope is larger than 3:4 slope and units in the gentler slope are placed facing a little bit upwards (see. Figure 5.5) which might slightly increase the roughness of the armour layer (i.e. decrease roughness coefficient), this large difference seems unrealistic.

Average γ_f		
slope	γ_f	γ_f_calibrated
3:4	0.51	0.68
1:2	0.43	0.56
1:2 smooth	0.76	1

Table 5.1 Average values of roughness coefficients
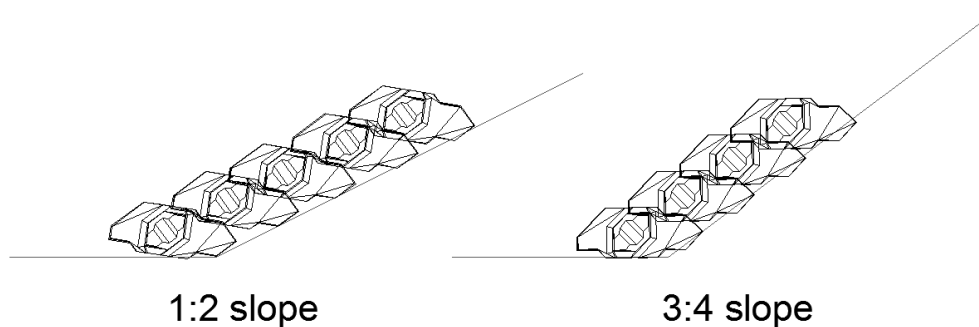
Figure 5.5 Placement of Xbloc+ unit (Rada Mora 2017)

A discussion of factors that might be playing a role in these deviations is provided in the next section.

5.2 SCATTER OF THE RESULTS

Figure 5.2, Figure 5.3 and Figure 5.4 show a large degree of scatter between the different series and therefore, empirical formulae does not predict overtopping rates accurately. The main factors that might influence this scatter are discussed below.

5.2.1 EFFECT OF THE ROCK CREST

Tests on the smooth slope are performed with a wooden plate and a rock crest. Figure 5.2 shows that 2% wave steepness is not affected by the presence of the crest as it fits with the empirical prediction assuming γ_f=1.0. However, results for 4% and 6% wave steepness are significantly reduced compared to the prediction for smooth slopes. Therefore, the effect of the rock crest does not have the same effect for swell and wind conditions.

During the performance of the tests of 2% wave steepness it was observed that most of the incoming waves had really high velocities and they passed over the structure with little interaction with the crest. Therefore, large unbroken waves are less affected by the rock crest as it is confirmed in Figure 4.23 where the influence of the rock crest berm is analysed. In contrast, lower overtopping discharges are more affected by the volume infiltrated through the crest as it represents a larger percentage of its total overtopping volume as compared to the water infiltrated during high overtopping discharges. Therefore, the presence of crest can lead to larger scatter in the smaller overtopping discharges.

5.2.1 PARAMETERS NOT INCLUDED IN EMPIRICAL FORMULAE

Breakwater's formula is really simplified and only depends on the relative crest freeboard R_c/H_{m0} and correction factors such as roughness coefficient. Therefore, correction factors end absorbing more information than what they are intrinsically representing.

In section 4.4, the influence of different parameters on wave overtopping is investigated. This analysis shows that parameters such as the wave period and slope angle have an influence on the overtopping rates. Thus, these missing parameters might be causing a poor estimation.

Although the scatter, Figure 4.12 shows that all test series have parallel trends. The two main parameters distinguishing one series from another are wave steepness and slope angle. Therefore, these two factors might be producing most of the scatter in the results.

Wave steepness is defined as the ratio between wave height and wave length (directly related to wave period). As the wave height is already included in the empirical prediction, the non-inclusion of the wave period in overtopping predictions can lead to inaccurate estimations of the wave overtopping discharges.

The slope angle has also an influence on wave overtopping. Figure 4.18 shows that higher overtopping rates are obtained for steeper slopes. This difference becomes more important for higher wave steepness (wind conditions). Hence, the influence of the slope angle is not represented by the actual empirical formulae and therefore, good predictions are hard to obtain.

Furthermore, the porosity of the armour influences the wave overtopping. No parameter directly accounts for this influence in the empirical prediction. Therefore, its effect is grouped up in the roughness coefficient.

5.2.2 DEFINED PARAMETERS IN EMPIRICAL FORMULAE GIVEN BY EUROTOP MANUAL

5.2.2.1 Wave height

For the calculation of wave overtopping, empirical formulae described in EurOtop manual use H_{m0} and $T_{m-1,0}$ measured in front of the structure to represent wave height and wave period. However, due to the fact that the structure is placed in intermediate waters, the highest waves break first when they feel the bottom, where the small waves stay unchanged. The significant wave height H_{m0} is affected as well as the wave height distribution which does not follow a Rayleigh distribution anymore because of wave breaking process. Therefore, considering other definitions of wave height, rather than the spectral wave height specified by the EurOtop manual, might reduce the scatter.

Dimensionless overtopping discharge is re-plotted using the statistical significant wave height, $H_{1/3}$ and the 2%-exceedance wave height, $H_{2\%}$ measured near the structure. Results are presented in Figure 5.6 and Figure 5.7. Note that Figure 4.12 is plotted next to the re-plotted figures for comparison purposes.

Figure 5.6 indicates that the introduction of $H_{1/3}$ measured near the structure does not give significant changes in the results. However, by using $H_{2\%}$ the scatter is reduced as shown in Figure 5.7. Still, some differences due to wave steepness are present, especially for swell conditions but deviations due to slope angle are reduced.
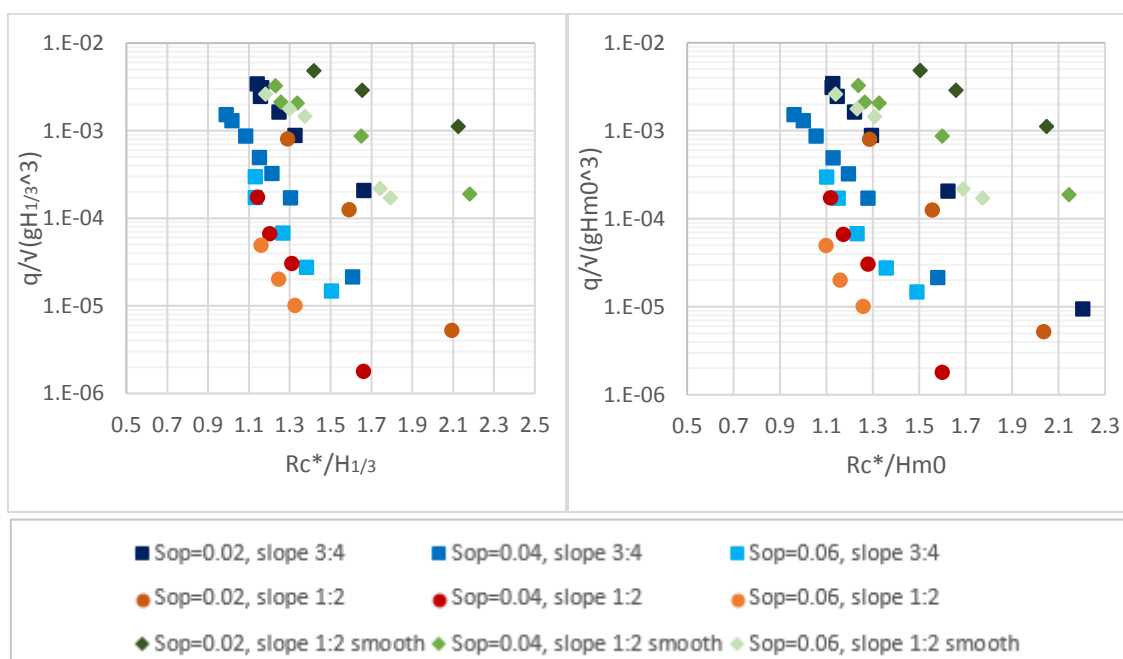
Figure 5.6 Measured dimensionless wave overtopping discharge using $H_{1/3}$
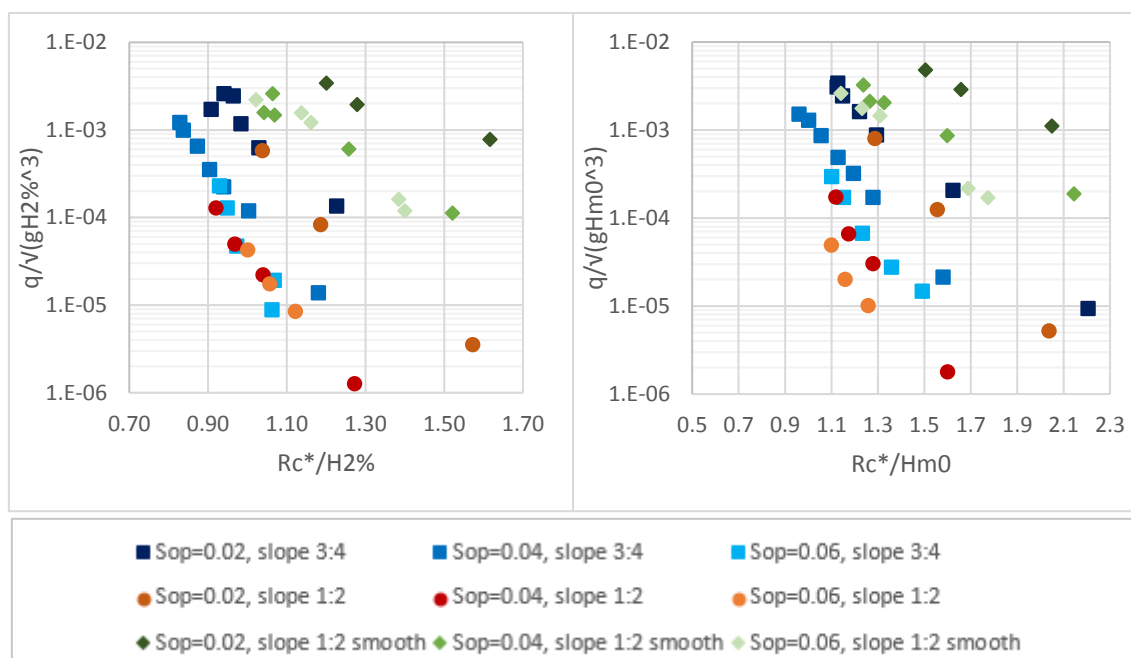
Figure 5.7 Measured dimensionless overtopping discharge using H2%

5.2.2.2 Roughness coefficient

Roughness is created by the irregular placement of the blocks or rocks forming the armour layer (more irregularities lead to higher roughness). However, the roughness factor, γ_f, not only takes into account how overtopping is influenced by the amour unit, other parameters not accounted for in the empirical formulae such as the armour porosity, the number of layers or the packing density also have an influence on the determination of the roughness coefficient.

Furthermore, the empirical formulae consider the roughness coefficient as a constant parameter. Although it is useful to define fixed values for each armour unit, this is not realistic. For instance, armour units at lower rows are placed deeper under water as compared to upper rows of the armour slope. Therefore, the roughness of the slope is not felt by the incoming waves at the same degree along the entire slope. Besides, surging waves are less affected by the roughness of the armour layer as they usually have a thicker water layer as compared to spilling or plunging waves.

The influence of the roughness coefficient on wave overtopping discharge was presented in section 4.4.6 and it indicates that the increase in wave overtopping is associated to an increase in roughness coefficient (see Figure 4.20). This confirms that the roughness coefficient is not a fixed value but increases with wave steepness (larger breaker parameters gives higher roughness coefficient). Therefore, the definition of a unique roughness coefficient regardless of wave conditions, also introduces inaccuracies on the wave overtopping prediction.

5.3 MODIFIED OVERTOPPING FORMULA

In order to reduce the scatter present in the results a modification of the overtopping predictor is investigated. Two parameters that, a priori, seem to be not properly represented are the wave steepness and the slope angle. As dike's formula considers the breaker parameter and the slope angle, this formula is taken as starting point.

Section 5.2.2.1 indicates that $H_{2\%}$ is a better descriptor than $H_{1/3}$ or H_{m0}. However, the determination of this parameter has not a standard procedure and usually general conversion rules are applied such as $H_{2\%}/H_{m0}=1.4$ (Verhagen et al. 2007). This type of relationships assumes a Rayleigh distribution and a Jonswap spectral shape with peak enhancement factor of 3.3 and therefore, the advantages of using $H_{2\%}$ disappears. Thus, and since the spectral significant wave height is taken as standard parameter in overtopping estimations, the approach for the modified overtopping formula is based on H_{m0} near the structure.

Moreover, note that although in Figure 4.20 is shown that the roughness coefficient is not constant, in this research it is assumed to be a fixed value as it is considered in the existing literature.

5.3.1 DIKE'S FORMULA

By using dike's formula wave steepness is better represented. As it is observed in Figure 5.8, well-defined trends are found for the armoured slopes and the smooth slope. However, the slope angle is still producing scatter. Therefore, a correction factor for the influence of the slope angle needs to be introduced.
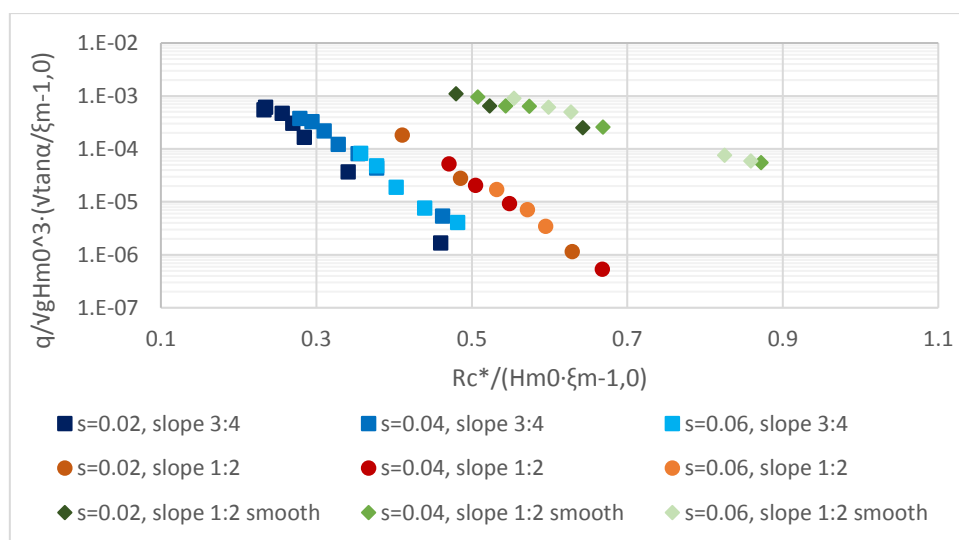
Figure 5.8 Dimensionless overtopping discharge expressed in terms of dike's formula

5.3.2 INTRODUCTION OF CORRECTION FACTORS

A correction factor of $(1-\tan\alpha)^{0.4}$ is found to be the optimum value to reduce the scatter produced by the poor representation of the slope angle in the prediction of wave overtopping.
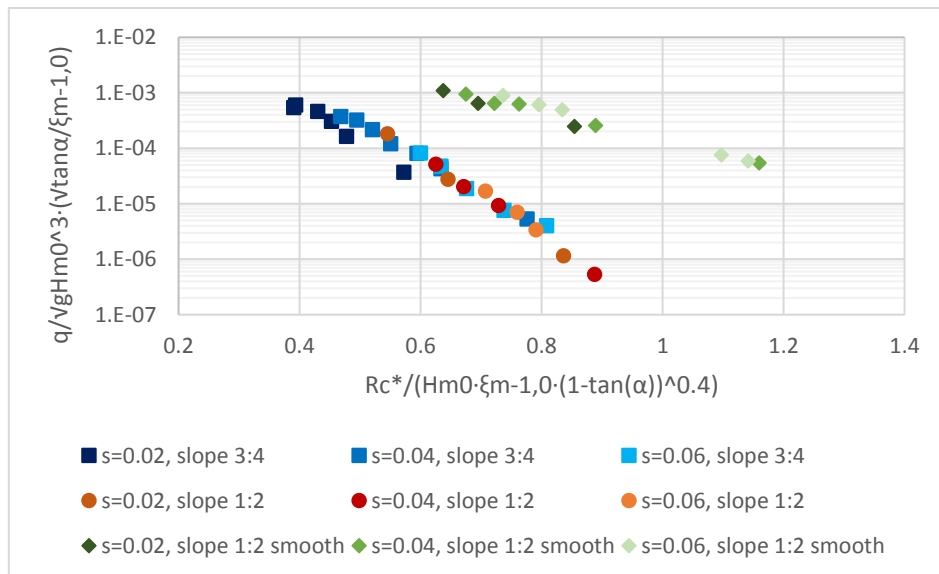
Figure 5.9 Dimensionless wave overtopping discharge after the introduction of slope corrector factor

Although the introduction of this correction factor reduces the scatter significantly and almost all the data points are in line, there are still some little deviations observed due to wave steepness. Thus, a correction for wave steepness is also studied.
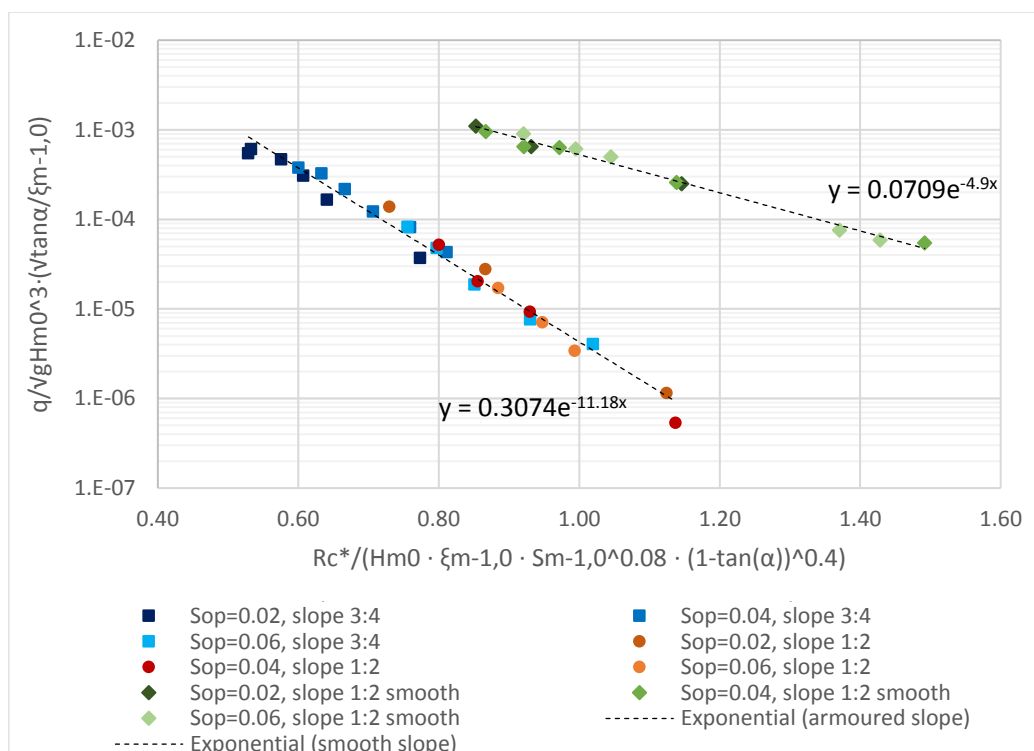
Figure 5.10 Dimensionless wave overtopping discharges after the introduction of slope and wave steepness correction factors

Figure 5.10 shows that by introducing a correction factor of $S_{m-1,0}^{0.08}$ to the empirical formulae the wave steepness is better represented and both smooth and armoured slopes are completely described by straight lines. Therefore, these two correction factors can be considered as a first step into the improvement of the empirical formulae. However, further analyses on other correction factors should be performed. For instance, during the

performance of the tests it is observed that the crest has a higher impact on wind conditions as compared to swell conditions. Thus, a correction of the influence of the rock crest based on the breaker parameter or wave steepness might be interesting to be studied.

After all these adjustments, the modified empirical formulae for the prediction of wave overtopping can be expressed as:

$$\frac{q}{\sqrt{gH_{m0}^3}} = \frac{0.023}{\sqrt{tan\alpha}} \xi_{m-1,0} \cdot \exp\left(-\left(2.7 \frac{R_c}{H_{m0}} \frac{1}{S_{m-1,0}^{-0.42} \cdot \tan(\alpha) \cdot (1 - \tan(\alpha))^{0.4} \cdot \gamma_f}\right)^{1.3}\right)$$

[5.3]

Note that expression [5.3] is bounded by the specific model set-up designed for this research and their derivations are only based on test results of this study. The applicability of this formula to other investigations is out of the scope, although validation of these modified formulae is recommended.

Furthermore, since dike's formula already considers the breaker parameter and the slope angle, it can be argued whether these corrector factors are a modification of the roughness coefficient or an actual correction for the wave steepness and slope angle. As mentioned in section 4.4.6, the roughness coefficient is not well represented as a constant parameter and its influence on wave overtopping is not the same under swell and wind conditions. However, in this research it is assumed constant. Therefore, further research on the influence of these, and other, parameters on the roughness coefficient must be performed to derive a conclusion.

5.4 DETERMINATION OF THE ROUGHNESS COEFFICIENT

5.4.1   BASED ON THE MODIFED EMPIRICAL FORMULA

Using the modified empirical formula (Eq. [5.3]), the roughness coefficient can be defined more accurately. In Figure 5.11, the empirical prediction is plotted using the roughness coefficients that best-fit with the test results. A 90% confidence band is also defined in order to check for reliability. It is observed that only one data point exceeds the 90% confidence band. The red point located in the lower part of the graph presents much deviation compared to other data points is due to the fact that small overtopping rates are more affected by the presence of the crest, which influence is not included in the formulae.
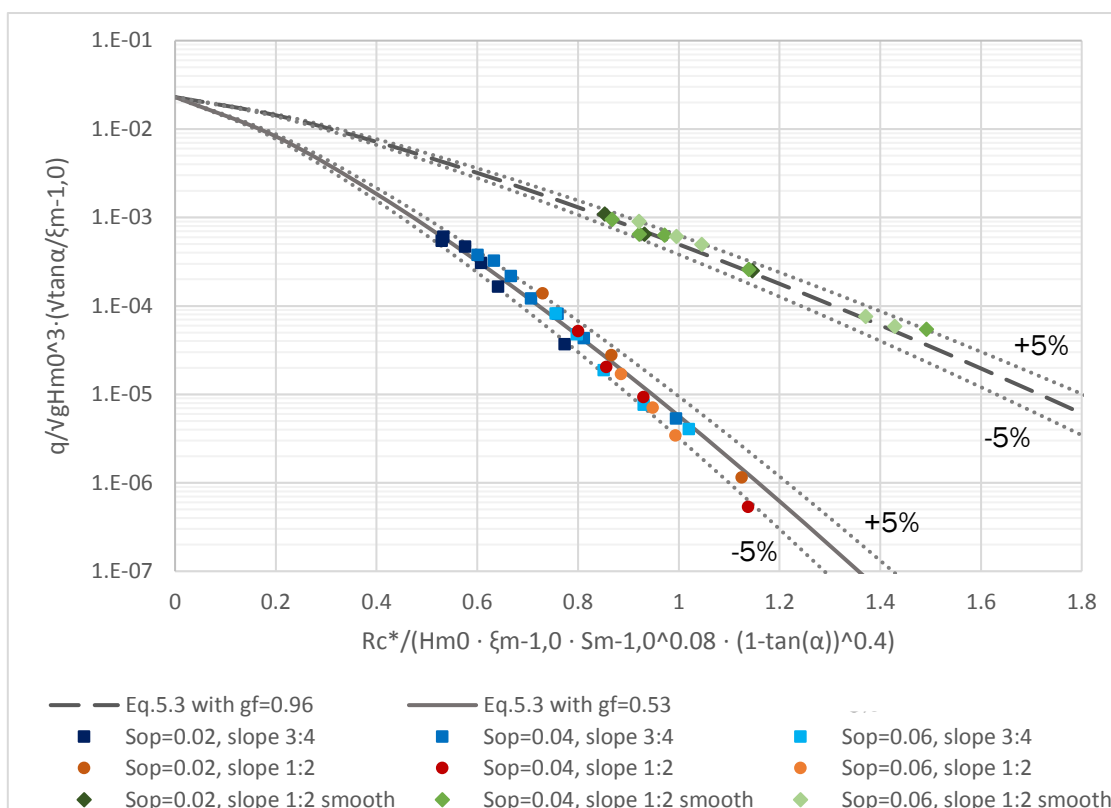
Figure 5.11 Dimensionless overtopping discharge compared to empirical prediction (Eq.5.3)

Using equation 5.3 the roughness coefficient can be estimated. As shown in Figure 5.11, the roughness coefficients are defined as 0.96 and 0.53 for smooth and armoured slopes, respectively. Smooth slopes have a predefined roughness coefficient of 1.0, therefore the results are 4% underestimated and an increase in the roughness coefficient for the Xbloc+ unit is undertaken. This calibration results in a roughness coefficient of 0.55. Table 5.2 summarizes the values of the roughness coefficients.

slope	γ_f	γ_f_calibrated
3:4	0.53	0.55
1:2	0.53	0.55
1:2 smooth	0.96	1

Table 5.2 Roughness coefficients for Xbloc+ armour unit derived from the modified overtopping equation

Note that this roughness coefficient is derived from the modified overtopping equation defined in this research. Thus, it is not comparable to any other coefficient present in the existing literature.

5.4.2 BASED ON THE EUROTOP MANUAL PROCEDURE

In section 5.1.1 the average roughness coefficients for the 3:4 slope structure and 1:2 slope structure are defined and factored based on the results obtained under smooth conditions. However, the crest berm is also present in the smooth structure and therefore, the smooth conditions are not "standard" and the roughness coefficients cannot be compared to the values provided in the EurOtop manual or CLASH programme.

The roughness coefficients presented in the EurOtop manual (2016) are derived based on the tests performed within the CLASH programme and adjusted by Bruce et al. (2009) based

on equation [5.2] which corresponds to the breakwaters equation. In CLASH tests, the roughness coefficient is derived from discharge measurements which were taken at $G_c=3D_n$ for rough structures (Pearson et al. 2004). These roughness coefficients were factored based on the results obtained under standard smooth conditions (measuring the overtopping discharge at the seaward edge of the structure and therefore, not affected by the crest berm).

As already mentioned in section 4.4.6, this expression can be rewritten as equation [5.4] which gives an average roughness coefficient of 0.49 for the armoured slope.

$$\gamma_f = -1.5 \frac{R_c}{H_{m0}} \cdot \left(\ln \left(\frac{q}{0.09\sqrt{gH_{m0}^3}} \right) \right)^{1/1.3}$$

[5.4]

In this research, test series conducted under smooth conditions are influenced by the presence of a berm except for swell waves (series 8) that did not show any reduction as it is discussed in section 4.4.8. Therefore, series 8 is taken as a reference for the standard smooth conditions which gives a roughness coefficient of 1.0.
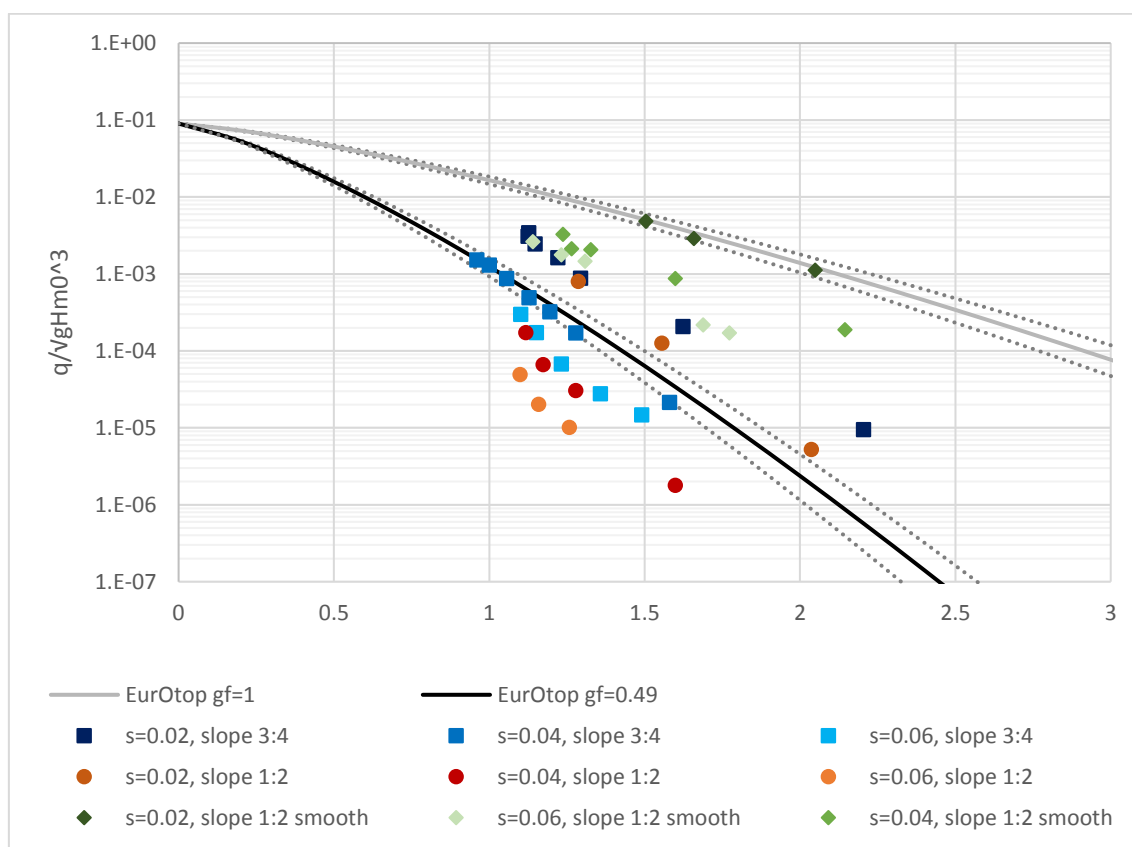
Figure 5.12 Determination of the roughness coefficient based on EurOtop manual procedure

In Figure 5.12 it is observed that based on the average roughness coefficient of 0.49, the empirical prediction overestimate wind waves and underestimate swell conditions. Although the high degree of scatter present, EurOtop manual also defined the roughness coefficient regardless of the scatter present in their results.

Figure 5.13 shows the deviations in CLASH results for the tests performed with standard Xblocs and one layer Cubes. Besides, the empirical prediction is drawn, which is based on the corresponding roughness coefficient defined for each type of armour unit. It is perceived that the empirical prediction usually underestimates the measurements. To quantify these deviations, the scatter index (SI) is calculated. The SI gives the percentage of the expected error of the prediction and it is derived by dividing the root mean square error (RMSE) by the mean of the observations as defined in equation [5.5].

$$SI = \left(\frac{1}{|logq_{meas}^*|} \cdot \sqrt{\frac{1}{n} \cdot \sum (logq_{est}^* - logq_{meas}^*)^2} \right) \cdot 100$$

[5.5]

Table 5.3 summarizes the outcomes and shows that the deviations have the same order of magnitude. Therefore, by taking the same approach defined by EurOtop manual, it can be stated that, although the scatter, a roughness coefficient of 0.49 can be assumed for the Xbloc+ unit.
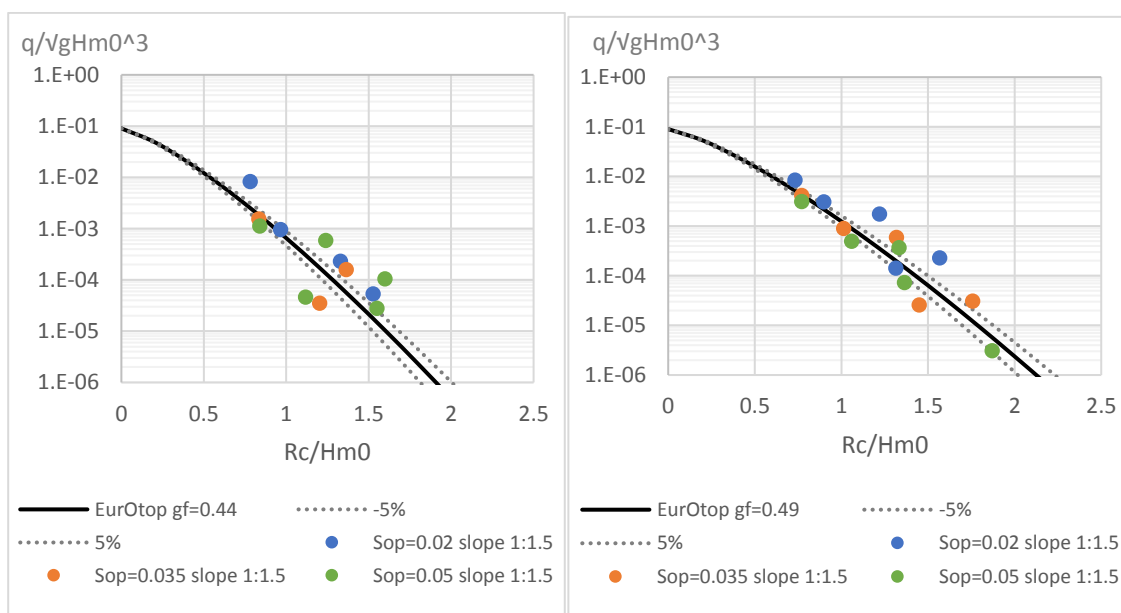
Figure 5.13 Dimensionless overtopping discharge measured within CLASH programme and its empirical prediction (left: Xbloc, right: 1L Cubes)

TYPE OF UNIT	SI
Xbloc+	19%
Xbloc (CLASH)	15%
1L Cubes (CLASH)	15%

Table 5.3 Scatter index for CLASH results and the measurements of this present research compared to the empirical prediction

As compared with other units such as the standard Xbloc (γ_f=0.44) and the one layer Cubes (γ_f=0.49)[1], it is perceived that the Xbloc+ units have a higher roughness coefficients with respect to the standard Xbloc which implies that it behaves smoother and this results in

---

[1] These roughness coefficients are derived by Bruce et al. (2009) and recommended by EurOtop (2016)

higher overtopping rates. Concerning one layer Cubes, both armour units behave similarly as they have the same roughness coefficient. However, one should bear in mind that roughness coefficients are dependent on the wave overtopping predictors and the used database as well as the scaled model configuration. In fact, the CLASH set-up and the configuration used for this research differ in some points previously mentioned in section 4.4.8 (i.e. different slope angle, presence/absence of foreshore) but in general, both model set-ups are similar enough to be able to compare their results.

5.5 COMPARISON OF THE PERCENTAGE OF OVERTOPPING WAVES WITH THE EMPIRICAL PREDICTION

As described in section 2.1.5.1.4, the percentage of overtopping wave can be estimated by equation [5.6].

The percentage of overtopping waves can also be estimated as described in EurOtop (2016). The empirical equation is a function of the armour freeboard, A_c, (instead of the crest freeboard, R_c), the nominal diameter, D_n, and the significant wave height, H_{m0}.

$$P_{ov} = \frac{N_{ow}}{N_w} = \exp\left(-\left(\frac{A_c \cdot D_n}{0.19 \cdot H_{m0}^2}\right)^{1.4}\right)$$

[5.6]

In which N_{ow} is the number of overtopping waves and N_w represents the total number of incident waves. For this study, the armour freeboard, A_c, is equal to the relative freeboard R_c.
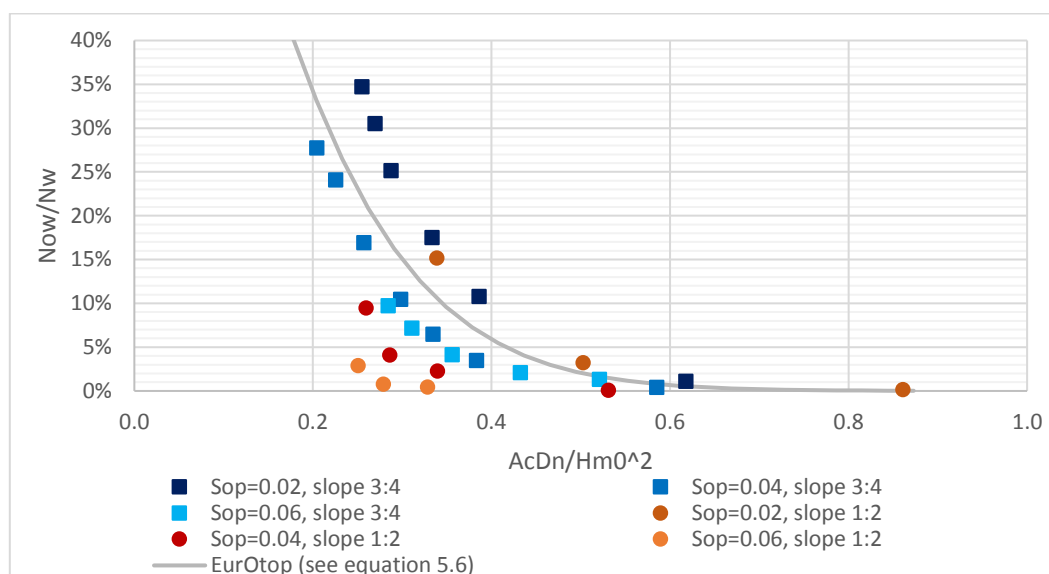
Figure 5.14 Comparison of the percentage of overtopping waves with the empirical formula

Figure 5.14 indicates that the existing formula overestimates the number of overtopping waves for long waves and underestimates the percentage of overtopping for short waves. The formula gives a good prediction for relative freeboards greater than 0.4. However, as the relative freeboard starts to decrease, the deviations become significant. Furthermore, higher differences are observed for the results obtained in the 1:2 slope. Therefore, further analyses on the prediction of the percentage of waves should be conducted in order to give a better representation of the reality. As a starting point, the introduction of a correction factor for the breaker parameter might be interesting to be studied since the difference of wave steepness and slope angle are not accounted for in the existing formula.

6 | CONCLUSIONS AND RECOMMENDATIONS

This chapter summarizes the conclusions of this research based on the results obtained from the small scale physical tests performed in the 2D wave flume. Furthermore, recommendations for further research in this area are given at the end of the chapter.

6.1 CONCLUSIONS

After the analysis of the test results, conclusions can be drawn. They are presented in terms of answers to the research questions formulated in Chapter 1.

1. *What is the wave overtopping discharge and percentage of overtopping waves over Xbloc+ armour layer?*

Nine series of tests were performed to determine the overtopping discharge and percentage of overtopping waves over Xbloc+ armour layer. Series differed in wave steepness and slope angle. Besides, three of the series were executed with a wooden plate to test a smooth slope.

Similar conclusions can be drawn for the wave overtopping discharge and the percentage of overtopping waves. It can be stated that:

- The wave overtopping discharge and the percentage of overtopping waves increase as wave height increases. Therefore, a reduction in the relative freeboard results in a higher percentage of overtopping waves and also, in a higher wave overtopping discharge.
- A 3:4 slope induces a higher number of overtopping waves and discharge as compared with a 1:2 slope since milder slopes are larger and thus, there is more space for dissipation.
- The longer the wave period, the higher the number of overtopping waves due to their greater wave energy.
- For swell conditions, a similar percentage of overtopping waves and overtopping rates are found between 3/4 and 1/2 slopes. Besides, waves with a 2% wave steepness have a larger deviation from the trendline calculated based on the EurOtop equation for breakwaters.
- Smooth slopes give greater overtopping rates as compared with rough armoured slopes

2. *Which parameters have an influence on wave overtopping results?*

From the analysis performed in this research, it can be concluded that the following parameters have an influence on wave overtopping:

- Wave height

Wave overtopping rates increase exponentially with wave height (H_{m0}) since higher wave heights leads to lower relative freeboards R_c/H_{m0}.

- Wave period

Although dimensionless wave overtopping discharge is less sensitive to changes in wave period than in wave height, wave overtopping rates are also influenced by wave period as these rates increase exponentially with wave period ($T_{m-1,0}$).

- Wave steepness

For low wave steepness a higher amount of overtopping is obtained as compared to higher wave steepness due to the different effect of the armour porosity and roughness on swell and wind waves.

- Slope angle

Steeper slopes induce higher overtopping rates. However, the slope angle of the structure has almost no influence under swell conditions since, as aforementioned, the properties of the armour (porosity, roughness) have a lower effect on surging waves as the water tongue is thicker compared to other type of breakers.

- Breaker parameter

Larger breaker parameters induce higher overtopping discharges as they represent more energetic waves.

- Roughness coefficient

Despite that the empirical formulae considers this parameter as a fixed value, the roughness coefficient is not constant. It ranges between 0.34 and 0.68 with an average of 0.49. Besides, it increases as the breaker parameter becomes larger (i.e. the armour layer is felt "smoother"). Therefore, surging waves are less affected by roughness and permeability as in this type of breaking the water layer running up and down the slope is thicker as compared with spilling or plunging breakers.

- Rock crest berm

Wind waves are more affected by the presence of the rock crest berm as compared to swell waves that have high velocities and pass over the structure with little interaction with the crest.

3. *Do the existing empirical formulae describe properly the wave overtopping?*

Accurate overtopping predictions are hard to obtain by means of the existing empirical formulae. Wave overtopping depends on a large number of factors and most of them are not included, or not well represented, by the overtopping predictors which, for the assessment of breakwaters, are only a function of the relative freeboard. Consequently, a high degree of scatter is observed when the empirical prediction for rubble mound structures is used. These deviations might be induced by:

- The effect of the rock protection placed on the crest berm. It is observed that the crest does not have the same influence on wind and swell waves as most of swell directly passes over the structure with little interaction with the crest.
- The parameters defined in empirical formulae included in EurOtop manual might not be the most appropriate to use for this case. It is seen that 2%-exceedance wave height gives a lower scatter compared to the results obtained by using the spectral wave height, H_{m0}, as suggested in the overtopping manual.
- The roughness coefficient is not well represented by a constant factor since the roughness and the permeability of the armour do not have the same impact regardless of the wave conditions.

- The exclusion of parameters that have an influence on wave overtopping such as slope angle and wave period are also increasing the scatter of the results.

Furthermore, the prediction of the percentage of overtopping waves is not accurate as important factors such as wave steepness and slope angle are not accounted for in the existing formula.

4. *How can the existing empirical prediction be improved in order to obtain more accurate estimations?*

By using the empirical formulae for dikes and embankments the overtopping prediction is more accurate. This formula includes the breaker parameter and the slope angle and therefore, gives a better representation of the wave overtopping. However, some scatter is still observed.

Thus, two correction factors are introduced in order to improve the overtopping prediction:

- Slope angle correction factor: $(1-\tan\alpha)^{0.4}$
- Wave steepness correction factor: $S_{m-1,0}^{0.08}$

Thus, the modified formula is expressed as:

$$\frac{q}{\sqrt{gH_{m0}^3}} = \frac{0.023}{\sqrt{\tan\alpha}}\xi_{m-1,0} \cdot \exp\left(-\left(2.7\frac{R_c}{H_{m0}}\frac{1}{S_{m-1,0}^{-0.42} \cdot \tan(\alpha) \cdot (1-\tan(\alpha))^{0.4} \cdot \gamma_f}\right)^{1.3}\right)$$

[6.1]

This formula gives accurate predictions as the measurements fit within a 90% confidence band.

5. *What value of roughness coefficient corresponds to this new armour unit?*

Based on the modified formula described by the equation [6.1], the Xbloc+ armour unit has a roughness coefficient of 0.55. However, this value is not comparable to the existing roughness coefficient given in the EurOtop manual as they are derived from different formulae.

Based on the approach followed by EurOtop, the roughness coefficient for the Xbloc+ can be assumed equal to 0.49. Therefore, Xbloc+ unit has a similar behaviour as one layer Cubes (γ_f=0.49) and gives higher overtopping rates as compared to the standard Xbloc (γ_f=0.44)

Although the breakwater equation for overtopping prediction gives some deviations from the measurements when a value of 0.49 is assumed, the same degree of scatter is observed in the predictions recommended by the CLASH programme and included in the EurOtop manual. Based on the statistical predictor Scatter Index (SI) a 15% of scatter is observed in the recommended predictions provided by EurOtop for Cubes and Xbloc while a roughness coefficient of 0.49 gives a 19% of scatter in the prediction of overtopping for the Xbloc+ armour tested in this research.

6.2 RECOMMENDATIONS

- Validation of the modified formulae

Further research should be done on validating equation [6.1] in order to check for the applicability of this new formulae to other experimental research. CLASH database or the

Neural Network tool (which it is based on the CLASH database) can be used in order to validate the correctness of the modifications.

- Inclusion of additional correction factors in the modified formula

Breakwater's formula does not describe properly wave overtopping. A first modification is introduced in this research. However, further studies should be performed to account for other parameters that might have an effect on overtopping prediction. For instance, it is observed that that crest and the properties of the armour (permeability, roughness) have a greater impact for wind waves. Therefore, some correction factor accounting for these effects should be further studied.

- Testing without a sloping foreshore

As the structure is placed in intermediate water, waves are affected by the foreshore by increasing in wave height due to shoaling process. By redoing the tests with a horizontal foreshore the influence of the foreshore on the results can be analysed and a correction factor for this effect can be further studied.

- Improvement of the definition of the roughness coefficient

This research confirms that the roughness coefficient varies although the existing empirical formulae assumes this factor as a constant. Therefore, analyses about the influence of the different parameters that might affect the roughness coefficient should be conducted to give a better representation of the roughness coefficient.

- Improvement of the prediction of the percentage of overtopping waves

The existing formula does not give an accurate prediction of the percentage of overtopping waves. Further analyses on the introduction of additional factors to improve this estimation are suggested. As a starting point, the introduction of a correction factor for the breaker parameter might be interesting to be studied.

- Check the region of validity of the wave overtopping formulae

The EurOtop manual considers for the dike's formula that for $\xi_{m-1,0}>2$ the wave overtopping discharge reaches a maximum. This maximum corresponds to the overtopping prediction for rubble mound structures. However, in this research, although being on the region of maximum overtopping (since breaker parameters are greater than 2), a maximum overtopping discharge is not found. Thus, checking the region of validity of the wave overtopping formulae is suggested.

REFERENCES

Allsop, W., 2003. Violent wave overtopping at the coast , when are we safe ? , (December 2015).

Bruce, T. et al., 2009. Overtopping performance of different armour units for rubble mound breakwaters. *Coastal Engineering*, 56(2), pp.166–179. Available at: http://dx.doi.org/10.1016/j.coastaleng.2008.03.015.

Burcharth, H., Liu, Z. & Troch, P., 1999. Scaling of Core Material in Rubble Mound Breakwater Model Tests. In COPEDEC, ed. *Fifth International Conference on Coastal and Port Engineering in Developing Countries: Proceedings of the COPEDEC V*. Cape Town, South Africa, 19-23 April, 1999, p. pp 1518-1528.

D'Angremond, K., van Roode, F.. & Verhagen, H.., 2008. *Breakwaters and closure dams* 2nd editio., VSSD.

EurOtop, 2016. EurOtop Manual on wave overtopping of sea. *Second edition. Pre-released October*.

EurOtop, 2007. EurOtop Wave Overtopping of Sea Defences and Related Structures : Assessment Manual. , (August).

Giroud, J.., 2010. Development of criteria for geotextile and granular filters. In *Proceedings of the 9th International Conference on Geosynthetics*. Guaruja, Brazil.

Hughes, S.A., 1993. *Physical Models and Laboratory Techniques in Coastal Engineering* W. Scientific, ed.,

Kortenhaus, A. et al., 2005. Quantification of Measurment Errors, Model and Scale Effects relative to Wave Overtopping. , Workpackag.

Mansard, E.P.D. & Funke, E.R., 1980. The Measurement of Incident and Reflected Spectra Using a least Squares Method. , pp.154–172.

Van der Meer, J.. & Janssen, J.P.F.M., 1995. *Wave run-up and wave overtopping at dikes. In: Wave Forces on Inclined and Vertical Wall Structures* Ed. N. Kob., ASCE.

Van der Meer, J., 1987. *Stability of rubble mound breakwaters. Stability formula for breakwaters armoured with ACCROPODE (R)*,

Molines, J., 2016. Wave overtopping and crown wall stability of cube and Cubipod-armored mound breakwaters.

Molines, J. & Medina, J.R., 2015a. Calibration of overtopping roughness factors for concrete armor units in non-breaking conditions using the CLASH database. , pp.1–31.

Molines, J. & Medina, J.R., 2015b. Calibration of overtopping roughness factors for concrete armor units in non-breaking conditions using the CLASH database. *Coastal Engineering*, 96, pp.62–70. Available at: http://dx.doi.org/10.1016/j.coastaleng.2014.11.008.

Muttray, M. & Reedijk, B., 2008. Design of Concrete Armour Layers. , (October), pp.1–17.

Owen, M.., 1980. *Design of seawalls allowing for wave overtopping*,

Pearson, J., Bruce, T., et al., 2004. *D24 Report on additional tests. Part B*,

Pearson, J., Meer, J.W. Van Der, et al., 2004. Overtopping performance of different armour units for rubble mound breakwaters. , pp.1–15.

Rada Mora, M.B., 2017. *Hydraulic performance of Xbloc+ armour unit*. TU Delft.

Salauddin, M., 2015. Physical model tests on new armour block Crablock for breakwaters to come to preliminary design guidance.

Schüttrumpf, H. & Oumeraci, H., 2005. Scale and Model effects in crest level design. In *Proc. 2nd Coastal Symposium*. Höfn. Iceland.

Steendam, G.J.A.N., 2004. The international database on wave overtopping. , pp.1–13.

Vanhoutte, L., 2008. Hydraulic stability of Cubipod armour units in Breaking conditions.

Verhaeghe, H., Rouck, J. De & Meer, J. Van Der, 2008. Combined classifier – quantifier model: A 2-phases neural model for prediction of wave overtopping at coastal structures. , 55, pp.357–374.

Verhagen, H., Van Vledder, G. & Arab, S., 2007. A practical method for design of coastal structures in shallow water. In *Proc. of the 31th International Conference on Coastal Engineering*. pp. 2912–2922.

Victor, L., Meer, J.W. Van Der & Troch, P., 2012. Probability distribution of individual wave overtopping volumes for smooth impermeable steep slopes with low crest freeboards. *Coastal Engineering*, 64, pp.87–101. Available at: http://dx.doi.org/10.1016/j.coastaleng.2012.01.003.

Vos, A., 2017. *Exploration into the mechanisms that govern the stability of an Xbloc+ v1 armour unit*. TU Delft.

Wolters, G., Hofland, B. & Wellens, P., 2014. Wave damping and permeability scaling in rubble mound breakwaters. , (1).

APPENDIX A: SCALING PROCESS

I.   SIMILITUDE REQUIREMENTS

Scale modelling must guarantee similarity in behaviour between the prototype and the model. Three types of similarity can be achieved:

- **Geometric similarity**

This condition is guaranteed if the scale ratios of all linear dimensions of the prototype and the model are equal. Therefore, the model has the same shape as the prototype.

- **Kinematical similarity**

Kinematical similarity exists if the ratio between all vectorial components of motion of the prototype and the model is the same for all particles at all time.

- **Dynamic similarity**

Two systems are dynamically similar if the ratios of all masses and forces acting on them are equal.

II.   SCALING LAW

For coastal structures, there are three relevant numbers for dynamic similarity: Froude (Fr), Reynolds (Re) and Weber (We). Unfortunately, the fulfilment of these three laws together is not possible to achieve.

- **Froude scaling**

The Froude number indicates the ratio between inertia and gravity forces. This ratio must be the same in the model as in the prototype.

$$\left(\frac{U}{\sqrt{g \cdot L}}\right)_p = \left(\frac{U}{\sqrt{g \cdot L}}\right)_m => \frac{N_u}{\sqrt{N_g N_L}} = 1$$

Froude criterion is valid for flow situations where the inertial forces are mainly balanced by gravitational forces. Therefore, it applies for most flows with free surface.

- **Reynolds scaling**

The Reynolds number gives the ratio between inertia and viscosity and makes sure that viscous forces are properly scaled. Therefore, this criterion is important when viscous forces are the dominating ones.

$$\left(\frac{\rho LU}{\mu}\right)_p = \left(\frac{\rho LU}{\mu}\right)_m => \frac{N_\rho N_L N_U}{N_\mu} = 1$$

It is clearly notice that Reynolds criterion is in conflict with Froude criterion. This implies that gravity and viscous forces cannot be both correctly scaled in the same scale model.

- Weber scaling

The Weber number is defined as the ratio between surface tension forces and inertia. It becomes important when air entrainment occurs, but also for breaking waves (surface stress acts as a membrane).

$$\left(\frac{\rho L U^2}{\sigma}\right)_p = \left(\frac{\rho L U^2}{\sigma}\right)_m => \frac{N_\rho N_L N_U}{N_\sigma} = 1$$

APPENDIX B: STABILITY CHECK

I.   ARMOUR LAYER

As discussed in section 2.2.1, the Reynolds number based on the characteristic dimension of the armour unit should exceed $3 \cdot 10^3$ in order to be stable. Besides, in order to neglect viscous effects the Reynolds number should be greater than 10^3.

Hughes (1993) defined the Reynolds number for the armour layer as follows:

$$Re = \frac{\sqrt{gH_s} \cdot D_n}{\nu} = \frac{\sqrt{9.81 \cdot 0.0938} \cdot 0.0291}{10^{-6}} = 2.8 \cdot 10^3$$

Therefore, stability of the armour layer can be considered met and scale effects due to viscosity are not expected.

II.   UNDERLAYER

Terzaghi's criteria for granular filters ensures the structure does not fail internally due to processes caused by the pressure developed between the armour layer and the core in geometrically closed granular filters.

According to Giroud (2010) , the classical Terzaghi's criteria are expressed by two equations:

For the stability of the interface between base material and filter material (retention criteria):

$$\frac{D_{15F}}{D_{85B}} < 4 \ or \ 5 \ => \ \frac{0.0102}{0.016} = 0.64$$

Therefore, this first stability requirement is met.

Secondly, for an adequate permeability of the filter layer to avoid its uplifting, the following condition is defined:

$$\frac{D_{15F}}{D_{15B}} > 4 \ or \ 5 => \ \frac{0.0102}{0.0024} = 4.25$$

Therefore, this second stability requirement is also met and the underlayer can be considered stable.

III.   TOE STABILITY

Toe protection is designed according to Van der Meer equation that relates the weight of the toe elements, the toe level and the damage (N_{od}).

Based on the dimensions of the toe, the ratio of the water depth on the toe (h_t) over the water depth near the toe (h) is 0.72. Therefore, the toe stability is based on the following formula given by Van der Meer:

$$\frac{H_s}{\Delta D_{n,50}} = \left(6.2 \cdot \left(\frac{h_t}{h} \right)^{2.7} + 2 \right) \cdot N_{od}$$

Assuming start of damage (N_{od}=0.5), a stability number of 4.1 is obtained.

Since the tests are performed until failure, a Hs of 14.3 cm is used considering 150% of the design significant wave height. This results in a D_{n50} of 21 mm which is converted to an available standard grading of 16-22.4 mm.

APPENDIX C: LABORATORY FOOTAGE

1 Cross section slope 3:4
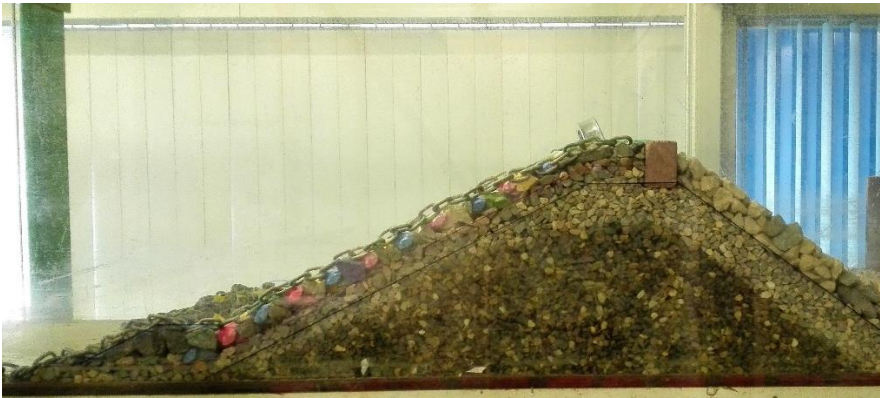
2 Cross section slope 1:2
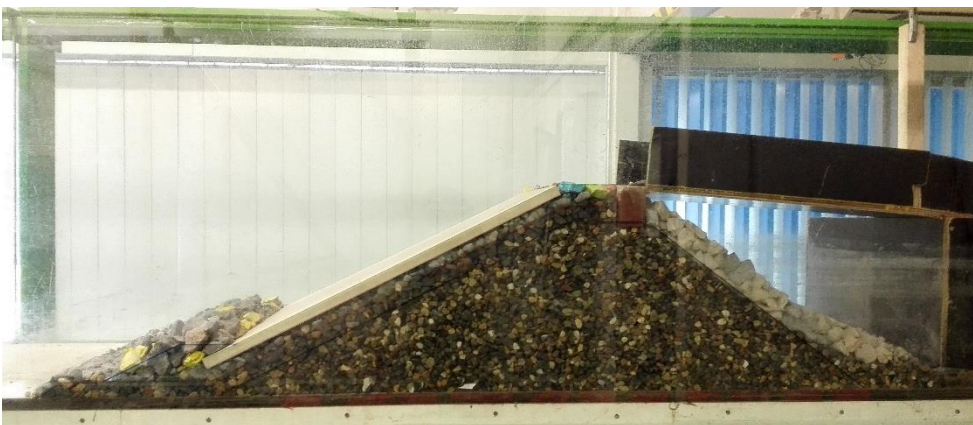
3 Cross section smooth slope 1:2

4 Top view (slope 3:4 initial blocs)

5 Top view (slope 3:4 modified blocs)

6 Top layer (slope 1:2)

7 Top layer (smooth slope 1:2)

8 Rear slope

9 Placement of the concrete unit

APPENDIX D: MEASURED WAVE CONDITIONS

In appendix D the measured incident wave conditions near the structure and at deep waters are presented.

Series	Test	Type of unit	Slope	Rc [m]	HmO/Hdesign	AT WAVE GENERATOR				DEEP WATER						NEAR THE STRUCTURE								
						HmO [m]	Tp [s]	Sop	Rc/HmO	HmO [m]	H1/3 [m]	Tp [s]	Tm-1,0 [s]	Sop	ξm-1,0	HmO [m]	H1/3 [m]	H2% [m]	Tp [s]	Tm-1,0 [s]	Sp	SmO-1	ξm-1,0	Kr
1	a	initial	0.727	0.124	60%	0.0571	0.960	0.04	2.17	0.0575	0.0570	0.955	0.932	0.040	3.526	0.0521	0.0539	0.0752	0.970	0.938	0.035	0.038	3.730	0.367
	b	initial	0.727	0.124	80%	0.0761	1.100	0.04	1.63	0.0808	0.0778	1.123	1.042	0.041	3.329	0.0747	0.0781	0.1087	1.123	1.063	0.038	0.042	3.530	0.421
	c	initial	0.727	0.124	100%	0.0952	1.240	0.04	1.30	0.0990	0.0962	1.208	1.164	0.043	3.359	0.0874	0.1102	0.1300	1.231	1.186	0.037	0.040	3.642	0.432
2	a	modified	0.727	0.124	60%	0.0563	1.343	0.02	2.20	0.0612	0.0590	1.362	1.250	0.021	4.586	0.0562	0.0548	0.0717	1.362	1.253	0.019	0.023	4.797	0.430
	b	modified	0.727	0.124	80%	0.0750	1.551	0.02	1.65	0.0834	0.0521	1.561	1.436	0.022	4.513	0.0764	0.0746	0.1011	1.600	1.450	0.019	0.023	4.763	0.467
	c	modified	0.727	0.124	100%	0.0938	1.734	0.02	1.32	0.1060	0.1019	1.840	1.603	0.020	4.470	0.0966	0.0943	0.1214	1.778	1.557	0.020	0.026	4.548	0.481
	d	modified	0.727	0.124	110%	0.1032	1.818	0.02	1.20	0.1077	0.1037	1.829	1.663	0.021	4.600	0.1040	0.1018	0.1291	1.829	1.608	0.020	0.026	4.527	0.490
	e	modified	0.727	0.124	120%	0.1125	1.899	0.02	1.10	0.1181	0.1131	1.882	1.736	0.021	4.586	0.1120	0.1111	0.1415	1.939	1.651	0.019	0.026	4.479	0.495
	f	modified	0.727	0.124	130%	0.1219	1.977	0.02	1.02	0.1276	0.1229	2.000	1.810	0.020	4.600	0.1156	0.1117	0.1348	2.000	1.811	0.019	0.023	4.836	0.507
	g	modified	0.727	0.124	140%	0.1313	2.051	0.02	0.94	0.1348	0.1290	2.065	1.866	0.020	4.614	0.1189	0.1174	0.1424	2.065	1.826	0.018	0.023	4.807	0.505
3	a	modified	0.727	0.124	60%	0.0563	0.950	0.04	2.20	0.0654	0.0645	0.955	0.903	0.046	3.206	0.0562	0.0555	0.0820	0.970	0.935	0.038	0.041	3.579	0.332
	b	modified	0.727	0.124	80%	0.0750	1.097	0.04	1.65	0.0895	0.0881	1.067	1.046	0.050	3.174	0.0785	0.0771	0.1050	1.103	1.055	0.041	0.045	3.419	0.356
	c	modified	0.727	0.124	100%	0.0938	1.226	0.04	1.32	0.1099	0.1075	1.231	1.163	0.046	3.185	0.0970	0.0951	0.1236	1.231	1.162	0.041	0.046	3.388	0.375
	d	modified	0.727	0.124	110%	0.1032	1.286	0.04	1.20	0.1182	0.1127	1.306	1.210	0.044	3.195	0.1038	0.1022	0.1319	1.333	1.199	0.037	0.046	3.379	0.391
	e	modified	0.727	0.124	120%	0.1125	1.343	0.04	1.10	0.1255	0.1221	1.362	1.259	0.043	3.226	0.1099	0.1076	0.1371	1.362	1.256	0.038	0.045	3.440	0.407
	f	modified	0.727	0.124	130%	0.1219	1.398	0.04	1.02	0.1368	0.1324	1.422	1.310	0.043	3.215	0.1184	0.1153	0.1432	1.422	1.291	0.038	0.045	3.406	0.423
	g	modified	0.727	0.124	140%	0.1313	1.451	0.04	0.94	0.1462	0.1407	1.422	1.360	0.046	3.229	0.1264	0.1243	0.1511	1.488	1.331	0.037	0.046	3.399	0.431
	h	modified	0.727	0.124	150%	0.1408	1.502	0.04	0.88	0.1575	0.1525	1.488	1.405	0.046	3.214	0.1328	0.1290	0.1539	1.524	1.383	0.037	0.044	3.445	0.432
4	a	modified	0.727	0.124	60%	0.0563	0.775	0.06	2.20	0.0486	0.0483	0.821	0.794	0.046	3.268	0.0426	0.0427	0.0637	0.781	0.802	0.045	0.042	3.528	0.270
	b	modified	0.727	0.124	80%	0.0750	0.895	0.06	1.65	0.0714	0.0928	0.928	0.889	0.053	3.018	0.0622	0.0629	0.0904	0.928	0.902	0.046	0.049	3.281	0.311
	c	modified	0.727	0.124	100%	0.0938	1.001	0.06	1.32	0.0903	0.0889	1.000	0.972	0.058	2.935	0.0832	0.0825	0.1167	1.049	0.984	0.048	0.055	3.096	0.327
	d	modified	0.727	0.124	110%	0.1032	1.050	0.06	1.20	0.0996	0.0985	1.049	1.010	0.058	2.906	0.0913	0.0897	0.1161	1.049	1.029	0.053	0.055	3.092	0.331
	e	modified	0.727	0.124	120%	0.1125	1.097	0.06	1.10	0.1089	0.1053	1.123	1.053	0.055	2.897	0.1006	0.0979	0.1274	1.123	1.070	0.051	0.056	3.063	0.336
	f	modified	0.727	0.124	130%	0.1219	1.141	0.06	1.02	0.1181	0.1127	1.164	1.091	0.056	2.882	0.1077	0.1096	0.1307	1.208	1.103	0.047	0.057	3.051	0.346
	g	modified	0.727	0.124	140%	0.1313	1.184	0.06	0.94	0.1285	0.1207	1.164	1.126	0.061	2.852	0.1126	0.1096	0.1334	1.208	1.140	0.049	0.055	3.084	0.354

Experimental study on the wave overtopping performance of Xbloc+ armour unit
Jimenez, A.

Series	Test	Type of unit	Slope	Rc [m]	HmO / Hdesign	AT WAVE GENERATOR			Rc/HmO	DEEP WATER						NEAR THE STRUCTURE								
						HmO [m]	Tp [s]	Sop		HmO [m]	H1/3 [m]	Tp [s]	Tm-1,0 [s]	Sop	ξm-1,0	HmO [m]	H1/3 [m]	H2% [m]	Tp [s]	Tm-1,0 [s]	Sp	Sm0-1	ξm-1,0	Kr
5	a	modified	0.510	0.140	60%	0.0644	1.437	0.02	2.17	0.0696	0.0679	1.422	1.327	0.022	3.203	0.0688	0.0669	0.0890	1.422	1.333	0.022	0.025	3.237	0.316
	b	modified	0.510	0.140	80%	0.0859	1.659	0.02	1.63	0.0916	0.0881	1.684	1.522	0.021	3.202	0.0900	0.0880	0.1180	1.684	1.510	0.020	0.025	3.205	0.352
	c	modified	0.510	0.140	100%	0.1074	1.855	0.02	1.30	0.1153	0.1106	1.882	1.694	0.021	3.176	0.1096	0.1093	0.1358	1.882	1.630	0.020	0.026	3.135	0.379
6	a	modified	0.510	0.140	60%	0.0644	1.016	0.04	2.17	0.0693	0.0678	1.016	0.980	0.043	2.370	0.0646	0.0637	0.0897	1.032	0.986	0.039	0.043	2.469	0.241
	b	modified	0.510	0.140	80%	0.0859	1.173	0.04	1.63	0.0934	0.0894	1.143	1.104	0.046	2.300	0.0875	0.0843	0.1100	1.185	1.113	0.040	0.045	2.395	0.265
	c	modified	0.510	0.140	100%	0.1074	1.312	0.04	1.30	0.1171	0.1107	1.306	1.228	0.044	2.285	0.1095	0.1068	0.1346	1.333	1.212	0.039	0.048	2.332	0.284
	d	modified	0.510	0.140	110%	0.1181	1.376	0.04	1.19	0.1265	0.1221	1.362	1.284	0.044	2.298	0.1193	0.1164	0.1446	1.422	1.261	0.038	0.048	2.324	0.306
	e	modified	0.510	0.140	120%	0.1288	1.437	0.04	1.09	0.1324	0.1290	1.422	1.336	0.042	2.338	0.1252	0.1225	0.1521	1.422	1.321	0.040	0.046	2.377	0.320
7	a	modified	0.510	0.140	66%	0.0783	0.914	0.06	1.79	0.0982	0.0938	0.901	0.870	0.077	1.767	0.0788	0.0779	0.0986	0.914	0.909	0.060	0.061	2.061	0.220
	b	modified	0.510	0.140	80%	0.0859	0.958	0.06	1.63	0.1015	0.0976	0.865	0.880	0.087	1.759	0.0831	0.0806	0.1004	1.000	0.924	0.053	0.062	2.042	0.227
	c	modified	0.510	0.140	100%	0.1074	1.071	0.06	1.30	0.1310	0.1251	1.103	1.057	0.069	1.859	0.1113	0.1056	0.1248	1.143	1.108	0.055	0.058	2.114	0.248
	d	modified	0.510	0.140	110%	0.1181	1.123	0.06	1.19	0.1471	0.1378	1.103	1.082	0.077	1.796	0.1208	0.1123	0.1325	1.103	1.107	0.064	0.063	2.028	0.252
	e	modified	0.510	0.140	120%	0.1288	1.173	0.06	1.09	0.1567	0.1452	1.208	1.157	0.069	1.861	0.1274	0.1207	0.1399	1.185	1.158	0.058	0.061	2.066	0.271
8	a	modified	0.510	0.140	60%	0.0644	1.437	0.02	2.17	0.0703	0.0678	1.422	1.309	0.022	3.143	0.0688	0.0661	0.0873	1.422	1.314	0.022	0.026	3.189	0.675
	b	modified	0.510	0.140	80%	0.0859	1.659	0.02	1.63	0.0894	0.0860	1.684	1.512	0.020	3.220	0.0905	0.0876	0.1173	1.684	1.498	0.020	0.026	3.171	0.629
	c	modified	0.510	0.140	100%	0.1074	1.855	0.02	1.30	0.1165	0.1116	1.882	1.688	0.021	3.149	0.1077	0.1064	0.1349	1.882	1.617	0.019	0.026	3.137	0.592
9	a	modified	0.510	0.140	60%	0.0644	1.016	0.04	2.17	0.0714	0.0704	1.049	0.981	0.042	2.337	0.0653	0.0642	0.0920	1.032	0.987	0.039	0.043	2.460	0.523
	b	modified	0.510	0.140	80%	0.0859	1.173	0.04	1.63	0.0957	0.0919	1.143	1.108	0.047	2.280	0.0882	0.0851	0.1121	1.185	1.115	0.040	0.045	2.390	0.529
	c	modified	0.510	0.140	100%	0.1074	1.312	0.04	1.30	0.1184	0.1130	1.280	1.226	0.046	2.268	0.1100	0.1069	0.1366	1.333	1.205	0.040	0.049	2.313	0.518
	d	modified	0.510	0.140	110%	0.1181	1.376	0.04	1.19	0.1464	0.1378	1.310	1.282	0.055	2.133	0.1178	0.1149	0.1430	1.391	1.255	0.039	0.048	2.328	0.520
	e	modified	0.510	0.140	120%	0.1288	1.437	0.04	1.09	0.1346	0.1314	1.422	1.338	0.043	2.322	0.1228	0.1187	0.1428	1.422	1.342	0.039	0.044	2.438	0.532
10	a	modified	0.510	0.140	66%	0.0783	0.914	0.06	1.79	0.0987	0.0942	0.901	0.871	0.078	1.765	0.0789	0.0781	0.1000	0.911	0.911	0.061	0.061	2.065	0.360
	b	modified	0.510	0.140	80%	0.0859	0.958	0.06	1.63	0.1032	0.0988	0.865	0.883	0.088	1.749	0.0829	0.0803	0.1011	1.000	0.925	0.053	0.062	2.046	0.374
	c	modified	0.510	0.140	100%	0.1074	1.071	0.06	1.30	0.1319	0.1255	1.103	1.059	0.069	1.856	0.1093	0.1029	0.1231	1.143	1.083	0.054	0.060	2.086	0.433
	d	modified	0.510	0.140	110%	0.1181	1.123	0.06	1.19	0.1464	0.1378	1.103	1.082	0.077	1.800	0.1185	0.1101	0.1284	1.185	1.113	0.054	0.061	2.058	0.442
	e	modified	0.510	0.140	120%	0.1288	1.173	0.06	1.09	0.1558	0.1445	1.231	1.172	0.066	1.890	0.1289	0.1214	0.1438	1.231	1.161	0.054	0.061	2.059	0.465

Experimental study on the wave overtopping performance of Xbloc+ armour unit
Jimenez, A.

APPENDIX E: MEASURED WAVE OVERTOPPING

The measured wave overtopping for each test series is presented in Appendix E.

Series	Test	Type of unit	Slope	Rc [m]	HmO [m]	H1/3 [m]	H2% [m]	Tp [s]	Tm-1,0 [s]	Sp	SmO-1	Ɛm-1,0	Kr	HmO/Hdesign	Δdepth [m]	Rc* [m]	Rc*/HmO	Now	Nw	Now/Nw	Volume outside bucket [l]	Total volume [l]	Test duration [s]	q [l/m/s]	q* [-]
												NEAR THE STRUCTURE													
1	a	initial	0.727	0.124	0.0521	0.0539	0.0890	0.970	0.938	0.035	0.038	3.730	0.367	55%	0.000	0.124	2.380	0	1222	0.0%	0.0	0.0	967	0.00E+00	0.00E+00
1	b	initial	0.727	0.124	0.0747	0.0781	0.1180	1.123	1.063	0.038	0.042	3.530	0.421	78%	0.000	0.124	1.660	2	1295	0.2%	0.0	0.2	1110	7.95E-04	1.24E-05
1	c	initial	0.727	0.124	0.0874	0.1102	0.1358	1.231	1.186	0.037	0.040	3.642	0.432	92%	0.000	0.124	1.419	49	1535	3.2%	0.0	3.1	1257	9.90E-03	1.22E-04
2	a	modified	0.727	0.124	0.0562	0.0548	0.0717	1.362	1.253	0.019	0.023	4.797	0.430	60%	0.000	0.124	2.205	1	1218	0.1%	0.0	0.1	1436	3.94E-04	9.44E-06
2	b	modified	0.727	0.124	0.0764	0.0746	0.1011	1.600	1.450	0.019	0.023	4.763	0.467	81%	0.000	0.124	1.624	14	1235	1.1%	0.0	5.5	1617	1.37E-02	2.07E-04
2	c	modified	0.727	0.124	0.0966	0.0943	0.1214	1.778	1.557	0.020	0.026	4.548	0.481	103%	-0.002	0.125	1.294	139	1288	10.8%	0.0	38.2	1841	8.30E-02	8.83E-04
2	d	modified	0.727	0.124	0.1040	0.1018	0.1291	1.829	1.608	0.020	0.026	4.527	0.490	111%	-0.006	0.127	1.221	223	1273	17.5%	0.0	79.9	1869	1.71E-01	1.63E-03
2	e	modified	0.727	0.124	0.1120	0.1111	0.1415	1.939	1.651	0.019	0.026	4.479	0.495	119%	-0.009	0.129	1.147	314	1248	25.2%	6.3	136.6	1894	2.88E-01	2.46E-03
2	f	modified	0.727	0.124	0.1156	0.1117	0.1348	2.000	1.811	0.019	0.023	4.836	0.507	123%	-0.012	0.130	1.125	379	1242	30.5%	17.0	194.6	2041	3.81E-01	3.10E-03
2	g	modified	0.727	0.124	0.1189	0.1174	0.1424	2.065	1.826	0.018	0.023	4.807	0.505	127%	-0.020	0.134	1.127	525	1512	34.7%	9.4	277.6	2524	4.40E-01	3.43E-03
3	a	modified	0.727	0.124	0.0562	0.0555	0.0820	0.970	0.935	0.038	0.041	3.579	0.332	60%	0.000	0.124	2.206	0	1161	0.0%	0.0	0.0	1156	0.00E+00	0.00E+00
3	b	modified	0.727	0.124	0.0785	0.0771	0.1050	1.103	1.055	0.041	0.045	3.419	0.356	84%	0.000	0.124	1.580	5	1158	0.4%	0.0	0.4	1032	1.48E-03	2.14E-05
3	c	modified	0.727	0.124	0.0970	0.0951	0.1236	1.231	1.162	0.041	0.046	3.388	0.375	103%	0.000	0.124	1.279	41	1179	3.5%	0.0	5.3	1301	1.62E-02	1.72E-04
3	d	modified	0.727	0.124	0.1038	0.1022	0.1319	1.333	1.199	0.037	0.046	3.379	0.391	111%	0.000	0.124	1.195	79	1216	6.5%	0.0	11.6	1372	3.38E-02	3.23E-04
3	e	modified	0.727	0.124	0.1099	0.1076	0.1371	1.362	1.256	0.038	0.045	3.440	0.407	117%	0.000	0.124	1.128	123	1175	10.5%	0.0	19.8	1411	5.62E-02	4.92E-04
3	f	modified	0.727	0.124	0.1184	0.1153	0.1432	1.422	1.291	0.038	0.045	3.406	0.423	126%	-0.002	0.125	1.056	205	1210	16.9%	0.0	40.3	1454	1.11E-01	8.69E-04
3	g	modified	0.727	0.124	0.1264	0.1243	0.1511	1.488	1.331	0.037	0.046	3.399	0.431	135%	-0.005	0.127	1.001	303	1257	24.1%	0.0	72.4	1582	1.83E-01	1.30E-03
3	h	modified	0.727	0.124	0.1328	0.1290	0.1539	1.524	1.383	0.037	0.044	3.445	0.432	142%	-0.007	0.128	0.960	334	1204	27.7%	0.0	90.4	1567	2.31E-01	1.52E-03
4	a	modified	0.727	0.124	0.0426	0.0427	0.0637	0.781	0.802	0.045	0.042	3.528	0.270	45%	0.000	0.124	2.914	0	1076	0.0%	0.0	0.0	831	0.00E+00	0.00E+00
4	b	modified	0.727	0.124	0.0622	0.0629	0.0904	0.928	0.902	0.046	0.049	3.281	0.311	66%	0.000	0.124	1.993	0	1096	0.0%	0.0	0.0	949	0.00E+00	0.00E+00
4	c	modified	0.727	0.124	0.0832	0.0825	0.1167	1.049	0.984	0.048	0.055	3.096	0.327	89%	0.000	0.124	1.491	18	1328	1.4%	0.0	0.3	1244	1.11E-03	1.48E-05
4	d	modified	0.727	0.124	0.0913	0.0897	0.1161	1.049	1.029	0.053	0.055	3.092	0.331	97%	0.000	0.124	1.358	34	1612	2.1%	0.0	1.0	1692	2.39E-03	2.76E-05
4	e	modified	0.727	0.124	0.1006	0.0979	0.1274	1.123	1.070	0.051	0.056	3.063	0.336	107%	0.000	0.124	1.233	55	1320	4.2%	0.0	2.7	1591	6.75E-03	6.76E-05
4	f	modified	0.727	0.124	0.1077	0.1096	0.1307	1.208	1.103	0.047	0.057	3.051	0.346	115%	0.000	0.124	1.151	93	1291	7.2%	0.0	6.4	1347	1.90E-02	1.72E-04
4	g	modified	0.727	0.124	0.1126	0.1096	0.1334	1.208	1.140	0.049	0.055	3.084	0.354	120%	0.000	0.124	1.101	126	1291	9.8%	0.0	13.5	1529	3.52E-02	2.98E-04

Experimental study on the wave overtopping performance of Xbloc+ armour unit
Jimenez, A.

Series	Test	Type of unit	Slope	Rc [m]	HmO [m]	H1/3 [m]	H2% [m]	Tp [s]	Tm-1,0 [s]	Sp	SmO-1	ξm-1,0	Kr	HmO/Hdesign	Δdepth [m]	Rc* [m]	Rc*/HmO	Now	Nw	Now/Nw	Volume outside bucket [l]	Total volume [l]	Test duration [s]	q [l/m/s]	q* [-]
													NEAR THE STRUCTURE												
5	a	modified	0.510	0.14	0.0688	0.0669	0.0890	1.422	1.333	0.022	0.025	3.237	0.316	64%	0.000	0.140	2.036	2	1164	0.2%	0.0	0.1	1455	2.96E-04	5.24E-06
	b	modified	0.510	0.14	0.0900	0.0880	0.1180	1.684	1.510	0.020	0.025	3.205	0.352	84%	0.000	0.140	1.556	43	1332	3.2%	0.0	4.9	1855	1.06E-02	1.25E-04
	c	modified	0.510	0.14	0.1096	0.1093	0.1358	1.882	1.630	0.020	0.026	3.135	0.379	102%	-0.002	0.141	1.286	184	1211	15.2%	0.0	42.0	1844	9.11E-02	8.01E-04
6	a	modified	0.510	0.14	0.0646	0.0637	0.0897	1.032	0.986	0.039	0.043	2.469	0.241	60%	0.000	0.140	2.167	0	1194	0.0%	0.0	0.0	1133	0.00E+00	0.00E+00
	b	modified	0.510	0.14	0.0875	0.0843	0.1100	1.185	1.113	0.040	0.045	2.395	0.265	82%	0.000	0.140	1.599	1	1187	0.1%	0.0	0.0	1264	1.46E-04	1.79E-06
	c	modified	0.510	0.14	0.1095	0.1068	0.1346	1.333	1.212	0.039	0.048	2.332	0.284	102%	0.000	0.140	1.279	30	1317	2.3%	0.0	1.3	1537	3.45E-03	3.04E-05
	d	modified	0.510	0.14	0.1193	0.1164	0.1446	1.422	1.261	0.038	0.048	2.324	0.306	111%	0.000	0.140	1.174	49	1195	4.1%	0.0	3.1	1441	8.57E-03	6.64E-05
	e	modified	0.510	0.14	0.1252	0.1225	0.1521	1.422	1.321	0.040	0.046	2.377	0.320	117%	0.000	0.140	1.118	113	1191	9.5%	0.0	9.3	1551	2.40E-02	1.73E-04
7	a	modified	0.510	0.14	0.0788	0.0779	0.0986	0.914	0.909	0.060	0.061	2.061	0.220	73%	0.000	0.140	1.777	0	971	0.0%	0.0	0.0	888	0.00E+00	0.00E+00
	b	modified	0.510	0.14	0.0831	0.0806	0.1004	1.000	0.924	0.053	0.062	2.042	0.227	77%	0.000	0.140	1.686	0	1296	0.0%	0.0	0.0	1182	0.00E+00	0.00E+00
	c	modified	0.510	0.14	0.1113	0.1056	0.1248	1.143	1.108	0.055	0.058	2.114	0.248	104%	0.000	0.140	1.258	6	1276	0.5%	0.0	0.4	1344	1.18E-03	1.01E-05
	d	modified	0.510	0.14	0.1208	0.1123	0.1325	1.103	1.107	0.064	0.063	2.028	0.252	112%	0.000	0.140	1.159	9	1146	0.8%	0.0	0.8	1251	2.65E-03	2.01E-05
	e	modified	0.510	0.14	0.1274	0.1207	0.1399	1.185	1.158	0.058	0.061	2.066	0.271	119%	0.000	0.140	1.099	33	1140	2.9%	0.0	2.3	1300	7.04E-03	4.94E-05
8	a	modified	0.510	0.14	0.0688	0.0661	0.0873	1.422	1.314	0.022	0.026	3.189	0.675	64%	-0.001	0.141	2.049	-	1410	-	0.0	26.9	1702	6.32E-02	1.12E-03
	b	modified	0.510	0.14	0.0905	0.0876	0.1173	1.684	1.498	0.020	0.026	3.171	0.629	84%	-0.010	0.145	1.658	-	1249	-	5.2	104.2	1695	2.46E-01	2.89E-03
	c	modified	0.510	0.14	0.1077	0.1064	0.1349	1.882	1.617	0.019	0.026	3.137	0.592	100%	-0.022	0.151	1.504	-	1279	-	12.4	254.7	1907	5.34E-01	4.83E-03
9	a	modified	0.510	0.14	0.0653	0.0642	0.0920	1.032	0.987	0.039	0.043	2.460	0.523	61%	0.000	0.140	2.145	-	1094	-	0.0	2.5	1028	9.85E-03	1.89E-04
	b	modified	0.510	0.14	0.0882	0.0851	0.1121	1.185	1.115	0.040	0.045	2.390	0.529	82%	-0.001	0.141	1.598	-	1162	-	0.0	21.6	1214	7.12E-02	8.68E-04
	c	modified	0.510	0.14	0.1100	0.1069	0.1366	1.333	1.205	0.040	0.049	2.313	0.518	102%	-0.006	0.143	1.327	-	1165	-	0.0	79.3	1348	2.35E-01	2.06E-03
	d	modified	0.510	0.14	0.1178	0.1149	0.1430	1.391	1.255	0.039	0.048	2.328	0.520	110%	-0.009	0.145	1.265	-	1246	-	6.0	99.7	1488	2.68E-01	2.12E-03
	e	modified	0.510	0.14	0.1228	0.1187	0.1428	1.422	1.342	0.039	0.044	2.438	0.532	114%	-0.012	0.146	1.238	-	1171	-	6.9	162.6	1481	4.39E-01	3.26E-03
10	a	modified	0.510	0.14	0.0789	0.0781	0.1000	0.911	0.911	0.061	0.061	2.065	0.360	74%	0.000	0.140	1.773	-	979	-	0.0	2.6	862	1.19E-02	1.71E-04
	b	modified	0.510	0.14	0.0829	0.0803	0.1011	1.000	0.925	0.053	0.062	2.046	0.374	77%	0.000	0.140	1.688	-	1103	-	0.0	4.1	1000	1.63E-02	2.18E-04
	c	modified	0.510	0.14	0.1093	0.1029	0.1231	1.143	1.083	0.054	0.060	2.086	0.433	102%	-0.003	0.142	1.308	-	1060	-	0.0	45.5	1104	1.65E-01	1.46E-03
	d	modified	0.510	0.14	0.1185	0.1101	0.1284	1.185	1.113	0.054	0.061	2.058	0.442	110%	-0.006	0.143	1.232	-	1081	-	0.0	66.2	1173	2.26E-01	1.77E-03
	e	modified	0.510	0.14	0.1289	0.1214	0.1438	1.231	1.161	0.054	0.061	2.059	0.465	120%	-0.007	0.144	1.140	-	1098	-	0.0	117.2	1239	3.79E-01	2.61E-03

Experimental study on the wave overtopping performance of Xbloc+ armour unit
Jimenez, A.